AWARD NUMBER: W81XWH-17-1-0354

TITLE: **Cutaneous Human Papillomaviruses as Co-Factors in Non-Melanoma Skin Cancer**

PRINCIPAL INVESTIGATOR: Nicholas A Wallace

CONTRACTING ORGANIZATION: Kansas State University

REPORT DATE: August 2020

TYPE OF REPORT: Annual

PREPARED FOR: U.S. Army Medical Research and Materiel Command
Fort Detrick, Maryland 21702-5012

REPORT DOCUMENTATION PAGE

Form Approved
OMB No. 0704-0188

1. REPORT DATE	2. REPORT TYPE	3. DATES COVERED
August 2020	Annual	08/01/2019-07/31/2020

4. TITLE AND SUBTITLE

Cutaneous Human Papillomaviruses as Co-Factors in Non-Melanoma Skin Cancer

5a. CONTRACT NUMBER

5b. GRANT NUMBER
W81XWH-17-1-0354

5c. PROGRAM ELEMENT NUMBER

6. AUTHOR(S)
Nicholas A. Wallace

E-Mail: nwallac@ksu.edu

5d. PROJECT NUMBER

5e. TASK NUMBER

5f. WORK UNIT NUMBER

7. PERFORMING ORGANIZATION NAME(S) AND ADDRESS(ES)

Kansas State University
1717 Claflin Road
Manhattan Ks, 66506

8. PERFORMING ORGANIZATION REPORT NUMBER

9. SPONSORING / MONITORING AGENCY NAME(S) AND ADDRESS(ES)

U.S. Army Medical Research and Materiel Command
Fort Detrick, Maryland 21702-5012

10. SPONSOR/MONITOR'S ACRONYM(S)

11. SPONSOR/MONITOR'S REPORT NUMBER(S)

12. DISTRIBUTION / AVAILABILITY STATEMENT

Approved for Public Release; Distribution Unlimited

13. SUPPLEMENTARY NOTES

14. ABSTRACT

We have made substantial strides in our efforts to better define β-HPV E6's ability to augment the mutagenic potential of genome destabilizing events. Our efforts have culminated in five peer reviewed manuscripts. All of the major tasks have been completed to 90- 100% of expectations. We were granted a no cost extension on this grant due to disruptions caused by COVID-19. Our expectation is that this additional time will allow us to complete the remaining work. Finally, we have been awarded two grants from the National Institutes of Health that will expand our work beyond the scope of this grant.

15. SUBJECT TERMS
Non-melanoma skin cancer, Cutaneous human papillomavirus infection, Ultraviolet irradiation, Ionizing radiation, DNA damage, Genome fidelity.

16. SECURITY CLASSIFICATION OF:			17. LIMITATION OF ABSTRACT	18. NUMBER OF PAGES	19a. NAME OF RESPONSIBLE PERSON
					USAMRMC
a. REPORT	b. ABSTRACT	c. THIS PAGE	UU		19b. TELEPHONE NUMBER *(include area code)*
U Unclassified	U Unclassified	U Unclassified	Unclassified		

Table of Contents

Page

1. **INTRODUCTION:** Genus β human papillomaviruses (β-HPVs) are believed to contribute to non-melanoma skin cancer by acting as a cofactor in UV-induced destabilization of the host genome. The purpose of this project is to test this hypothesis by measuring the ability of the E6 protein from β-HPV to disrupt cellular signaling in response to challenges to genome fidelity. We are examining non-homologous end joining, nucleotide excision repair, and the Hippo Pathway. Mechanistically, we are testing disruptions of this pathway that are either dependent or independent of β-HPV E6's degradation of p300, a cellular histone acetyltransferase.
2. **KEYWORDS:** Non-melanoma skin cancer, Cutaneous human papillomavirus infection, Ultraviolet irradiation, Ionizing radiation, DNA damage, Genome fidelity.
3. **ACCOMPLISHMENTS:** *The PI is reminded that the recipient organization is required to obtain prior written approval from the awarding agency Grants Officer whenever there are significant changes in the project or its direction.*

Career Development Specific Tasks: During the first reporting period, I have made significant advancements toward my goal of establishing myself as a leader in the non-melanoma skin cancer research. This is will allow me to make continued contributions to the PRCRP topic area, "Melanoma and Other Skin Cancers

- **Career Development Specific Major Task 1:** Receive Career and Research Advice from Experts in Cancer Causing Viruses
  - **Projected Completion date** (from SOW): August 1, 2020
  - **Completion Percentage:** ~95% (detailed in subsequent sections, calculated from percentage of milestones met)

Research Specific Tasks: My research continues to highlight the oncogenic risk of cutaneous human papillomavirus infection co-occurring with exposure to military relevant risk factors UV and ionizing radiation. My findings are consistent with β-HPV infections contributing to non-melanoma skin cancer in military personnel.

- **Specific Aim 1 Major Task 1:** Characterize β-HPV E6's attenuation of DNA crosslink repair.
  - **Projected Completion date** (from SOW): May 1, 2019
  - **Completion Percentage:** 100% (detailed in subsequent sections)
    - We have extended our efforts beyond the original task after completing the work proposed in the SOW.
- **Specific Aim 1 Major Task 2:** Determine the Extent to which β-HPV E6 Attenuates Non-Homologous End Joining Repair (NHEJ) of DNA Lesions
  - **Projected Completion date** (from SOW): August 1, 2020
  - **Completion Percentage:** 95% (detailed in subsequent sections)
- **Specific Aim 2 Major Task 1:** Defining β-HPV E6's inhibition of the Hippo Pathway (HP)
  - **Projected Completion date** (from SOW): February 1, 2019
  - **Completion Percentage:** 95% (detailed in subsequent sections)
- **Specific Aim 2 Major Task 2:** Determine the mechanism of β-HPV E6's inhibition of the HP.
  - **Projected Completion date** (from SOW): August 1, 2020

        - **Completion Percentage:** 100% (detailed in subsequent sections)
            - We have extended our efforts beyond the original task after completing the work proposed in the SOW.
    - **Specific Aim 3 Major Task 1:** P300-Independent Disruption of DNA Crosslink Repair
        - **Projected Completion date** (from SOW): August 1, 2018
        - **Completion Percentage:** 95% (detailed in subsequent sections)
            - We have completed this task as much as possible and are currently examining the other p300-independent phenotypes that we identified during the completion of AIM2. This adheres with the theme of the proposal.
    - **Specific Aim 3 Major Task 2:** Determine the mechanism of β-HPV E6's p300-independent inhibition of DNA crosslink repair.
        - **Projected Completion date** (from SOW): August 1, 2020
        - **Completion Percentage:** 100% (detailed in subsequent sections)
            - We have completed this task as much as possible and are currently examining β-HPV E6 in the context of a common mutation found in NMSC. This adheres with the theme of the proposal.

What was accomplished under these goals?

CAREER DEVELOPMENT-SPECIFIC TASKS

Major Task 1: Receive Career and Research Advice from Experts in Cancer Causing Viruses

Subtask 1: Present Research Annually to Drs. Laimonis and Giam's Research Teams

● Last reporting Period Summary: I met with Dr. Giam and Uniformed Services University Health Sciences Microbiology faculty in person. I also presented my research to Dr. Laimonis primarily via email and phone conversations.

● Second Reporting Period: I communicated with Dr. Giam about my progress via email. I met with Dr. Laimonis twice in person to discuss my work.

● Third Reporting Period: I communicated with Dr. Giam about my progress via email. I met with Dr. Laimonis twice in person to discuss my work. My third and fourth visits with Dr. Laimonis were cancelled due to COVID-19 restrictions. We have exchanged emails instead.

Subtask 2: Attend and Present Research at Marquee HPV Research Conferences

● Last reporting Period Summary: I attended several regional conferences in between these meetings highlighted by 17th Annual Symposium in Virology hosted by the University of Nebraska's Center for Virology.

● Second Reporting Period: I attended the 2018 and 2019 DNA Tumor Virus Meetings and chaired a session in the 2018 meeting. I also presented at the 2019 International Papillomavirus Meeting. I also attended the 18th Annual Symposium in Virology hosted by the University of Nebraska's Center for Virology. In total, my lab and I presented work related to this project 4 times at international conferences and 3 times at a national conference.

● Third Reporting Period: I attended the 2019 Midwest Symposium on Papilloma and Polyom viruses. I presented at this meeting. My students presented at this meeting and at the American Society of Virology Meeting for a total of 3 international/national conference presentations. Several other speaking engagments were cancelled due to the pandemic.

Subtask 3: Monthly Discussion of Career Progress and Grant Submission Strategy with Dr. Laimonis.

Dr. Laimonis and I continue discuss my career regularly. This has included regular grant revisions and career guidance. These interactions have been incalculably helpful as I've navigate my pre-tenure career. Thanks to his advice, support from the CDMRP and hard work from my lab members, I have been encouraged to go up for tenure early and will submit my tenure packet in August 2020. I have also obtained two grants funded by the National Institutes of Health and submitted an unsuccessful proposal to the CDMRP.

Subtask 4: Discuss Scientific and Professional Progress with Dr. Clem (KSU Faculty Advisor).

With Dr. Clem's mentorship, I have seen my lab's output grow over the last year. My new lab's location near him continues to be beneficial.

Milestones Achieved:

(1) Presentation of project data at preeminent meetings annually, (12, 24 36 Months)
    a. In this funding period, project data was presented 3 times at noteworthy national and international meetings. It was also presented several other times at local/regional events.
        i. 7 other presentations were cancelled due to the ongoing pandemic.

(2) Submit major grant proposal to extend project by the end of the second budget period (24 Months)
    a. In funding period 1 I submitted the two grants described below:
        i. A proposal to the American Cancer Center was resubmitted titled, *"*Genus Beta Human Papillomavirus E6 Impairs Genome Fidelity". This grant would provide support to expand the efforts funded by the CDMRP from 2019-2023. Notably, there is no overlap to the work supported by the CDMRP and this milestone was completed over 1 year earlier than projected.
            1. **Update: This grant was not funded, but its score improved and it was resubmitted during budget period 3.**
        ii. I am a junior investigator on a COBRE proposal (P20) resubmitted to the National Institute of General Medical Sciences. This work would also extend the efforts funded by the CDMRP with complimentary analysis of the oncogenic potential of cutaneous HPV infections. There is no overlap with the CDMRP funded project.
            1. **Update: This grant was funded during budget period 3.**
    b. I also submitted an R15 proposal to the National Institutes of Health entitled, "High Risk Genus Alpha HPV Oncogenes Dysregulate Translesion Synthesis". This grant received a favorable score but was not funded. There is no overlap with this CDMRP funded project.
        i. **Update: This grant was funded during budget period 3.**
(3) If necessary, revise and resubmit grant. (24, 36 Months)
    a. All three grants described above were resubmitted during budget period 2 and are awaiting review.
        i. **During the third budget period, two of the three grants listed above were funded and the third was resubmitted.**
(4) Publish Findings in Peer Reviewed Journal (24, 36 Months)

a. **A total of 10 manuscripts have been published from our group during overall period of support from this grant.**
b. Three manuscripts were published ahead of schedule during the first funding period.
    i. Loss of Genome Fidelity: Beta HPVs and the DNA Damage Response. Wendel SO, Wallace NA Front. Microbiol. 2017 PMID:29187845 LINK
    ii. Characterizing DNA Repair Processes at Transient and Long-lasting Double-strand DNA Breaks by Immunofluorescence Microscopy. Murthy V, Dacus D, Gamez M, Hu C, Wendel SO, Snow J, Kahn A, Walterhouse SH, Wallace NA. 2018 PMID: 29939192 LINK
    iii. The Curious Case of APOBEC3 Activation by Cancer Associated Human Papillomaviruses. Wallace NA, Munger K. 2018 PMID: 29324878 LINK
c. Two more manuscripts were published during the second budget period. References are listed below
    i. Cervical cancer cell lines are sensitive to sub-erthemal UV exposure. Gu W., Sun S., Kahn A., Dacus D., Wendel SO., McMillan N., Wallace NA. 2019 PMID: 30517878 LINK
    ii. mSphere of Influence: the Value of Simplicity in Experiments and Solidarity among Lab Members. Wallace NA. 2019. PMID: 31217299 LINK
d. Five more manuscripts were published during the third budget period. References are listed below
    i. Beta Human Papillomavirus 8E6 Attenuates LATS Phosphorylation after Failed Cytokinesis. D Dacus, C Cotton, TX McCallister, NA Wallace. 2020. PMID: 32238586. LINK
    ii. β-HPV 8E6 combined with TERT expression promotes long-term proliferation and genome instability after cytokinesis failure. D Dacus, E Riforgiate, NA Wallace 2020 LINK
    iii. DNA repair gene expression is increased in HPV positive head and neck squamous cell carcinomas. AJ Holcomb, L Brown, O Tawfik, R Madan, Y Shnayder, SM Thomas, NA Wallace 2020 LINK
    iv. β-HPV 8E6 Attenuates ATM and ATR Signaling in Response to UV Damage. JA Snow, V Murthy, D Dacus, C Hu, NA Wallace. 2019. PMID: 31779191 LINK
    v. Catching hpv in the homologous recombination cookie jar. NA Wallace. 2020. PMID: 31744663 LINK

(5) Gain career advice from experts in viral oncology
a. I have had extensive interactions with my formal mentors and given talks at 5 different regional/national conferences (**DNA Tumor Virus Meeting; Midwest Papillomavirus and Polyomavirus Symposium**; **Kansas IDEA Network of Biomedical Research Excellence's Annual Symposium; Kansas University Medical Center's Viral Pathogenesis Symposium; University of Nebraska's Center for Virology Fly Swat Meeting**).

RESEARCH-SPECIFIC TASKS

<u>Specific Aim 1: To define the p300 inhibition of DNA repair by β-HPV E6</u>

Major Task 1: Characterize β-HPV E6's attenuation of DNA crosslink repair.

A peer-reviewed manuscript (Snow et al; 2019) describing our data was published in the journal Pathogens during the third budget period.

Subtask 1: Obtain HRPO approval to isolate keratinocytes from neonatal foreskins and complete onboarding of Changkun Hu.

This was completed during the first budget period.

Subtask 2: Examine XPA phosphorylation and Stabilization using Immunoblot at representative time points following UV exposure. This will be done in vector control, β-HPV E6 and β-HPV ΔE6 expressing cells.

The work for this subtask was completed during budget period 3 and published after peer review in a special issue of the journal Pathogens. I have included the figure from the paper (Snow et al 2019) with data relevant to this subtask (Figure 1A-D). They demonstrate the β-HPV E6 (referred to as 8E6 in the paper and figure) reduce phosphorylation of XPA. In addition, we also found that β-HPV E6 also reduced expression of XPA (Figure 1B). This work as done in primary HFKs and TERT-immortalized HFKs. These data were also summarized more thoroughly in the report for the second budget period.

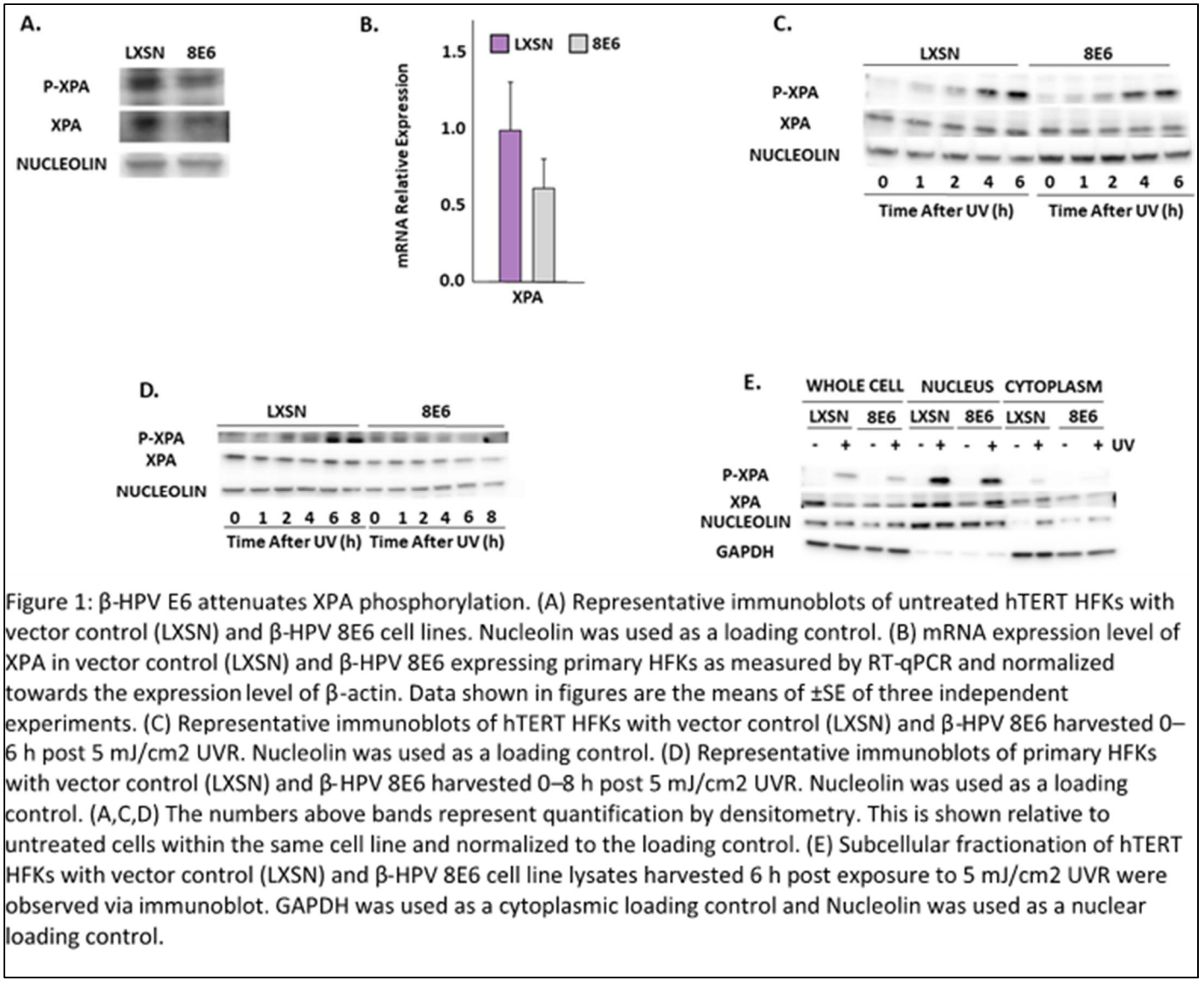

Figure 1: β-HPV E6 attenuates XPA phosphorylation. (A) Representative immunoblots of untreated hTERT HFKs with vector control (LXSN) and β-HPV 8E6 cell lines. Nucleolin was used as a loading control. (B) mRNA expression level of XPA in vector control (LXSN) and β-HPV 8E6 expressing primary HFKs as measured by RT-qPCR and normalized towards the expression level of β-actin. Data shown in figures are the means of ±SE of three independent experiments. (C) Representative immunoblots of hTERT HFKs with vector control (LXSN) and β-HPV 8E6 harvested 0–6 h post 5 mJ/cm2 UVR. Nucleolin was used as a loading control. (D) Representative immunoblots of primary HFKs with vector control (LXSN) and β-HPV 8E6 harvested 0–8 h post 5 mJ/cm2 UVR. Nucleolin was used as a loading control. (A,C,D) The numbers above bands represent quantification by densitometry. This is shown relative to untreated cells within the same cell line and normalized to the loading control. (E) Subcellular fractionation of hTERT HFKs with vector control (LXSN) and β-HPV 8E6 cell line lysates harvested 6 h post exposure to 5 mJ/cm2 UVR were observed via immunoblot. GAPDH was used as a cytoplasmic loading control and Nucleolin was used as a nuclear loading control.

Subtask 3: Determine if DNA crosslink repair is rescued by exogenous expression of XPA and ATR.

During budget period 2, our data suggested that excess ATR or XPA would not rescue crosslink repair. This was because β-HPV E6 blocked ATR activity. The data demonstrating this can be found in Figure 2 and in the previously mentioned manuscript.

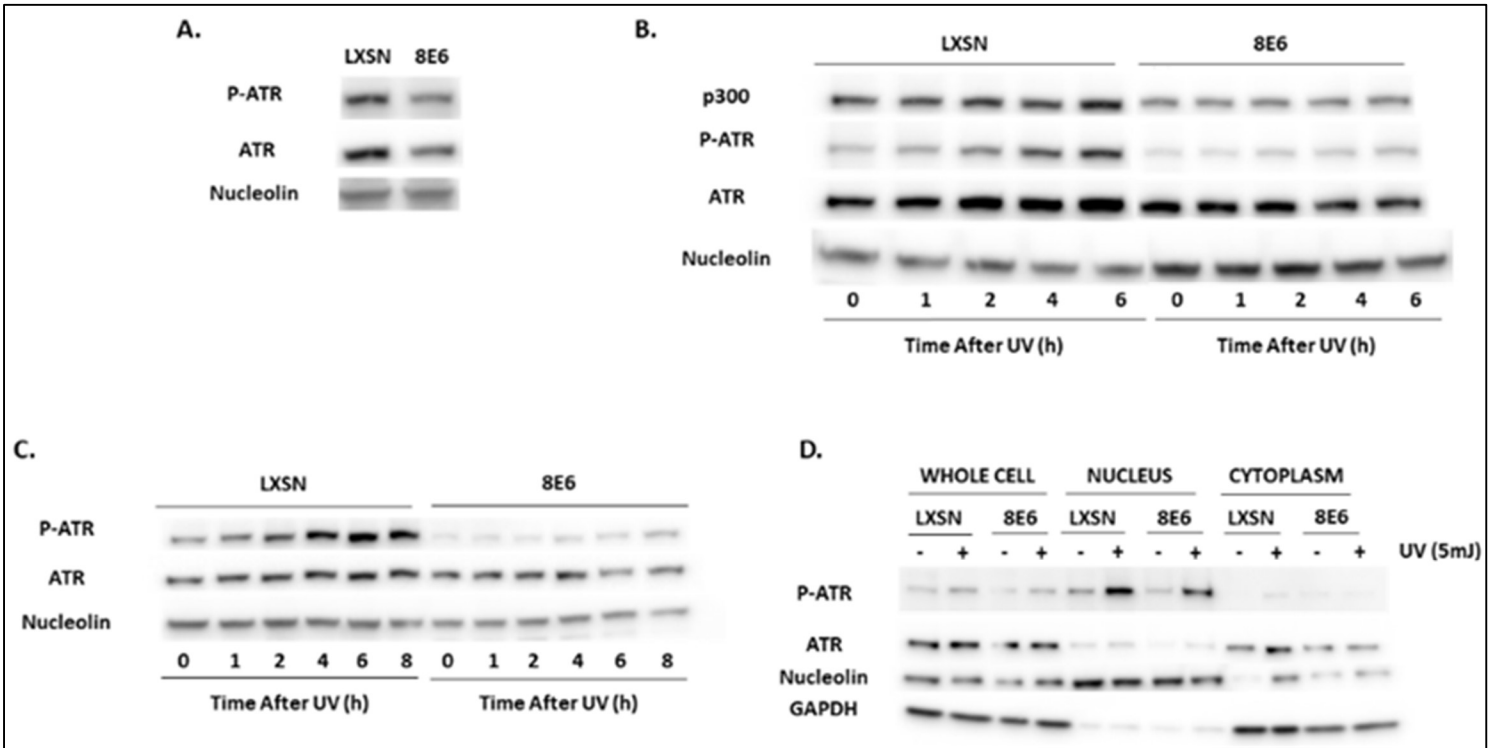

Figure 2: β-HPV 8E6 attenuates ATR activation. (A) Representative immunoblots of untreated hTERT HFKs with vector control (LXSN) and β-HPV 8E6 cell lines. Nucleolin was used as a loading control. (B) Representative immunoblots of hTERT HFKs with vector control (LXSN) and β-HPV 8E6 harvested 0–6 h post 5 mJ/cm2 UVR. Nucleolin was used as a loading control. (C) Representative immunoblots of primary HFKs with vector control (LXSN) and β-HPV 8E6 harvested 0–8 h post 5 mJ/cm2 UVR. Nucleolin was used as a loading control. (A–C) The numbers above bands represent quantification by densitometry. This is shown relative to untreated cells within the same cell line and normalized to the loading control. (D) Subcellular fractionation of hTERT HFKs with vector control (LXSN) and β-HPV 8E6 cell line lysates harvested 6 h post exposure to 5 mJ/cm2 UVR were observed via immunoblot. GAPDH was used as a cytoplasmic loading control and Nucleolin was used as a nuclear loading control.

As a result, we examined ATR phosphorylation targets. This demonstrated that β-HPV E6 has a broad but not universal ability to hinder ATR-mediated phosphorylation and is shown figure 3-4 and can also be found in Snow et al 2019. Notably, β-HVP E6 increased the frequency of cells in S-phase before and after UV (Figure 3F). This is expected to promote mutagenesis and HPV replication as genomes are more at risk during replication and HPV requires replicating cells for their proliferation. β-HPV E6 also decreases POLη expression and repair complexes formation. This extends the known signaling impact of β-HPV E6 to the translesion synthesis (TLS) pathway. TLS protects replication forks from collapsing until UV damage is repaired. This prevents replication forks from collapsing into double stranded DNA breaks (DSBs). Attenuation of the TLS pathway provides an explanation for our prior observation that β-HPV E6 makes UV-induced DSBs more likely. These data were also summarized more thoroughly in the report for the second budget period.

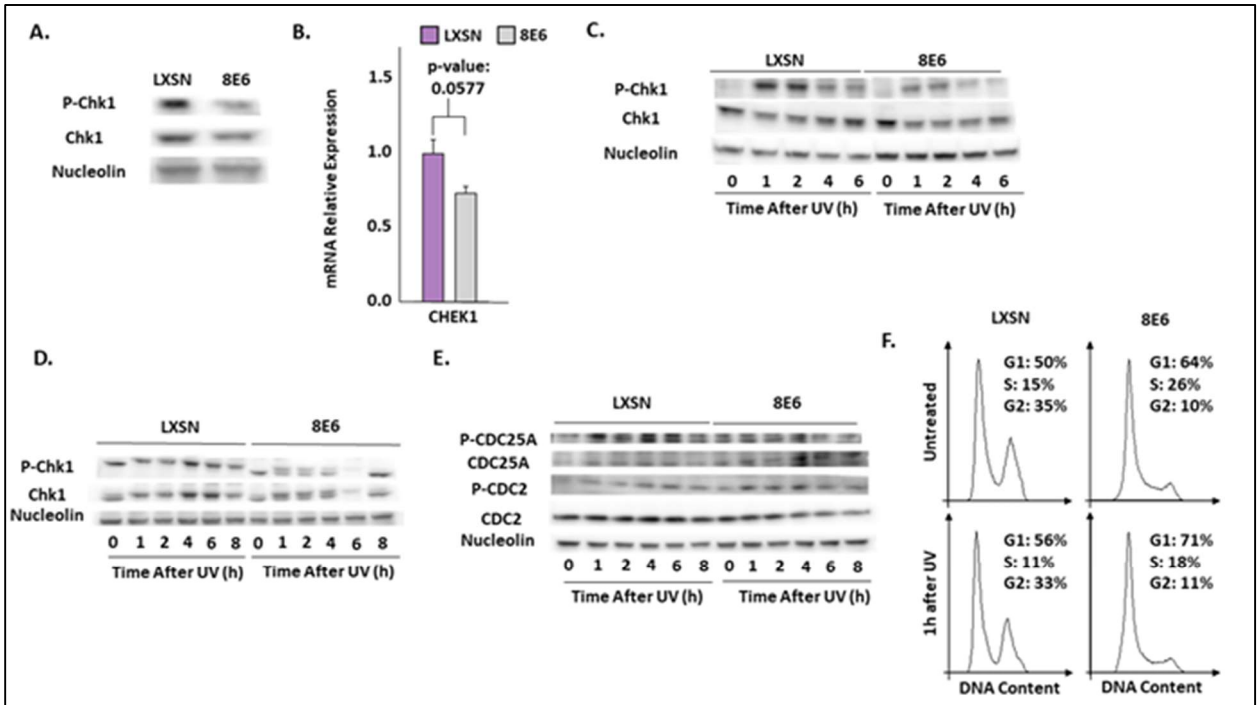

Figure 3: β-HPV 8E6 attenuates CHK1 phosphorylation. (A) Representative immunoblots of untreated hTERT HFKs with vector control (LXSN) and β-HPV 8E6 cell lines. Nucleolin was used as a loading control. (B) mRNA expression level of CHEK1 in vector control (LXSN) and β-HPV 8E6 expressing primary HFKs as measured by RT-qPCR and normalized towards the expression level of β-actin. Data shown in figures are the means of ±SE of three independent experiments. (C) Representative immunoblots of hTERT HFKs with vector control (LXSN) and β-HPV 8E6 harvested 0–6 h post 5mJ/cm2 UVR. Nucleolin was used as a loading control. (D) Representative immunoblots of primary HFKs with vector control (LXSN) and β-HPV 8E6 harvested 0–8 h post 5 mJ/cm2 UVR. Nucleolin was used as a loading control. (E) Representative immunoblots of hTERT HFKs with vector control (LXSN) and β-HPV 8E6 harvested 0–8 h post 5 mJ/cm2 UVR. Nucleolin was used as a loading control. (A, C–E) The numbers above bands represent quantification by densitometry. This is shown relative to untreated cells within the same cell line and normalized to the loading control. (F) Cell cycle analysis of hTERT HFKs with LXSN vector control and β-HPV 8E6 1 h post 5 mJ/cm2 UVR.

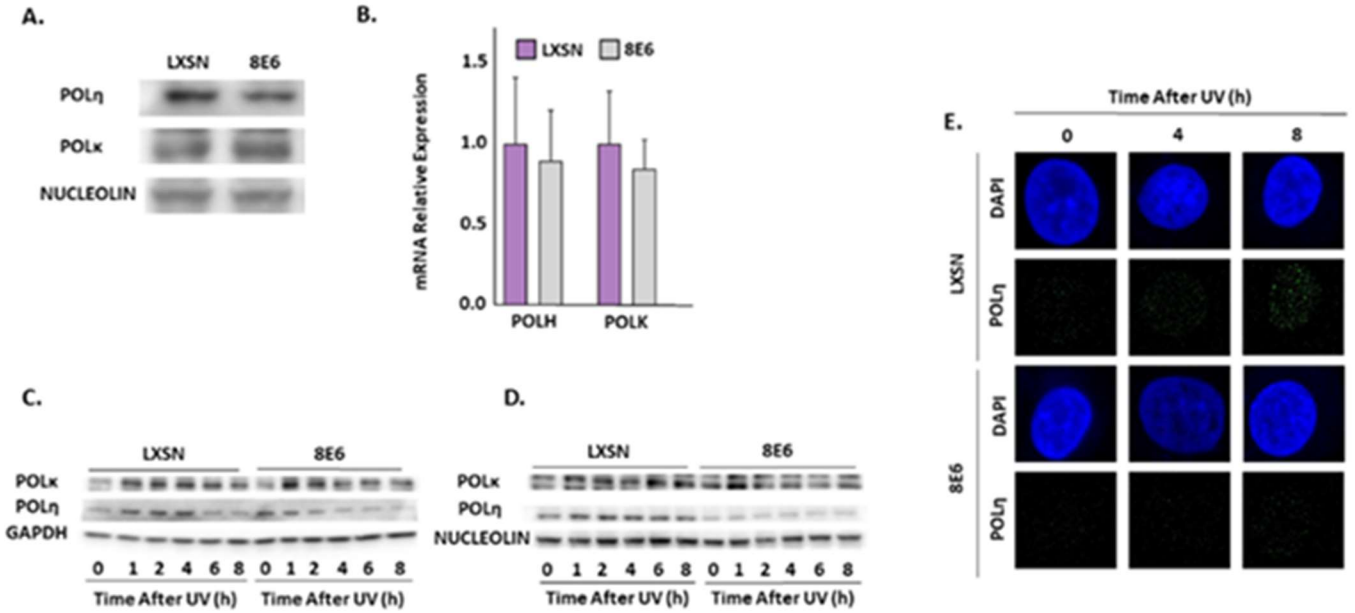

Figure 4: β-HPV 8E6 attenuates POLη abundance. (A) Representative immunoblots of untreated hTERT HFKs vector control (LXSN) and β-HPV 8E6 cell lines. Nucleolin was used as a loading control. (B) mRNA expression level of POLH and POLK in vector control (LXSN) and β-HPV 8E6 expressing primary HFKs as measured by RT-qPCR and normalized towards the expression level of β-actin. Data shown in figures are the means of ±SE of three independent experiments. (C) Representative immunoblots of hTERT HFKs with vector control (LXSN) and β-HPV 8E6 harvested 0–8 h post 5 mJ/cm2 UVR. GAPDH was used as a loading control. (D) Representative immunoblots of primary HFKs with vector control (LXSN) and β-HPV 8E6 harvested 0–8 h post 5 mJ/cm2 UVR. Nucleolin was used as a loading control. (A,C,D) The numbers above bands represent quantification by densitometry. This is shown relative to untreated cells within the same cell line and normalized to the loading control. (E) Representative immunofluorescence microscopy images of hTERT HFKs. POLη (green) and nuclei stained (blue) with DAPI.

<u>Subtask 4: Define the subcellular localization of XPA using immunofluorescence microscopy and immunoblots, before and after UV.</u>

We have shown that β-HPV E6 changes the subcellular localization of XPA by both microscopy and immunoblots of subcellular fractionations. These data were published in Snow et al 2019 and are summarized here in Figure 1E and Figure 5. They were also discussed in more detail in the report for budget period 1 and 2.

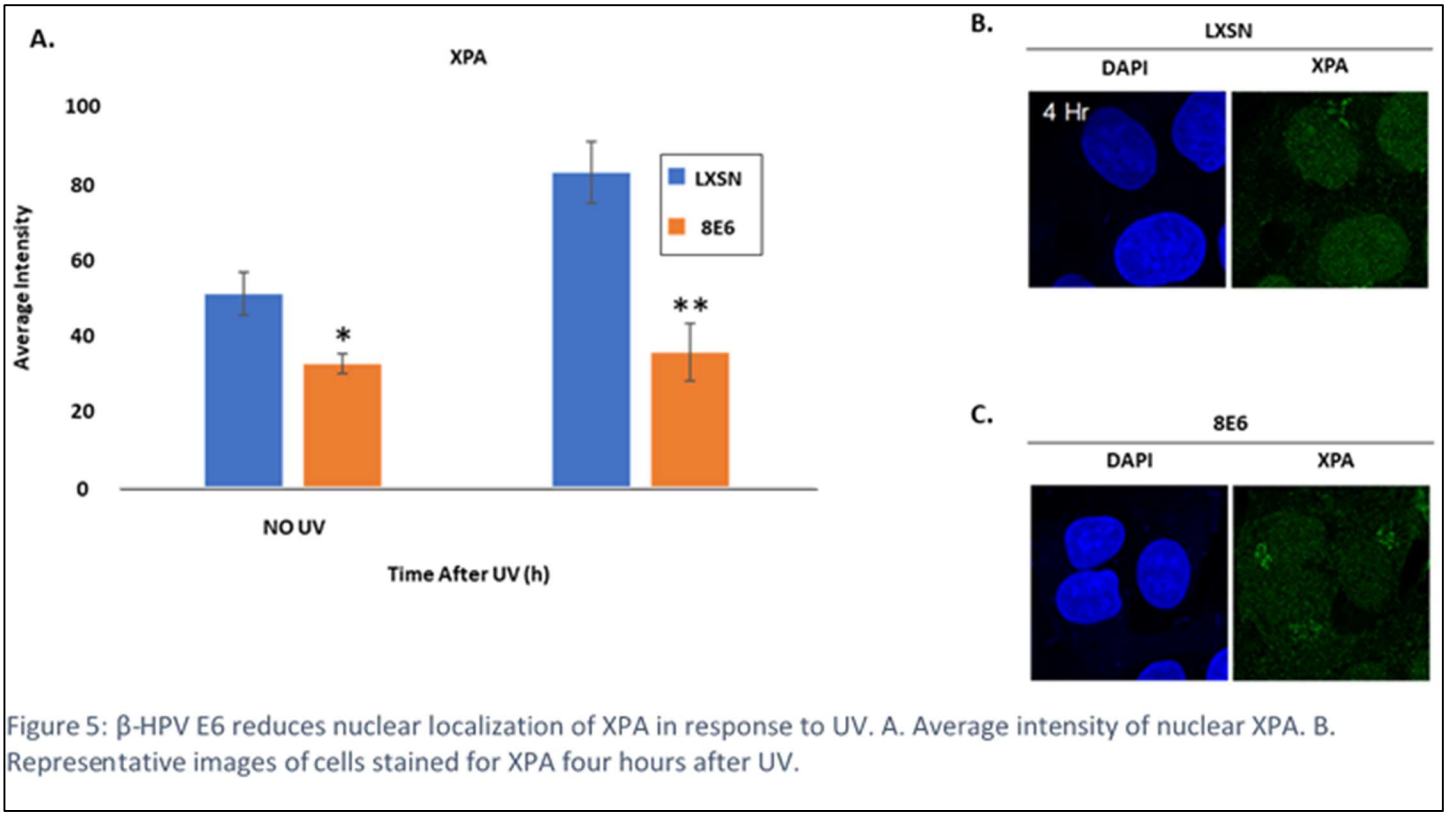

Figure 5: β-HPV E6 reduces nuclear localization of XPA in response to UV. A. Average intensity of nuclear XPA. B. Representative images of cells stained for XPA four hours after UV.

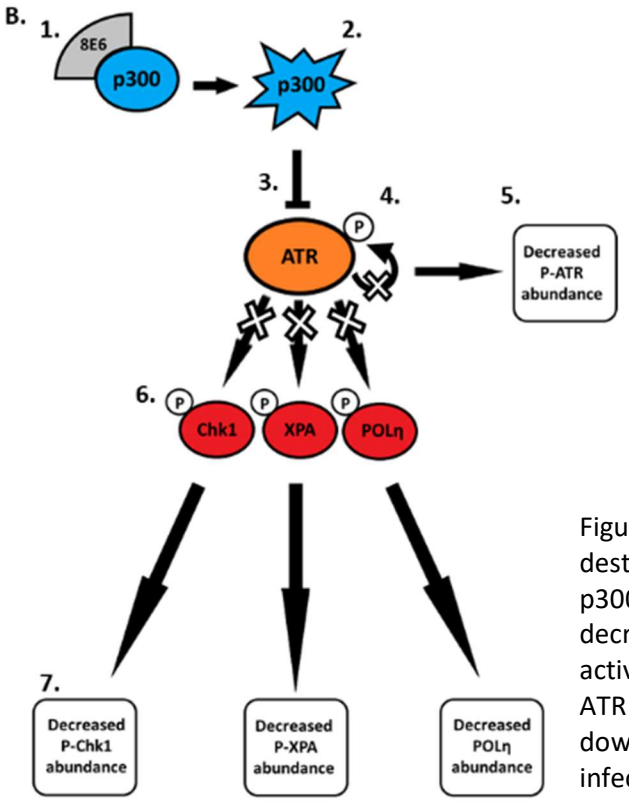

Figure 6: β-HPV 8E6 binds to p300 (1) causing p300 to become destabilized and subsequentially degraded (2). The decrease in p300 levels leads to less ATR transcription (3). This leads to a decrease in ATR autophosphorylation (4) resulting in less activated ATR available (5). Limited availability of activated ATR leads to a decrease in ATR-dependent phosphorylation of downstream proteins (6) causing changes in β-HPV 8E6 infected cells (7).

<u>Subtask 5: Determine if β-HPV E6 changes the abundance of other crosslink repair proteins using immunoblotting to detect the abundance of NER proteins before and after UV.</u>

This subtask was completed in budget period 2. We provide Figure 6 as a summary of the inhibition of ATR signaling discovered with the support from this grant.

Milestones Achieved:

Milestones Achieved: We will learn…

Milestones Achieved: We will …

(1) obtain oversight from HRPO necessary to avoid unintentional or unethical mistreatment of the human subjects.

This was completed during the first budget period.

(2) get the staff necessary to complete this aim.

This was completed during the first budget period.

(3) learn whether β-HPV E6 alters XPA phosphorylation and stabilization after UV and whether any changes are p300-dependent.

This was completed and published in budget period 3.

(4) learn whether β-HPV E6 acts through XPA- and ATR-dependent mechanisms to prevent crosslink repair.

We found that β-HPV E6 inhibits ATR activation and expression meaning that it ultimately represses crosslink repair by decreasing ATR expression and activation. An extension of this observation is that β-HPV E6 acts indirectly through XPA.

(5) learn whether β-HPV E6 changes the subcellular localization of XPA following UV and whether any changes are p300-dependent.

This was completed and published in budget period 3.

(6) learn if β-HPV E6 changes the abundance of NER proteins in cells with and without UV exposure.

This was completed and published in budget period 3.

Major Task 2: Determine the Extent to which β-HPV E6 Attenuates Non-Homologous End Joining Repair (NHEJ) of DNA Lesions

<u>Subtask 1: Define β-HPV E6's ability to disrupt DNApk expression and autophosphorylation by immunoblot.</u>

Most of this subtask was completed during the first and second budget periods. We have shown that β-HPV E6 decreases DNApk autophosphorylation in response to DNA damage. These data are currently

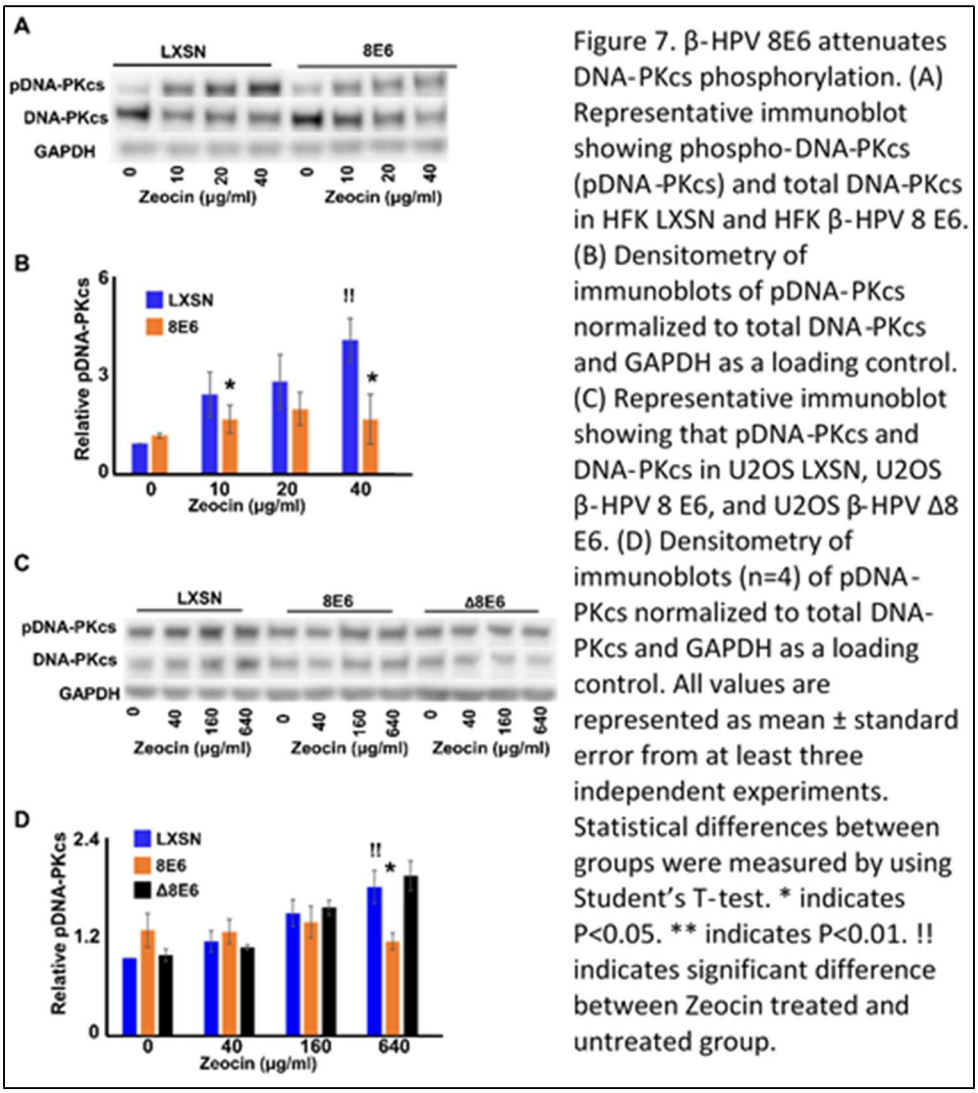

Figure 7. β-HPV 8E6 attenuates DNA-PKcs phosphorylation. (A) Representative immunoblot showing phospho-DNA-PKcs (pDNA-PKcs) and total DNA-PKcs in HFK LXSN and HFK β-HPV 8 E6. (B) Densitometry of immunoblots of pDNA-PKcs normalized to total DNA-PKcs and GAPDH as a loading control. (C) Representative immunoblot showing that pDNA-PKcs and DNA-PKcs in U2OS LXSN, U2OS β-HPV 8 E6, and U2OS β-HPV Δ8 E6. (D) Densitometry of immunoblots (n=4) of pDNA-PKcs normalized to total DNA-PKcs and GAPDH as a loading control. All values are represented as mean ± standard error from at least three independent experiments. Statistical differences between groups were measured by using Student's T-test. * indicates $P<0.05$. ** indicates $P<0.01$. !! indicates significant difference between Zeocin treated and untreated group.

under-review at the peer-reviewed journal Cancer (Hu, Bugbee and Wallace 2020). They have been repeated in Keratinocytes (HFKs) and U2OS cells (Figure 7).

<u>Subtask 2: Determine the effect of β-HPV E6 on the expression of NHEJ proteins by immunoblot.</u>

We have shown that β-HPV E6 does not decrease canonical NHEJ protein abundance by immunoblot. These data are also included in the submitted manuscript (Hu, Bugbee and Wallace 2020). See figure 8.

<u>Subtask 3: Define the ability of β-HPV E6 to impair NHEJ using a fluorescence based reporter system (traffic light reporter assay).</u>

We have taken two approaches to the previously reported problems with the broken flow cytometer at Kansas State University. First, we requested permission to buy a table top flow cytometer using funds from this grant. That request is currently being processed and evaluated. In the meantime, we converted a flow cytometry based assay for NHEJ to be detectable by immunoblot. Specifically, we use Cas9-directed endonucleases to make DSB cuts downstream of the GAPDH promoter and upstream of the CD4 open reading frame. When this is repaired by NHEJ, cells constitutively express CD4. We found this was detectable by immunoblot. To confirm that the CD4 expression was due to NHEJ, we used ATM and DNApk inhibitors (Ku55933 and NU7441, respectively). As expected, ATM inhibition increased NHEJ (determined by CD4 abundance), while DNApk inhibition abolished NHEJ. We then used this assay to demonstrate that β-HPV E6 decreased NHEJ in HFKs and U2OS cells. Further, at least some of this

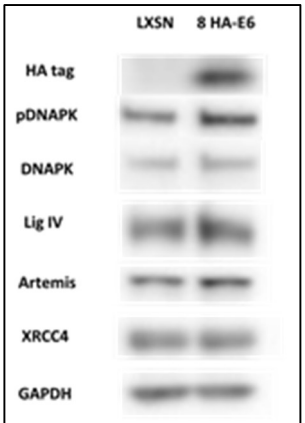

Figure 8: NHEJ protein abundance is not decreased by β-HPV E6.

inhibitory effect was p300-independent. These data are also included in the previously mentioned manuscript. Please see Figure 10)

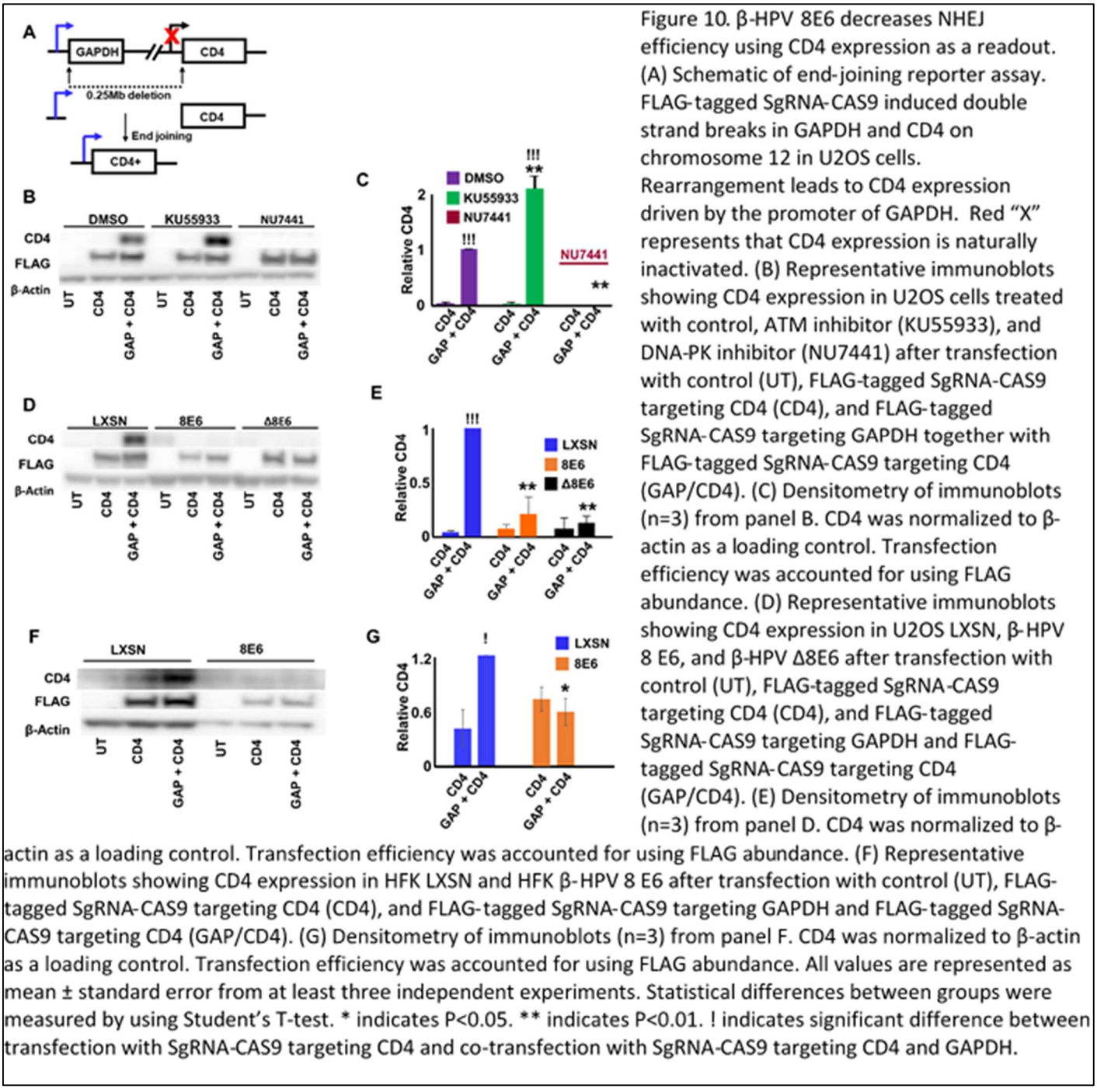

Figure 10. β-HPV 8E6 decreases NHEJ efficiency using CD4 expression as a readout. (A) Schematic of end-joining reporter assay. FLAG-tagged SgRNA-CAS9 induced double strand breaks in GAPDH and CD4 on chromosome 12 in U2OS cells. Rearrangement leads to CD4 expression driven by the promoter of GAPDH. Red "X" represents that CD4 expression is naturally inactivated. (B) Representative immunoblots showing CD4 expression in U2OS cells treated with control, ATM inhibitor (KU55933), and DNA-PK inhibitor (NU7441) after transfection with control (UT), FLAG-tagged SgRNA-CAS9 targeting CD4 (CD4), and FLAG-tagged SgRNA-CAS9 targeting GAPDH together with FLAG-tagged SgRNA-CAS9 targeting CD4 (GAP/CD4). (C) Densitometry of immunoblots (n=3) from panel B. CD4 was normalized to β-actin as a loading control. Transfection efficiency was accounted for using FLAG abundance. (D) Representative immunoblots showing CD4 expression in U2OS LXSN, β-HPV 8 E6, and β-HPV Δ8E6 after transfection with control (UT), FLAG-tagged SgRNA-CAS9 targeting CD4 (CD4), and FLAG-tagged SgRNA-CAS9 targeting GAPDH and FLAG-tagged SgRNA-CAS9 targeting CD4 (GAP/CD4). (E) Densitometry of immunoblots (n=3) from panel D. CD4 was normalized to β-actin as a loading control. Transfection efficiency was accounted for using FLAG abundance. (F) Representative immunoblots showing CD4 expression in HFK LXSN and HFK β-HPV 8 E6 after transfection with control (UT), FLAG-tagged SgRNA-CAS9 targeting CD4 (CD4), and FLAG-tagged SgRNA-CAS9 targeting GAPDH and FLAG-tagged SgRNA-CAS9 targeting CD4 (GAP/CD4). (G) Densitometry of immunoblots (n=3) from panel F. CD4 was normalized to β-actin as a loading control. Transfection efficiency was accounted for using FLAG abundance. All values are represented as mean ± standard error from at least three independent experiments. Statistical differences between groups were measured by using Student's T-test. * indicates P<0.05. ** indicates P<0.01. ! indicates significant difference between transfection with SgRNA-CAS9 targeting CD4 and co-transfection with SgRNA-CAS9 targeting CD4 and GAPDH.

<u>Subtask 4: Determine the ability of β-HPV E6 to prevent NHEJ repair foci formation by immunofluorescence microscopy.</u>

This subtask was completed during budget period 2. During the previous reporting period, we also reported that β-HPV E6 significantly increased the presence of pDNApk and RAD51 co-localization at DSBs. These co-localized foci are likely catastrophic for cells because NHEJ (indicated by pDNApk) removes the type of single strand overhangs that must occur for RAD51 foci to exist. This is predicted to

result in large deletions. We are currently using the Cas9 technology described in Figure 10 to create a DSB at a known genomic location and using targeted deep sequencing to define the mutagenic consequences of β-HPV E6 expression at a DSB.

Finally, we found that β-HPV E6 attenuated ATM activation and phosphorylation of ATM target proteins in response to UV. These data were included in a recently accepted manuscript (Snow et al 2019) and are shown in Figure 11.

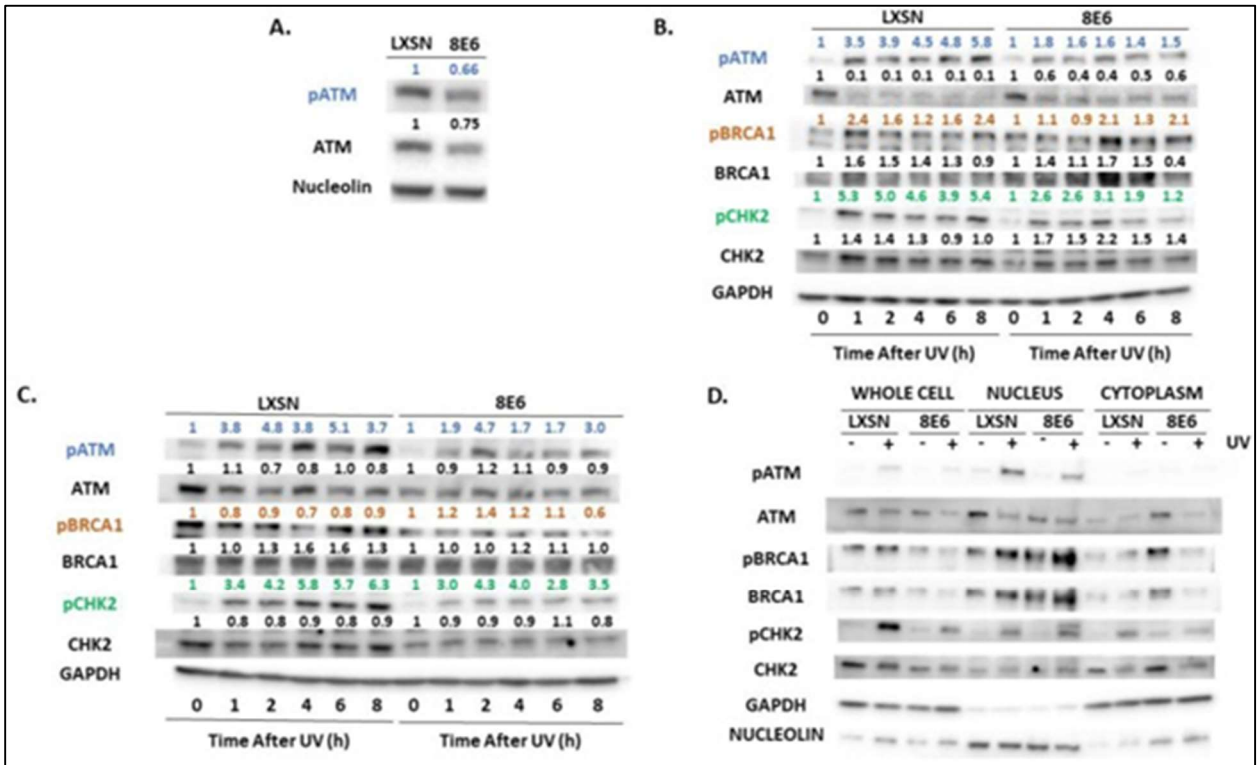

Figure 11: β-HPV 8E6 attenuates ATM activation. (**A**) Representative immunoblots of untreated hTERT HFKs with vector control (LXSN) and β-HPV 8E6 cell lines. Nucleolin was used as a loading control. (**B**) Representative immunoblots of hTERT HFKs with vector control (LXSN) and β-HPV 8E6 harvested 0–8 h post 5 mJ/cm^2 UVR. GAPDH was used as a loading control. (**C**) Representative immunoblots of primary HFKs with vector control (LXSN) and β-HPV 8E6 harvested 0–8 h post 5 mJ/cm^2 UVR. GAPDH was used as a loading control. (**A–C**) The numbers above bands represent quantification by densitometry. This is shown relative to untreated cells within the same cell line and normalized to the loading control. (**D**) Subcellular fractionation of hTERT HFKs with vector control (LXSN) and β-HPV 8E6 cell line lysates harvested 6 h post exposure to 5 mJ/cm^2 UVR were observed via immunoblot. GAPDH was used as a cytoplasmic loading control and Nucleolin was used as a nuclear loading control.

Milestones Achieved: We will…

(1) *learn the extent to which β-HPV E6 prevents DNApk expression and activation as well as whether this phenotype is p300-dependent.*

Thus this milestone was met and surpassed. We found p300-dependent attenuation of DNApk activation and p300-indpendent attenuation of NHEJ.

(2) *learn whether β-HPV E6 decreases the abundance of NHEJ proteins and whether these changes are dependent on p300 degradation.*

This milestone was achieved during the first budget period.

(3) *learn whether β-HPV E6 inhibits the repair of double strand breaks by the non-homologous end joining pathway as well as the role of p300 in any inhibition.*

Unfortunately, technical difficulties beyond our control or ability to resolve (broken flow cytometer equipment) have prevented this milestone from being met as described. We have achieved the desired result using an alternative method, but still need to conduct the originally proposed experiment.

(4) *learn the extent to which β-HPV E6 prevents non-homologous end joining proteins from forming repair foci and the p300-dependence of any such phenotype.*

This goal was met and surpassed. Further, relevant data has been published in a peer reviewed journal.

Specific Aim 2: Determine the breadth and mechanism of β-HPV E6's Hippo Pathway (HP) Inhibition

We are preparing a manuscript for submission to the Journal of Virology based on the data from Specific Aim 2. This is the highest ranked journal in virology. We expect to submit the manuscript in early Fall.

Major Task 1: Defining β-HPV E6's inhibition of the HP

Subtask 1: Obtain HRPO approval to isolate keratinocytes from neonatal foreskins.

This was completed during the first budget period.

Subtask 2: Determine the impact of β-HPV E6 on the phosphorylation of HP proteins by immunoblot.

This was completed during the first budget period.

Subtask 3: Define the subcellular localization of HP proteins in cells by immunofluorescence microscopy.

This was completed during the first budget period.

Subtask 4: Determine the extent to which β-HPV E6 promotes TEAD promoter activity by luciferase reporter assay.

This task was completed during the third budget period and published in the Journal of Virology (Dacus et al 2020) along with the data described in Subtasks 1-4. Relevant data for the other three subtasks was

provided in the previous reporting period. Figure 12 contains the relevant data.

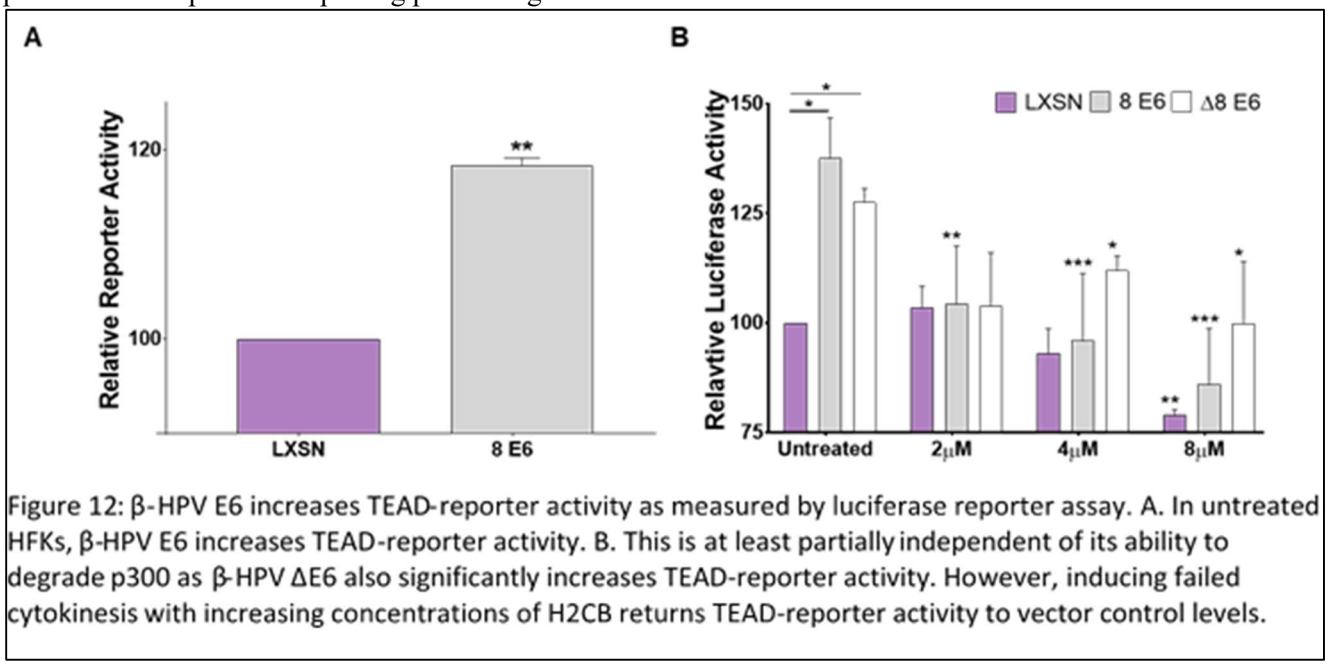

Figure 12: β-HPV E6 increases TEAD-reporter activity as measured by luciferase reporter assay. A. In untreated HFKs, β-HPV E6 increases TEAD-reporter activity. B. This is at least partially independent of its ability to degrade p300 as β-HPV ΔE6 also significantly increases TEAD-reporter activity. However, inducing failed cytokinesis with increasing concentrations of H2CB returns TEAD-reporter activity to vector control levels.

Subtask 5: Define the prevalence of multipolar mitosis and micronuclei formation in β-HPV E6 expressing cells by immunofluorescence microscopy.

As reported for budget period two, our data supports the idea that β-HPV E6 promotes multipolar mitosis and demonstrates that micronuclei are increased by β-HPV E6. We are currently limited in our ability to detect multipolar mitoses because of the less than ideal frequency of mitotic cells in vector control HFKs. To combat this restriction, we are actively working out the conditions to increase the frequency of cells in mitosis by employing a double thymidine block.

Milestones Achieved: We will…

(1) obtain oversight from HRPO necessary to avoid unintentional or unethical mistreatment of the human subjects.

This was completed during the first budget period.

(2) learn whether β-HPV E6 alters the phosphorylation of Hippo pathway proteins and if any such changes are p300-dependent.

This was completed during the first budget period.

learn whether β-HPV E6 prevents the subcellular localization of Hippo proteins induced by failed cytokinesis and if any such inhibition is p300-dependent

This was completed during the first budget period.

(3) learn whether β-HPV E6 increase TEAD promoter activity after failed cytokinesis and if they can whether or not it is a p300-dependent phenotype.

We completed this task, showing that TEAD promoter activity was increased in basal cells in a p300 dependent manner by β-HPV E6 however after failed cytokinesis TEAD promoter activity was

decreased when β-HPV E6 was expressed. We have independently confirmed these results using rtPCR and an *in silico* screen.

(4) learn whether β-HPV E6 increases the likelihood of multipolar mitosis and micronuclei formation after failed cytokinesis as well as the role of p300-degradation in any such increases.

This subtask is mostly complete. We have observed an increase in micronuclei and aneuploidy associated with β-HPV E6 expression. We had difficulty detecting mitotic cells of any kind and adjusting our experimental design to observe cells arrested in mitosis to circumnavigate this issue.

Major Task 2: Determine the mechanism of β-HPV E6's inhibition of the HP.

Subtask 1: Define the abundance of HP proteins by immunoblot. This will be done in vector control, β-HPV E6 and β-HPV ΔE6 expressing cells.

This was completed during the first budget period.

Subtask 2: Determine if p300 is involved in β-HPV E6-induced changes to the abundance of HP proteins using β-HPV ΔE6 mutant and immunoblot.

This was completed during the first budget period.

Subtask 3: Determine if p300 is present at HP gene promoters by chromatin immunoprecipitation and qPCR.

We completed the planned qPCR experiments but did not see any change in HP gene expression (Fiugre 22). As a result, we did not continue with the planned chromatin immunoprecipitation experiment.

Subtask 4: Perform an unbiased analysis of β-HPV E6's effect on the HP using HP PCR Array purchased from Qiagen and validated by qPCR as well as immunoblot.

This was completed during the first budget period.

Milestones Achieved: We will learn…

(1) whether β-HPV E6 changes the abundance of select HP proteins by destabilizing p300.

This was completed during the first budget period.

(2) whether p300 is at the promoters of HP genes and whether β-HPV E6 changes the abundance of p300 at these promoters.

Our rtPCR data demonstrate that HP gene expression is not decreased by β-HPV E6. As a result, there was no value in determining the mechanism of β-HPV E6's non-existent modification of HP expression. We do see an increase in LATS2 protein abundance suggesting an increase in protein stability.

(3) the comprehensive impact of β-HPV E6 on HP gene expression.

This was completed during the first budget period.

Specific Aim 3: Determine how β-HPV E6 induces p300-independent inhibition of DNA repair.

Major Task 1: P300-Independent Disruption of DNA Crosslink Repair

Subtask 1: Finish Onboarding for Dalton Dacus and obtain HRPO approval to isolate keratinocytes from neonatal foreskins.

This was completed during the first budget period.

Subtask 2: Define ICL-repair in HT1080 cells where β-HPV cannot degrade p300 by immunofluorescence microscopy using antibodies against UV-induced ICLs.

As discussed in the report for budget period 2, we have shifted the focus of this subtask to better characterizing the ability of β-HPV E6 to induce aneuploidy. This has been a very fruitful effort, leading to a recently accepted manuscript in the peer-reviewed journal, Virology (Dacus, Riforgiate and Wallace 2020). In this manuscript, we show that that β-HPV E6 becomes particularly capable of mitigating the long term anti-proliferative effects of failed cytokinesis when the viral gene is expressed in cells immortalized by telomerase activity. This does not affect β-HPV E6's ability to alter Hippo pathway signaling, but does allow cells to maintain longer term proliferation and accumulate aneuploidy. The relevant data for this work is provided in figures 13-17.

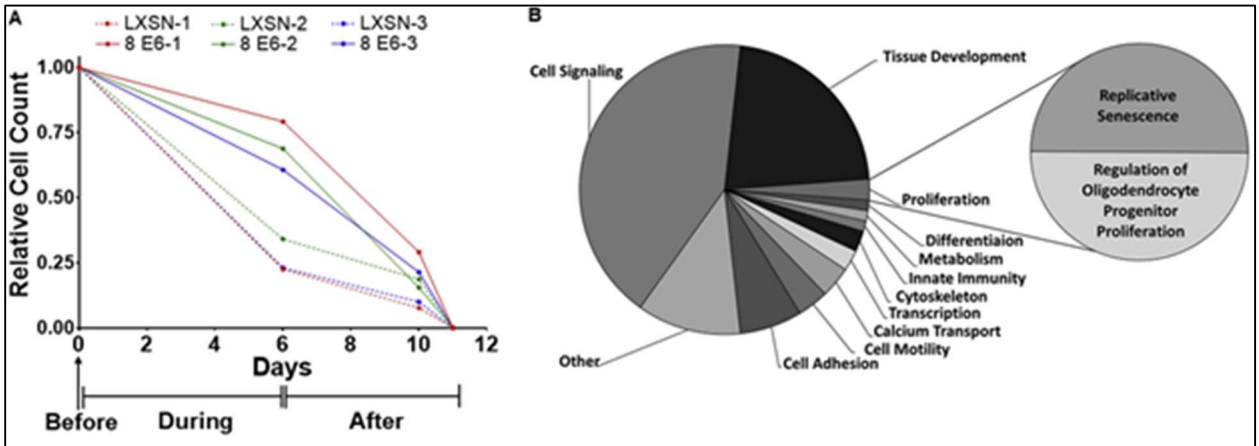

Fig. 13: H2CB-induced failed cytokinesis prevents long-term proliferation. (A) Three growth curves (biological replicates) comparing HFK LXSN and β-HPV 8E6 cells before, during, and after 6 days of H2CB exposure in 6-well tissue culture plates. HFK LXSN (dashed) and β-HPV 8E6 (solid) data with the same color and number (red, 1; green, 2; and blue, 3) were treated in parallel. (B) Two charts representing GO analysis of common mutations in cSCC. The larger chart on the left represents nodes of similar GO: biological process terms. The smaller chart represents the two GO: biological process terms within the "Proliferation" node. TERT expression allows β-HPV 8E6 HFKs growth after H2CB-induced failed cytokinesis.

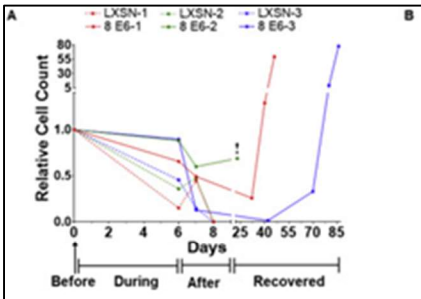

B

Cell Type	% Recovered
LXSN	0% (3/3)
8 E6	0% (3/3)
LXSN + *TERT*	~11% (1/9)
8 E6 + *TERT*	100% (9/9)

Fig. 14. TERT expression promotes recovery from failed cytokinesis. (A) Three growth curves (biological replicates) comparing TERT-HFK LXSN and β-HPV 8E6 cells before, during, after, and recovered from 6 days of H2CB exposure in 6-well tissue culture plates. LXSN (dashed) and β-HPV 8E6 (solid) data with the same color and number (red, 1; green, 2; and blue, 3) were treated in parallel. ! signifies the premature end of the long-term cultivation due to bacterial contamination. (B) Percent of HFK and TERT-HFK cells capable of long-term growth after 6 days in H2CB.

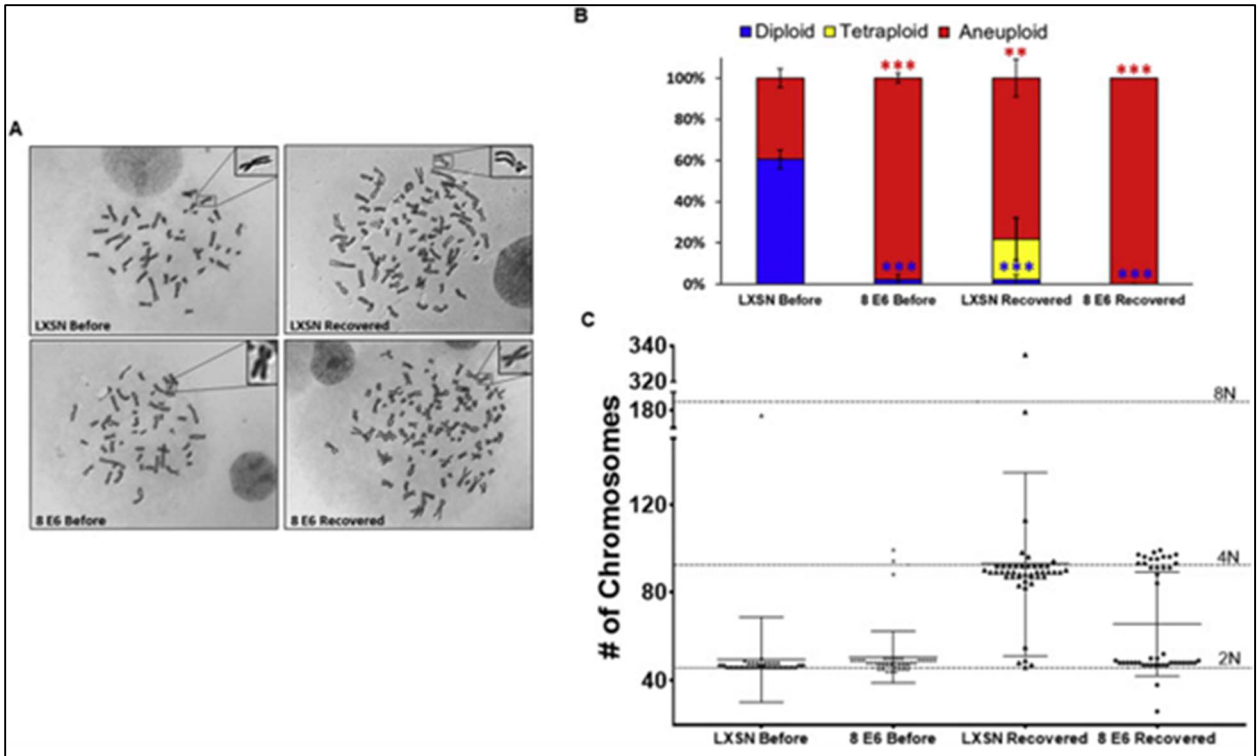

Fig. 15. β-HPV 8E6 and cytokinesis failure induce changes in ploidy. (A) Representative images of metaphase spreads. Insert on the top-right corner shows a magnified chromosome. (B) Relative frequency of diploidy (blue), tetraploidy (yellow), and aneuploidy (red) before H2CB treatment and once cells recovered. Red and blue asterisks denote a significant difference from 'LXSN Before' for aneuploidy and diploidy, respectively. (C) Graphical presentation of the distribution of the number of chromosomes among ≥ 45 cells analyzed by metaphase spreads (before or recovered from 6 days of H2CB exposure). Horizontal-dotted lines represent 46 (2 N), 92 (4 N), or 184 (8 N) chromosomes. ** denotes significant difference between indicated samples $p \leq 0.01$, *** denotes $p \leq 0.001$ (Student's t-test).

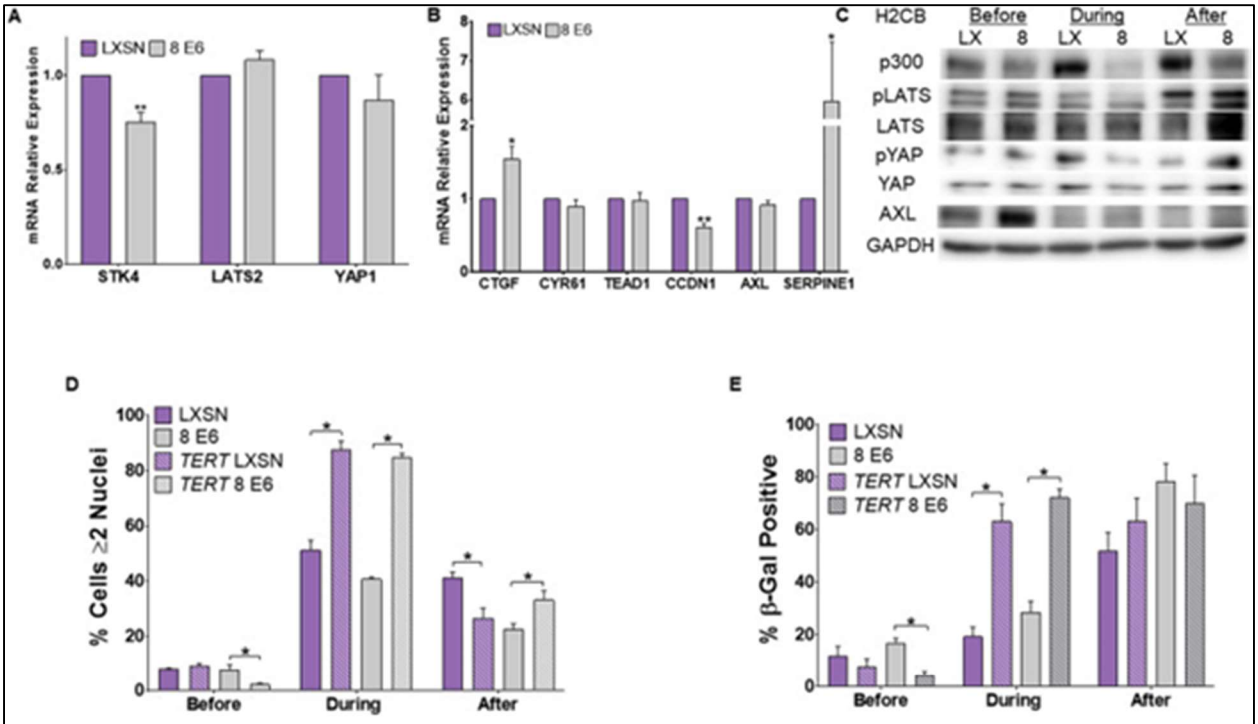

Fig. 16: Responses to H2CB-induced failed cytokinesis in TERT-HFK. Expression of (A) canonical HP genes and (B) TEAD-regulated genes in TERT-HFKs measured by RT-qPCR and normalized to β-actin mRNA. (C) Representative immunoblot of HP proteins in TERT-HFK cells before, during, and after H2CB exposure. (D) Quantification of cells with more than 1 nucleus before, during, and after H2CB exposure. (E) Quantification of SA β-Gal staining in HFK cells vs TERT-HFK before, during, and after H2CB treatment. Figures depict means ± standard error of the mean. n ≥ 3. * denotes significant difference between indicated samples * denotes $p \leq 0.05$, ** denotes $p \leq 0.01$. (Student's t-test).

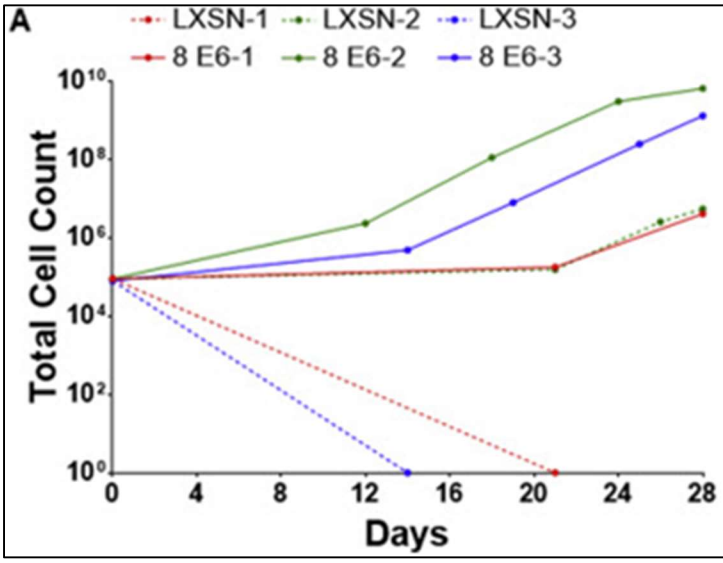

Fig. 17. TERT-HFK recovering from H2CB-induced cytokinesis failure. (A) Three growth curves (one of 2 additional 10 cm biological replicates) comparing TERT-HFK-LXSN and -β-HPV 8E6 once recovered from 6 days of H2CB exposure in 10 cm tissue culture plates. LXSN (dashed) and β-HPV 8E6 (solid) data with the same color and number (red, 1; green, 2; and blue, 3) were treated in parallel.

Subtask 3: Define ICL-repair when exogenous expression of degradation resistant p300 prevents β-HPV E6 from degrading p300 using immunofluorescence microscopy with antibodies against UV-induced ICLs.

As noted in the previous annual report and prior sections of this one, we are now the characterizing micronuclei found in cells expressing β-HPV E6. Specifically, we found that micronuclei caused by β-HPV E6 are on average smaller than those in control cells (Figure A). This is independent of p300 degradation and shared with between multiple β-HPV E6 proteins. In contrast, β-HPV E6 does not change the frequency of H2AX staining or the intensity of DAPI staining (Figure B and C). Finally, we determined if β-HPV E6 changed the frequency of centromeres in micronuclei using cenpA as a marker for centromeres. There was a modest p300-dependent increase in centromere staining that accompanied β-HPV E6 expression (Figure D).

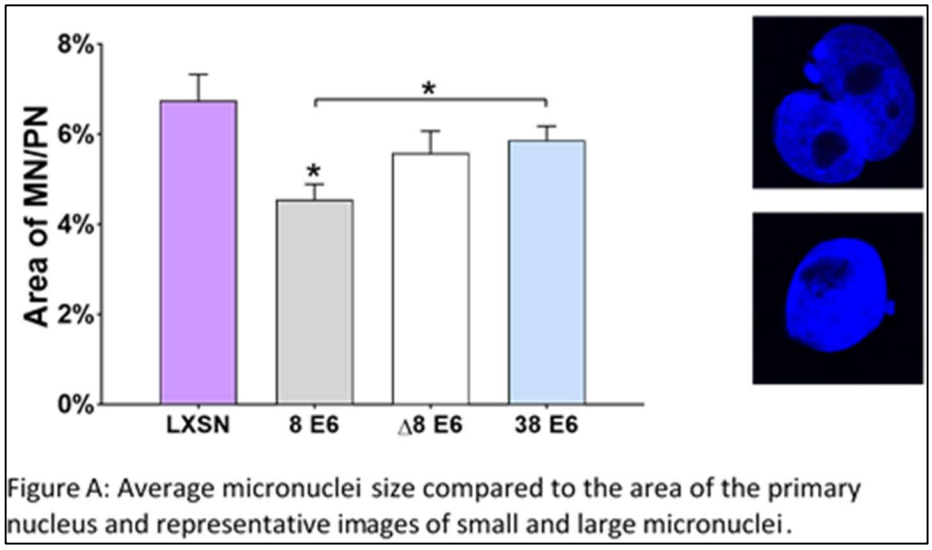

Figure A: Average micronuclei size compared to the area of the primary nucleus and representative images of small and large micronuclei.

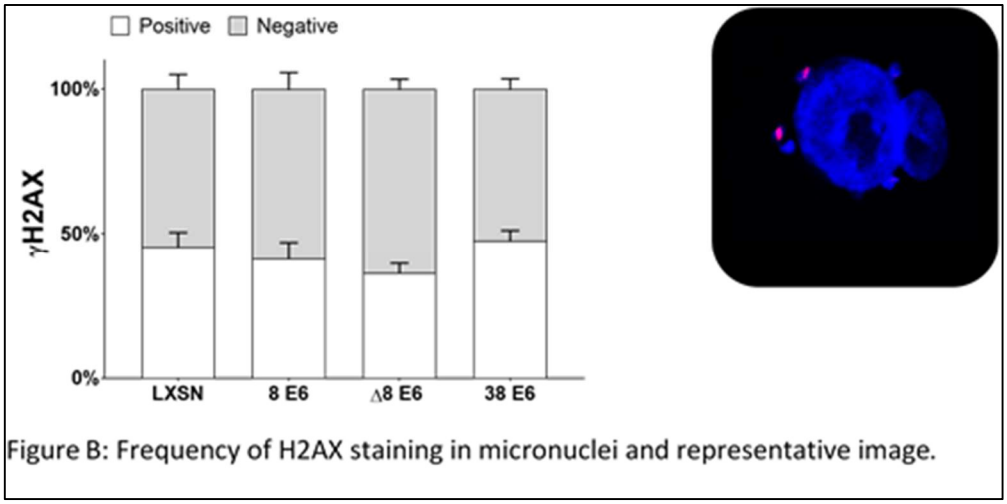

Figure B: Frequency of H2AX staining in micronuclei and representative image.

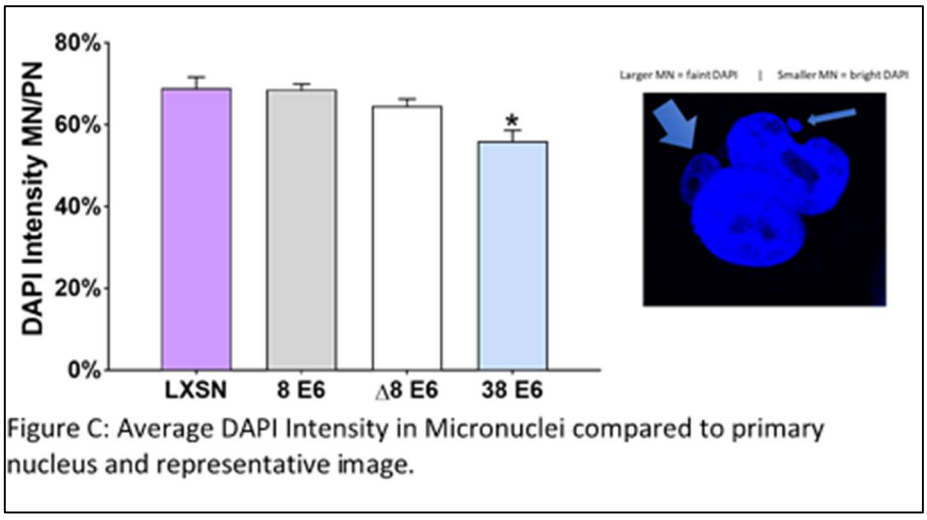

Figure C: Average DAPI Intensity in Micronuclei compared to primary nucleus and representative image.

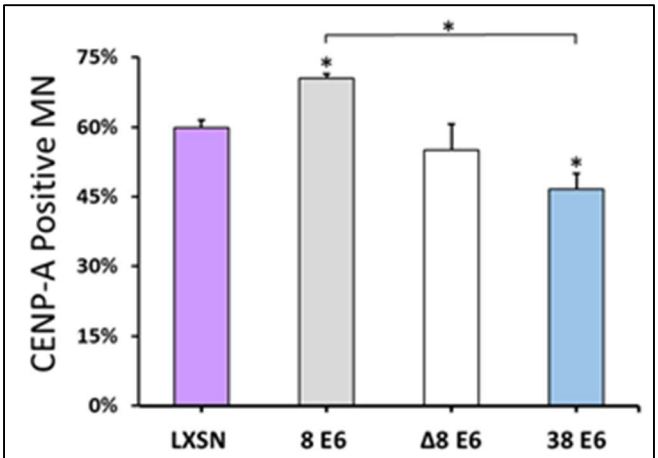

Figure D: Frequency of CENP-A staining in micronuclei.

Subtask 4: Determine if β-HPV E6 can further impede crosslink repair in cells where ATR and p300 are targeted for RNAi mediated degradation (Assayed by immunofluorescence microscopy).

We have completed and executed the MTA (Kansas State University and International Agency for Research on Cancer) that allowed us to obtain cells expressing other genes from other β-HPVs. The ongoing pandemic delayed this exchange but the cells were recently obtained and we are beginning to define aneuploidy and micronucleation in them.

Milestones Achieved: We will…

(1) obtain oversight from HRPO necessary to avoid unintentional or unethical mistreatment of the human subjects.

This was completed during the first budget period.

(2) get the staff necessary to complete this aim.

This was completed during the first budget period.

(3) learn the extent to which β-HPV E6 prevents ICL repair through p300-independent mechanisms.

Our shift in focus has been very fruitful, resulting in the manuscript described above. We consider ourselves to have achieved and surpassed this milestone.

(4) learn the extent to which β-HPV E6 prevents ICL repair through p300- and ATR-independent mechanisms.

We have obtained the materials to conduct the work described in subtask four and are eagerly pursuing this end.

Major Task 2: Determine the mechanism of β-HPV E6's p300-independent inhibition of DNA crosslink repair.

As described above, we have refocused our attention. Remaining within the framework of our proposal, we have extending the efforts of AIM 2 by defining how β-HPV E6 expressing cells recover from failed cytokinesis. These data were combined with data from Major Task 1 and published in Dalton Riforgiate and Wallace 2020.

Subtask 1: Define the extent to which BCL6 inhibition prevents β-HPV E6 from preventing DNA crosslink repair by immunofluorescence microscopy and chemical inhibition and RNAi-mediated knockdown of BCL6.

We accomplished our goal of understand how β-HPV E6 expressing cells recovered from H2CB-induced failed cytokinesis and identified a common cellular mutation that acted synergistically with β-HPV E6 to promote recovery. These data have been described in preceding sections and as mentioned can be found in the peer-reviewed manuscript Dacus, Riforgiate and Wallace 2020. This was incorporated in Subtasks 1-4 of this Major task.

Subtask 2: Determine if β-HPV E6 interacts with ATR/ATRIP using Co-immunoprecipitation reactions.

See above

Subtask 3: Determine if BCL6 is acting as a transcriptional repressor of ATR expression using chromatin immunoprecipitation.

See above

Subtask 4: Define the impact of β-HPV E6 on BCL6 protein stability and transcription using immunoblots and qPCR.

See above

Subtask 5: Identify novel β-HPV E6 interacting proteins by mass spectrometry with validation by co-immunoprecipitation.

We have continued our efforts to understand p300-independent activities of β-HPV E6 with regard to DSB repair. Specifically building off of the observation that β-HPV ΔE6 attenuated, we have defined a p300-independent mechanism of NHEJ inhibition. β-HPV ΔE6 and β-HPV E6 both prevent the induction of a repair complex essential for NHEJ. Namely, XRCC4 foci are not induced by the DSBs created from zeocin exposure. These data are shown in figure 18 and are under-review in the journal Cancers. In this figure we also show that DNA-PK mediated phosphorylation is attenuated by β-HPV E6, but this phenotype was p300-dependent.

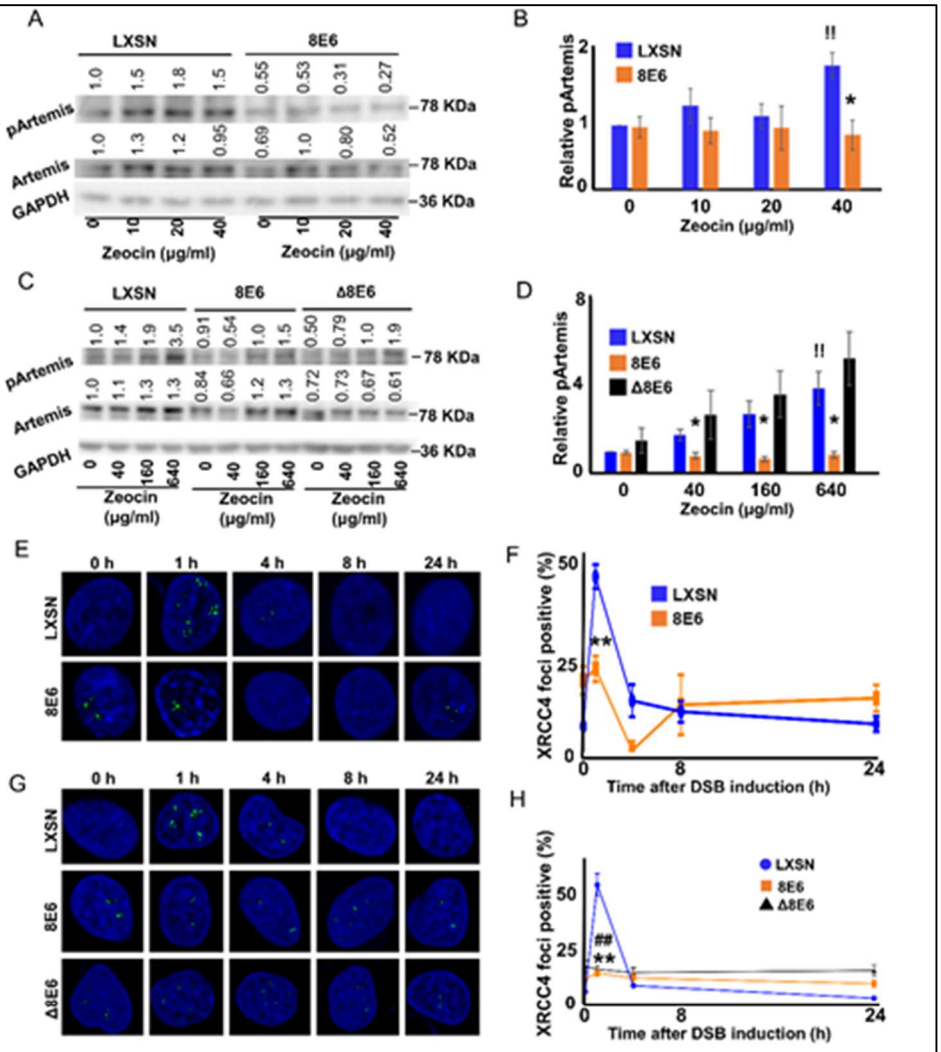

Figure 5. β-HPV 8E6 decreases pDNA-PKcs target proteins pArtemis abundance and XRCC4 foci formation. (A) Representative immunoblot showing pArtemis and total Artemis in HFK LXSN and HFK β-HPV 8 E6. (B) Densitometry of immunoblots (n=4) of pArtemis normalized to total Artemis and to GAPDH as a loading control. (C) Representative immunoblot showing that pArtemis and total Artemis in U2OS LXSN, U2OS β-HPV 8 E6, or U2OS β-HPV Δ8 E6. (D) Densitometry of immunoblots (n=4) of pArtemis normalized to total Artemis and to GAPDH as a loading control. (E) Representative images of XRCC4 foci in HFK cell lines 0-24 hours following Zeocin exposure. (F) Percentages of XRCC4 foci positive (>2) HFK cells following DSB induction. (G) Representative images of XRCC4 foci in U2OS cell lines 0-24 hours following Zeocin exposure. (H) Percentages of XRCC4 foci positive (>2) U2OS cells following DSB induction. All values are represented as mean ± standard error from at least three independent experiments. Statistical differences between groups were measured by using Student's T-test. * indicates P<0.05. ** indicates P<0.01. !! indicates significant difference between Zeocin treated and untreated group. ## indicates significant difference between U2OS β-HPV Δ8 E6 and control.

Milestone(s) Achieved: We will learn…

(1) whether β-HPV E6 inhibits ICL repair through BCL6 inhibition.

We have not been able to complete the originally proposed milestones, because our BCL6 result produced a phenotype that was too small/variable for further characterization. To honor our commitment to the award, we have instead extended our work in two ways to identify β-HPV E6's p300-dependent and -independent genome destabilizing activity. We have published a manuscript describing how β-HPV E6 acts synergistically with telomerase activation to promote long term proliferation after failed cytokinesis. Second, we identified β-HPV E6's p300-independent ability to impair NHEJ and a mechanism for this attenuation (inhibition of XRCC4 foci formation).

(2) whether β-HPV E6 interacts with ATR/ATRIP.

See above.

(3) whether β-HPV E6 induced increases in BCL6 result in transcriptional repression of ATR.

See above.

(4) the extent to which β-HPV E6 chances BCL6 protein stability.

See above.

(5) the extent to which β-HPV E6 changes BCL6 transcription.

See above.

(6) the identity of novel β-HPV E6 interacting proteins.

See above.

- **What opportunities for training and professional development has the project provided?**
  - Both graduate students funded in this project have twice presented their work at an international conference (DNA tumor virus meeting). Dalton Dacus also presented his work at a virtual assembly of the American Society for Virology. The PI received significant mentoring from Drs. Laimins, Gao and Clem. Further, he was invited to give 15 seminars on his work at Universities across the country and internationally.
- **How were the results disseminated to communities of interest?**
  - Our group is highly engaged in the dissemination of our findings to the local regional and international communities of interest.
  - We have a very active twitter account (@wallacehpvlab) that we use to communicate our work to a network of followers.
  - We have engaged over 100 community members in hands-on tours of our lab during each reporting period, prior to COVID-19. These outreach activities are not available now. We have however continued our efforts to use our proximity to a US military base (Fort Riley) to facilitate engagement with the military health community. Specifically, we spoke with Drs. Julia Gaston and Colleen Mitchel. We cannot be certain as no identifying information is collected from our guests.

        - Before COVID-19 limited our outreach efforts, we participated in events organized by the K-State Office for the Advancement of Women in Science and Engineering to promote the participation of women in science (Girls Reaching Our World and EXploring sCIence, Technology and Enginnering).
        - The PI also gave a public lecture as part of the local "Science on Tap" series.
    - **What do you plan to do during the next reporting period to accomplish the goals?**
        - Dr. Wallace will continue his career development adapting to the realities presented by COVID-19. Specifically, we will engage with his mentors virtually and continue to grow his connections by presenting at virtual conferences.
        - We are in the process of implementing two next gen sequencing based experiments related to this grant but supported from outside sources of funding.
        - We expect to publish at least one additional paper from the work supported here.
        - We have resubmitted our application to the American Cancer Society and hope for positive news later this month. An R01 grant application to the National Institutes of Health will be submitted on topics relevant to the work funded here.
4. **IMPACT:** *Describe distinctive contributions, major accomplishments, innovations, successes, or any change in practice or behavior that has come about as a result of the project relative to:*
    - **What was the impact on the development of the principal discipline(s) of the project?**
        - β-HPV infections are believed to cause cancer by increasing the ability of sunlight and radiation to cause skin cancer. We have hypothesized that they do this by preventing the cells they infect from properly responding to damaged DNA. In this period, we have published five manuscripts (Three of these were relevant to this funding). The data presented in these papers support this idea by showing the proteins from this virus destabilize the host genome. These results are important for the military community in particular for two reasons. 1. Military service is a risk factor for skin cancers. 2. Military service is associated with increased sun and radiation exposure.
    - **What was the impact on other disciplines?**
        - Our work has broad impacts as it helps clarify the role of p300 in signaling pathways known to suppress tumors. This includes investigators studying the Hippo Pathway, chromosome segregation and maintenance, double strand break repair, cell cycle regulation and crosslink repair.
    - **What was the impact on technology transfer?**
        - *The overall goal of this project is to determine the oncogenic potential of β-HPV infections so that anti-viral drugs or vaccines can be developed. Our results remain supportive of this goal.*

- **What was the impact on society beyond science and technology?**
  - Efforts to prevent cancer will always have the potential to impact society at large. Our work remains impactful in this manner.
  - Our outreach and engagement efforts also help grow lay knowledge of science and encourage participation in science by underrepresented members of society

5. **CHANGES/PROBLEMS:** *The Project Director/Principal Investigator (PD/PI) is reminded that the recipient organization is required to obtain prior written approval from the awarding agency Grants Officer whenever there are significant changes in the project or its direction. If not previously reported in writing, provide the following additional information or state, "Nothing to Report," if applicable:*
   - **Changes in approach and reasons for change**
     - *We have continued and expanded the new course described in our report for budget period 2.*
   - **Actual or anticipated problems or delays and actions or plans to resolve them**
     - We have requested permission to buy a bench top flow cytometry sorter that we reported as broken in budget period 2. We are in the process of getting a quote for this piece of equipment.
   - **Changes that had a significant impact on expenditures**
     - none
   - **Significant changes in use or care of human subjects, vertebrate animals, biohazards, and/or select agents**
     - Nothing to report
   - **Significant changes in use or care of human subjects**
     - Nothing to report
   - **Significant changes in use or care of vertebrate animals.**
     - Nothing to report
   - **Significant changes in use of biohazards and/or select agents**
     - Nothing to report
6. **PRODUCTS:** *List any products resulting from the project during the reporting period. If there is nothing to report under a particular item, state "Nothing to Report."*
   - **Publications, conference papers, and presentations**.
     - **Journal publications.**

1. Dacus D, Riforgiate E, Wallace NA. “β-HPV 8E6 Combined with TERT Expression Promote Long-Term Proliferation and Genome Instability After Cytokinesis Failure.” Virology, 2020
2. Holcomb A, Brown L, Tawfik O, Madan R, Shnayder Y, Thomas SM, Wallace NA. “Overexpression of Homologous Repair Proteins in Human Papillomavirus Positive Head and Neck Squamous Cell Carcinoma.” Virology, 2020
3. Dacus D, Cotton C, McCallister TX, Wallace NA. “Beta Human Papillomavirus 8E6 Attenuates LATS Phosphorylation after Failed Cytokinesis” Journal of Virology, 2020

4. Wallace NA. “Catching HPV in the Homologous Recombination Cooking Jar” Trends in Microbiology, 2020.
5. Snow JA, Murthy V, Dacus D, Hu C, Wallace NA. “β-HPV 8E6 Attenuates ATM and ATR Signaling in Response to UV Damage” Pathogens 2019

- **Books or other non-periodical, one-time publications.**
  - Nothing to report
- **Other publications, conference papers, and presentations.**

1. Louisiana State University, Shreveport Health Science Center, (2020) “HPV Oncogenes Induce and Disrupt Translesion Synthesis”

2. University of Kansas Cancer Center (2019) “HPV Oncogenes Induce and Disrupt Translesion Synthesis”

3. Department of Microbiology, Molecular Genetics & Immunology, University of Kansas Medical Center (2019) “HPV Oncogenes Induce and Disrupt Translesion Synthesis”

4. Center for Molecular Medicine’s Symposium on the missing links in HPV-Biology: Focus on Head & Neck cancer and Skin Cancer, Cologne, Germany (2019) “Interference of HPV with DNA Damage and Repair Pathway”

5. Virginia Commonwealth University Philips Institute for Oral Health Research (2018) “HPV Oncogenes Induce and Disrupt Translesion Synthesis”

6. Wake Forest University School of Medicine Microbiology and Immunology (2018) “HPV Oncogenes Induce and Disrupt Translesion Synthesis”

7. University of Kansas, Lawrence, KS (2018) “HPV Oncogenes Induce and Disrupt Translesion Synthesis”

8. 6th Workshop on Emerging Issues in Oncogenic Virus Research. Manduria, Italy. (2020) “β-HPV E6 Attenuates UV Repair” (Abstract Accepted, Conference Cancelled)

9. Midwest HPV Conference, Indiana University School of Medicine (2019) “HPV Oncogenes and Genome Stability”

10. Designing Molecules Workshop and Conference. Japan Society for Promotion of Science and K-State Department of Chemistry. (2019) “HPV Oncogenes Induce and Disrupt Translesion Synthesis”

- **Website(s) or other Internet site(s)**
  - **www.WallaceLabKSU.weebly.com**
    - **This is our personal lab website. It broadcasts our twitter handle and announces major accomplishments.**
  - @wallaceHPVlab is our twitter handle.
    - This twitter account disseminates the daily activities and science news from our group. We use it to connect with our over 800 followers. It is an effective outreach tool.
- **Technologies or techniques**
  - Nothing to report
- **Inventions, patent applications, and/or licenses**
  - Nothing to report
- **Other Products**
  - Nothing to report

7. **PARTICIPANTS & OTHER COLLABORATING ORGANIZATIONS**
   - **What individuals have worked on the project?**

Name:	*Dalton Dacus*
Project Role:	*Graduate Student*
Researcher Identifier (e.g. ORCID ID):	*Not Applicable*
Nearest person month worked:	*12*
Contribution to Project:	Mr. Dacus performed most of analysis of the hippo pathway (Aim 2) and some of the work for AIM3
Funding Support:	*CDMRP and Wallace Startup funds*

-

Name:	*Changkun Hu*
Project Role:	*Graduate Student*
Researcher Identifier (e.g. ORCID ID):	*Not Applicable*
Nearest person month worked:	*12*

Contribution to Project:	*Mr. Hu has performed the analysis of the NHEJ pathway.*
Funding Support:	*CDMRP and Wallace Startup Funds*

-

Name:	*Jazmine Snow*
Project Role:	*Research Assistant*
Researcher Identifier (e.g. ORCID ID):	*Not Applicable*
Nearest person month worked:	*4*
Contribution to Project:	*Ms. Snow has performed the characterization of ATM and ATR signaling described above in Specific AIM 1.*
Funding Support:	*Wallace Startup funds*

-

Name:	*Nicholas Wallace*
Project Role:	*Primary Investigator*
Researcher Identifier (e.g. ORCID ID):	*0000-0002-3971-716X*
Nearest person month worked:	*3*
Contribution to Project:	*Dr. Wallace oversaw the work on each projects. He wrote and edited all manuscripts. He also submitted grants to fund future relevant studies. He mentored the graduate students, post doc and research assistant in his lab. He also presented the lab's findings to external and internal audiences.*
Funding Support:	*CDMRP Support and NIH Support*

-

Name:	*Laimonis Laimins*
Project Role:	*Designated Mentor*
Researcher Identifier (e.g. ORCID ID):	0000-0002-6314-623X
Nearest person month worked:	*1*

Contribution to Project:	*Dr. Laimins advised and mentored Dr. Wallace as necessary throughout the budget period.*
Funding Support:	*Dr. Laimins is supported by 2 RO1's from the NCI and 1 R21 from NIAID.*

- **Has there been a change in the active other support of the PD/PI(s) or senior/key personnel since the last reporting period?**
  - Nothing to Report.
- **What other organizations were involved as partners?**
  - Nothing to Report.

8. **SPECIAL REPORTING REQUIREMENTS**
   - Nothing to Report
   - **APPENDICES:** PDF versions of the five manuscripts published during this reporting period are appended below.

Virology 549 (2020) 32–38

Contents lists available at ScienceDirect

Virology

journal homepage: www.elsevier.com/locate/virology

β-HPV 8E6 combined with *TERT* expression promotes long-term proliferation and genome instability after cytokinesis failure

Dalton Dacus, Elizabeth Riforgiate, Nicholas A. Wallace*

Division of Biology, Kansas State University, Manhattan, KS, USA

ARTICLE INFO

Keywords:
Aneuploid
Polyploid
Chromosome
Skin cancer
β-HPV
Telomerase

ABSTRACT

Human papillomavirus (HPV) is a family of viruses divided into five genera: alpha, beta, gamma, mu, and nu. There is an ongoing discussion about whether beta genus HPVs (β-HPVs) contribute to cutaneous squamous cell carcinoma (cSCC). The data presented here add to this conversation by determining how a β-HPV E6 protein (β-HPV 8E6) alters the cellular response to cytokinesis failure. Specifically, cells were observed after cytokinesis failure was induced by dihydrocytochalasin B (H2CB). β-HPV 8E6 attenuated the immediate toxicity associated with H2CB but did not promote long-term proliferation after H2CB. Immortalization by telomerase reverse transcriptase (*TERT)* activation also rarely allowed cells to sustain proliferation after H2CB exposure. In contrast, *TERT* expression combined with β-HPV 8E6 expression allowed cells to proliferate for months following cytokinesis failure. However, this continued proliferation comes with genome destabilizing consequences. Cells that survived H2CB-induced cytokinesis failure suffered from changes in ploidy.

1. Introduction

Cutaneous squamous cell carcinoma (cSCC) is one of the most common malignancies worldwide (Lomas et al., 2012; Alam and Ratner, 2001). The annual rate of cSCC has risen for thirty straight years (Hollestein et al., 2014). These malignancies represent a tremendous financial burden, especially in fair-skinned populations. As a result, the United States currently spends $3.8 billion annually on treatments (Deady et al., 2014). UV radiation, light skin color, and immunosuppression are the major risk factors implicated in the development of cSCC (Fahradyan et al., 2017). Additionally, it has been hypothesized that cutaneous human papillomavirus of the beta genus (β-HPV) may be another factor in cSCC progression (Howley and Pfister, 2015a; McLaughlin-Drubin, 2015; Tommasino, 2017).

β-HPV types 5 and 8 were first isolated from sun-exposed skin lesions found in individuals with the rare genetic disorder, epidermodysplasia verruciformis (EV) (Orth, 2008). People with EV are prone to β-HPV infections and cSCC (Orth, 2008; Nunes et al., 2018). A similar association has been observed in people taking immunosuppressive drugs after organ transplants (Genders et al., 2015; Boyle et al., 1984; Boxman et al., 1997). Further, animal and epidemiological studies also suggest β-HPV infections are associated with cSCC (Tommasino, 2017; Chahoud et al., 2016; Patel et al., 2008). Yet β-HPV expression in immunocompetent individuals drops significantly as healthy skin progresses to precancerous actinic keratosis (AK), then onto cSCC (Nunes et al., 2018; Winer et al., 2017; Hampras et al., 2017; Weissenborn et al., 2005, 2009; Howley and Pfister, 2015b). *In vitro* assays suggest that β-HPV proteins, particularly β-HPV E6, alter cell signaling to promote proliferation, impairing genome stability in the process (Wendel and Wallace, 2017; Rollison et al., 2019). These data have led some to hypothesize that β-HPV augments the mutational burden associated with UV, promoting the early stages of malignant conversion. In what has been called the “hit-and-run” model of viral oncogenesis, these mutations result in a tumor that no longer relies on continued viral gene expression (Aldabagh et al., 2013; Hufbauer and Akgül, 2017; de Koning et al., 2007). While this model has merit, other factors seem to dictate the oncogenic potential of β-HPV infections. For example, a recent publication from Strickley et al. helped solidify the growing consensus that immune status is a central determinant of the oncogenic potential associated with β-HPV infections (Strickley et al., 2019). Other factors may also increase or decrease the risk associated with these infections. Given how widespread β-HPV infections are, it remains important to understand the genetic changes that could augment their deleterious characteristics.

The work described here focuses on the maintenance of genome fidelity during cell division. Live cell microscopy and brightfield microscopy demonstrate that failed cytokinesis occurs about 10% of the time that skin cells enter mitosis (Wallace et al., 2014; Dacus et al.,

* Corresponding author.
E-mail address: nwallac@ksu.edu (N.A. Wallace).

https://doi.org/10.1016/j.virol.2020.07.016
Received 6 July 2020; Received in revised form 28 July 2020; Accepted 29 July 2020
Available online 04 August 2020
0042-6822/

2020). When this occurs, if the cells continue proliferating, they will suffer changes in ploidy (Hayashi and Karlseder, 2013; Alonso-Lecue et al., 2017; Lens and Medema, 2019). Responses to failed cytokinesis are often studied after induction by dihydrocytochalasin B (H2CB). H2CB causes cytokinesis failure by inhibiting actin polymerization. One study used this approach to show that the Hippo pathway kinase LATS was responsible for orchestrating the cellular response to failed cytokinesis, by inducing p53 accumulation and preventing further proliferation (Ganem et al., 2014). β-HPV 8E6 expression inhibits this buildup of p53 by attenuating LATS activation in a p300-dependent manner (Dacus et al., 2020). Despite the impairment of relevant signaling events, β-HPV 8E6 only imparted transient protection from failed cytokinesis. While β-HPV 8E6 expressing cells tolerated the immediate impact of failed cytokinesis, they were not capable of sustained proliferation. Mutations that activate telomerase are common in cSCC and are associated with growth advantages (Cheng et al., 2015; Griewank et al., 2013; Pópulo et al., 2014). Like β-HPV 8E6 expression, *TERT* expression had a limited ability to promote proliferation after failed cytokinesis. However, expression of β-HPV 8E6 in cells immortalized by telomerase activation promoted short- and long-term proliferation after failed cytokinesis. The survival of H2CB-induced failed cytokinesis was associated with increased aneuploidy.

2. Results

β-HPV 8E6 expressing HFK cannot sustain proliferation after H2CB-induced failed cytokinesis. β-HPV 8E6 hinders the cellular response to genome destabilizing events, including DNA damage and failed cytokinesis (Wendel and Wallace, 2017; Dacus et al., 2020). This study examines the consequences of β-HPV 8E6's impairment of signaling events stemming from H2CB-induced cytokinesis failure. β-HPV 8E6 reduces H2CB-induced activation of a Hippo tumor suppressor pathway kinase (LATS), p53 stabilization, and the accumulation of apoptotic markers. β-HPV 8E6 also increases the expression of pro-proliferative TEAD-responsive genes. To determine if these alterations allowed cells to survive H2CB-induced failed cytokinesis, we exposed vector control human foreskin keratinocytes (HFK LXSN) and β-HPV 8E6 expressing HFK (HFK β-HPV 8E6) to media containing 4 μM of H2CB for 6 days (Ganem et al., 2014). Cells counted on day 0 are referred to as 'before' H2CB. After 6 days of H2CB exposure, cells were counted and are referred to as 'during'. H2CB was washed out and cells were placed in growth media. Cells were monitored until they reached approximately 90% confluency or stopped proliferating (referred to as 'after'). At this point, viable cultures were counted, passaged, and considered to have recovered (recovered-HFK LXSN or recovered-HFK β-HPV 8E6) from H2CB exposure. Three independent biological replicates found similar results. β-HPV 8E6 attenuated the immediate consequences of H2CB-associated toxicity (compare the number of HFK LXSN and HFK β-HPV 8E6 after 6 days of H2CB exposure in Fig. 1A). However, neither cell line was capable of sustained proliferation after H2CB (Fig. 1A).

β-HPV infections occur in different genetic backgrounds, some of which could act synergistically with β-HPV 8E6 to allow cells to recover from H2CB-induced failed cytokinesis (Martincorena et al., 2015). Given the links between β-HPV and cSCC development, recurrent genetic contributors to cSCC development were examined to identify candidate alterations. Specifically, common mutations from sequencing data of 68 cSCC were ranked by their frequency (Pickering et al., 2014; Li et al., 2015; Gao et al., 2013; Cerami et al., 2012) (Supplemental Data 1). Then, a gene ontology analysis was performed on the top 10% of mutations using the web-based gene ontology software, PANTHER (Mi et al., 2017; The Gene Ontology Resourc, 2019; Ashburner et al., 2000) (Fig. 1B). The biological process "replicative senescence" contained within the "proliferation" node contained commonly mutated genes in cSCC. A complementary gene ontology software also identified "replicative senescence" among the cellular responses enriched within cSCC mutated genes (data not shown). This broad unbiased approach was complimented with a literature-based prioritization of the mutated genes. Among the genes in the "replicative senescence" node, mutations in *TERT* (the gene encoding telomerase reverse transcriptase, a component of telomerase) were notable. Multiple other studies have identified telomerase activating mutations within *TERT* promoter region in cSCC (Cheng et al., 2015; Griewank et al., 2013; Pópulo et al., 2014; Scott et al., 2014). Enhanced telomerase activity can promote proliferation despite damage and stress that would normally remove cells from the cell cycle (Urquidi et al., 2000; Victorelli and Passos, 2017; Davoli et al., 2010). It also allows cells immortalized by telomerase activation to continue growing after exposure to cytochalasin B, an unsaturated derivative of H2CB, which shares the ability to inhibit cell division, but unlike H2CB, it affects sugar transport (31, 48–51). These observations suggest that *TERT* activation is a relevant alteration in cSCC and that it could act on its own or synergize with β-HPV 8E6 to promote growth after cytokinesis failure.

To determine if *TERT* activation could promote survival from H2CB, β-HPV 8E6 expression was examined in HFK immortalized by telomerase activation (*TERT*-HFK). Specifically, the effects of H2CB on long term proliferation were studied in previously characterized HA-tagged β-HPV 8E6 and vector control *TERT*-HFKs (*TERT*-HFK β-HPV 8E6 and *TERT*-HFK LXSN, respectively) (Wang et al., 2016; Dickson et al., 2000). β-HPV 8E6 maintained its previously reported ability to alter the response to H2CB and increase TEAD-responsive gene expression in this genetic background (Supplementary Fig. 1A–C). Further, H2CB exposure was more effective at inducing binucleation and senescence (indicated by senescence-associated β-Galactosidase or SA β-Gal staining) in *TERT*-HFK cells (Supplementary Fig. 1D,E). These data confirmed that both β-HPV 8E6 and H2CB retained their reported activities in *TERT*-HFK cells. Next, the impact of H2CB exposure (6 days of 4 μM H2CB) on long-term proliferation was defined for three biological replicates using the growth conditions described in Fig. 1A. β-HPV 8E6 continued to reduce cell death in *TERT*-HFKs during H2CB exposure (compare cell lines at day 6 in Fig. 2A). However, β-HPV 8E6 was also able to promote recovery from H2CB-induced failed cytokinesis in this genetic background (recovered-*TERT*-HFK β-HPV 8E6). In each of these long-term growth assays, *TERT*-HFK β-HPV 8E6 survived for at least 17 days after H2CB exposure (Fig. 2A). Unfortunately, one repeat was contaminated and could not be expanded after survival. In contrast, none of the attempts to grow *TERT*-HFK LXSN after H2CB exposure were successful (recovered-*TERT*-HFK LXSN).

To obtain recovered-*TERT*-HFK LXSN to compare to recovered-*TERT*-HFK β-HPV 8E6 cells, 6 additional replicates were performed in a format with a larger initial population of cells (expansion from a 6-well to 10-cm plate format). In these conditions, only one of the *TERT*-HFK LXSN cell lines survived (See Fig. 2B). *TERT*-HFK β-HPV 8E6 cells also survived in each of the experiments conducted in 10-cm plates. Representative growth data for these cells can be found in Supplementary Figure 2. Recovered-*TERT*-HFK cells were expanded to determine the genomic consequences of surviving H2CB.

3. β-HPV 8E6 exacerbates aneuploidy in *TERT*-HFKs after recovering from failed cytokinesis

Failed cytokinesis jeopardizes genome integrity, particularly when cells continue to proliferate afterward (Hayashi and Karlseder, 2013; Storchova and Kuffer, 2008; Ganem et al., 2007). To determine if the cells that survived H2CB-induced failed cytokinesis had impaired genomic instability, differential interference contrast microscopy of condensed chromosomes from metaphase spreads was used to compare the ploidy of *TERT*-HFK LXSN to recovered-*TERT*-HFK LXSN cells (Fig. 3A). While most *TERT*-HFK LXSN were diploid before H2CB treatment, many recovered-*TERT*-HFK LXSN cells had aneuploid genomes. A small subset of recovered-*TERT*-HFK LXSN cells had tetraploid genomes (Fig. 3B). Chromosome abnormalities were exacerbated by β-HPV 8E6 in the cell line paired with the only recovered-*TERT*-HFK

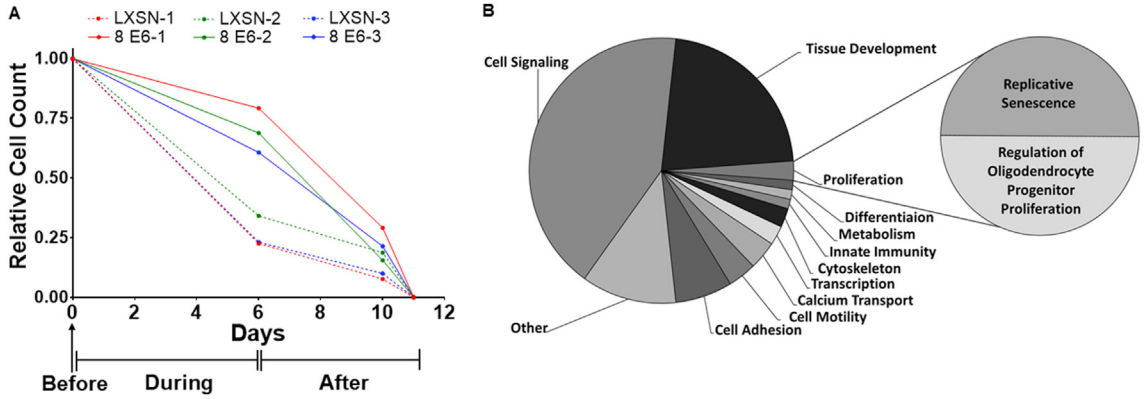

Fig. 1. H2CB-induced failed cytokinesis prevents long-term proliferation. (A) Three growth curves (biological replicates) comparing HFK LXSN and β-HPV 8E6 cells before, during, and after 6 days of H2CB exposure in 6-well tissue culture plates. HFK LXSN (dashed) and β-HPV 8E6 (solid) data with the same color and number (red, 1; green, 2; and blue, 3) were treated in parallel. (B) Two charts representing GO analysis of common mutations in cSCC. The larger chart on the left represents nodes of similar GO: biological process terms. The smaller chart represents the two GO: biological process terms within the "Proliferation" node. *TERT* expression allows β-HPV 8E6 HFKs growth after H2CB-induced failed cytokinesis. (For interpretation of the references to color in this figure legend, the reader is referred to the Web version of this article.)

LXSN cell line. Most *TERT*-HFK β-HPV 8E6 cells had aneuploid genomes before H2CB exposure and all the recovered-*TERT*-HFK β-HPV 8E6 were aneuploid (Fig. 3B, C). The length of time in passage is unlikely to explain these data as the cells were analyzed after a similar time in culture. Further, the results were nearly identical when ploidy was determined immediately after recovery or several passages later (data not shown).

4. Discussion

β-HPVs promote the proliferation of damaged skin cells (Howley and Pfister, 2015a; Tommasino, 2017; Rollison et al., 2019; Wallace et al., 2014; Dacus et al., 2020). β-HPV 8E6 is a critical contributor to this phenotype and acts at least in part by suppressing apoptotic responses (Dacus et al., 2020; Underbrink et al., 2008). As a result, β-HPV infections have been hypothesized to allow the accumulation of potentially tumorigenic mutations. Here, we examine the ability of β-HPV 8E6 to act along with *TERT* expression to facilitate the survival of cells that do not divide after replicating their genomes. We summarize our observations in Fig. 4. When cytokinesis failure was induced by H2CB, HFK were unable to sustain long-term growth (Fig. 4A). β-HPV 8E6 did not change this outcome (Fig. 4B). Immortalization by telomerase activation rarely allowed cells to recover from.

H2CB exposure (Fig. 4C). However, the combination of β-HPV 8E6 expression and *TERT* expression allowed cells to sustain proliferation for months (presumably indefinitely) after cytokinesis failure and augmented genomic instability (Fig. 4D).

When comparing HFK and *TERT*-HFK cell lines some caution should be exercised as they were generated from different donors. However, phenotypes are frequently replicated across.

Keratinocytes from separate persons (White et al., 2012; Howie et al., 2011; Meyers et al., 2017). More specific to this study and these cells, the previously reported attenuation of the Hippo pathway kinase LATS activation by β-HPV 8E6 was conserved between both HFK and *TERT*-HFK cell lines (Supplementary Figure 1 and (Dacus et al., 2020)). These data are consistent with the established idea that telomerase activation promotes carcinogenesis and suggest that β-HPV infections may augment the transformative power of telomerase activation.

Our data also provides other, more specific insights. For instance, we found that β-HPV 8E6 made *TERT*-HFKs approximately 2.5 times more likely to be aneuploid (Fig. 3C). To our knowledge, this is the first report associating changes in ploidy with β-HPV 8E6. The observation is in line with reports from the Tommasino Lab that describe changes in ploidy in β-HPV 38 E6 and E7 immortalized keratinocytes (Gabet et al., 2008). Unlike our report, they demonstrated that ectopic *TERT* expression reduced aneuploidy, likely by reducing the chromosomal rearrangements, anaphase bridges, and multipolar mitoses associated with β-HPV 38 E6/E7 immortalization. This could be the result of differences between β-HPV 38 E6 and β-HPV 8E6 or they might be explained by the presence/absence of the β-HPV E7 protein (Tommasino, 2017; Howley and Pfister, 2015b).

In vitro studies on β-HPVs tend to examine the effects of stimuli over a short time interval (hours to days). However, the average β-HPV infection persists for six to eleven months (de Koning et al., 2007; Hampras et al., 2014). *TERT*-HFK cells provide a system to replicate lengthier conditions and our data demonstrates the utility of such an

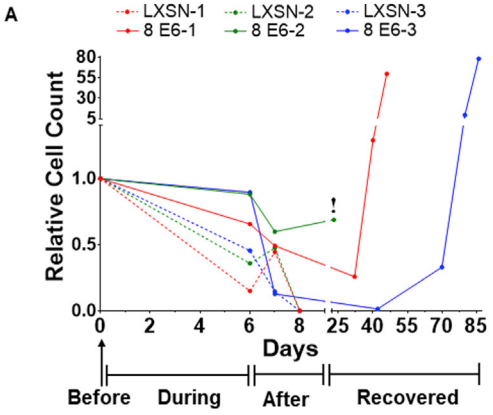

B

Cell Type	% Recovered
LXSN	0% (3/3)
8 E6	0% (3/3)
LXSN + *TERT*	~11% (1/9)
8 E6 + *TERT*	100% (9/9)

Fig. 2. *TERT* expression promotes recovery from failed cytokinesis. (A) Three growth curves (biological replicates) comparing *TERT*-HFK LXSN and β-HPV 8E6 cells before, during, after, and recovered from 6 days of H2CB exposure in 6-well tissue culture plates. LXSN (dashed) and β-HPV 8E6 (solid) data with the same color and number (red, 1; green, 2; and blue, 3) were treated in parallel. **!** signifies the premature end of the long-term cultivation due to bacterial contamination. (B) Percent of HFK and *TERT*-HFK cells capable of long-term growth after 6 days in H2CB. (For interpretation of the references to color in this figure legend, the reader is referred to the Web version of this article.)

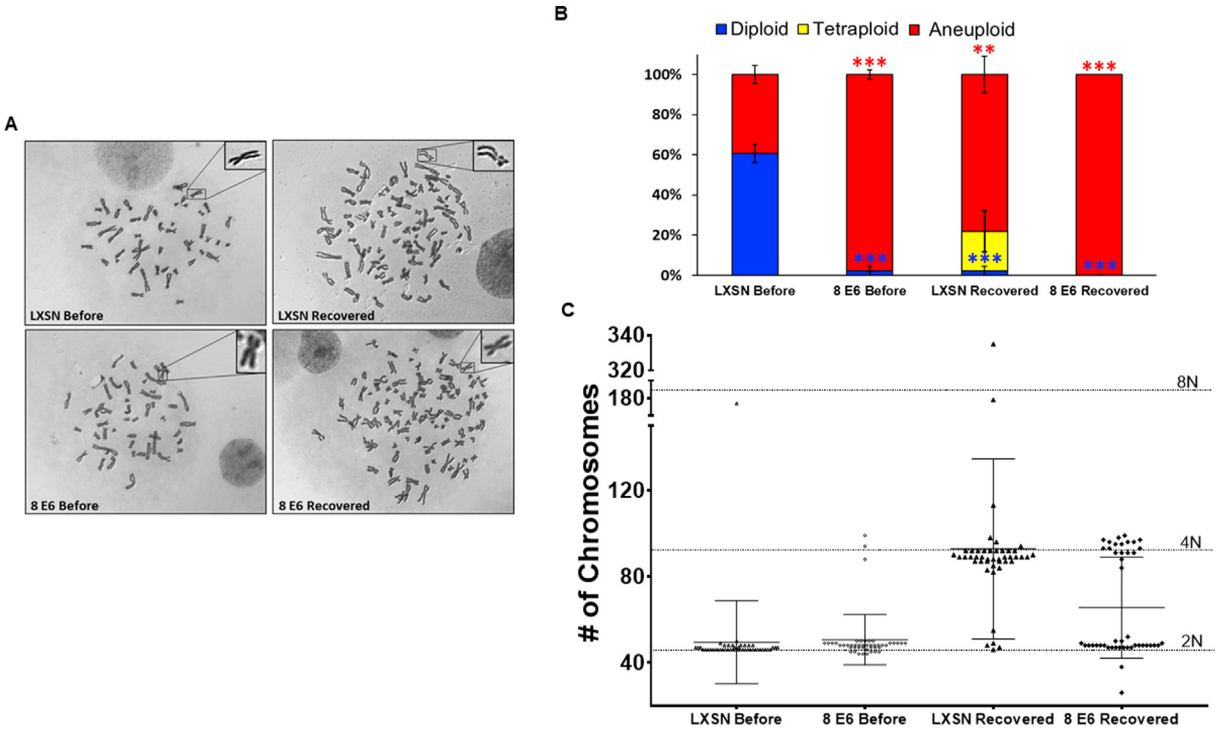

Fig. 3. β-HPV 8E6 and cytokinesis failure induce changes in ploidy. (A) Representative images of metaphase spreads. Insert on the top-right corner shows a magnified chromosome. (B) Relative frequency of diploidy (blue), tetraploidy (yellow), and aneuploidy (red) before H2CB treatment and once cells recovered. Red and blue asterisks denote a significant difference from 'LXSN Before' for aneuploidy and diploidy, respectively. (C) Graphical presentation of the distribution of the number of chromosomes among ≥ 45 cells analyzed by metaphase spreads (before or recovered from 6 days of H2CB exposure). Horizontal-dotted lines represent 46 (2 N), 92 (4 N), or 184 (8 N) chromosomes. ** denotes significant difference between indicated samples $p \leq 0.01$, *** denotes $p \leq 0.001$ (Student's *t*-test). (For interpretation of the references to color in this figure legend, the reader is referred to the Web version of this article.)

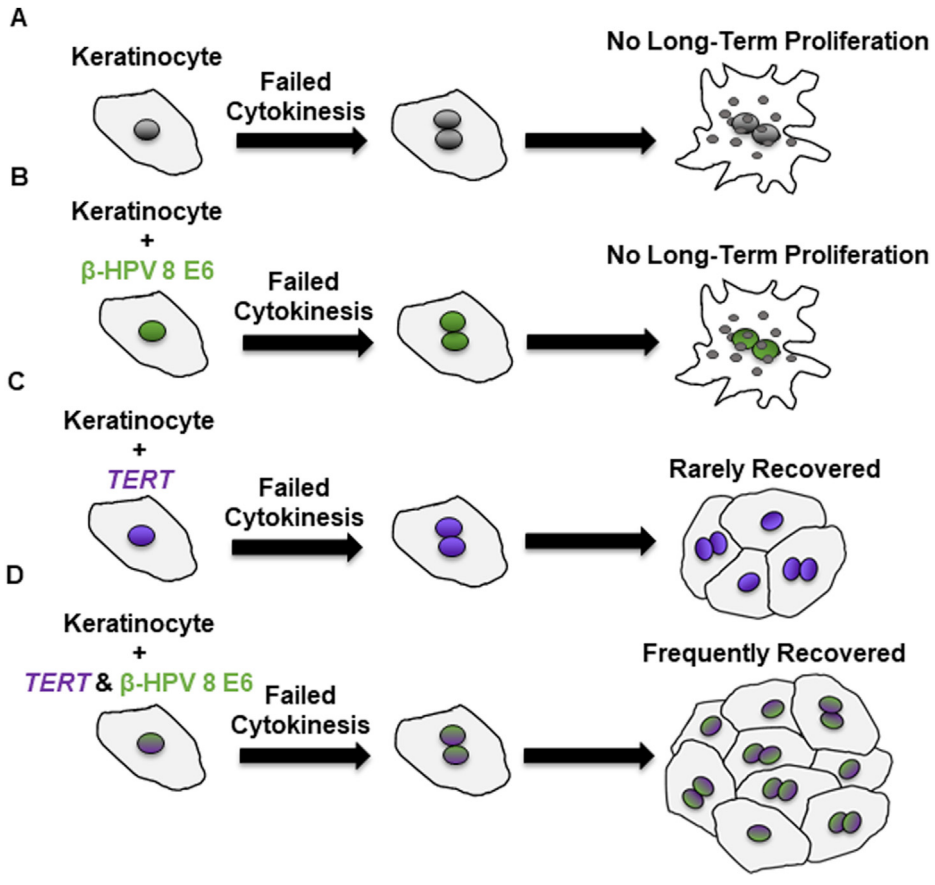

Fig. 4. β-HPV 8E6 and telomerase activation affect cell fate after failed cytokinesis. (A) Keratinocytes that experience H2CB-induced cytokinesis failure become binucleated (indicated by two nuclei inside the cell) resulting in cell death and inhibition of long-term proliferation. (B) β-HPV 8E6 (indicated by green nuclei) reduces the death associated with cytokinesis failure but cells remain unable to sustain long-term proliferation. (C) Keratinocytes immortalized by *TERT* activation (indicated by purple nuclei) experience H2CB-associated binucleation and toxicity, but unlike primary keratinocytes, a small number recover. (D) *TERT* immortalized keratinocytes that co-express β-HPV 8E6 (indicated by green/purple nuclei) regularly survive H2CB-exposure but have high levels of aneuploidy. (For interpretation of the references to color in this figure legend, the reader is referred to the Web version of this article.)

approach. By removing the restrictive nature of primary cell growth, we were able to describe the changes in ploidy stemming from failed cytokinesis. Based on our data, caution should be exercised when examining these systems as *TERT* expression can change the cellular response to genome destabilizing events.

Indeed, our data offers proof of principle that phenotypes associated with β-HPV E6 can change based on the genetic context of viral gene expression. There may be genetic environments where cutaneous papillomavirus infections promote cSCC and others where the same infections prevent cSCC. If this were true, it might help explain conflicting reports that describe these infections as oncogenic and oncopreventative (Howley and Pfister, 2015a; Aldabagh et al., 2013; Strickley et al., 2019; Hasche et al., 2018). Moving forward, it will be interesting to determine the ability of β-HPV E6 to synergize with other common mutations and the mechanism by which β-HPV 8E6 increases aneuploidy.

5. Material and methods

5.1. Cell culture

Primary HFK were derived from neonatal human foreskins. HFK and *TERT*-immortalized-HFK (obtained from Michael Underbrink, University of Texas Medical Branch) were grown in EpiLife medium supplemented with calcium chloride (60 μM), human keratinocyte growth supplement (ThermoFisher Scientific), and penicillin-streptomycin. HPV genes were cloned, transfected, and confirmed as previously described (Wallace et al., 2014). In order not to activate the Hippo pathway via contact inhibition, we carefully monitored the cell density in all experiments. Experiments were aborted if unintended differences in seeding resulted in cell densities that were more than 10% different among cell lines at the beginning of an experiment.

5.2. cBioPortal and gene ontology analysis

Software from (www.cbioportal.org) was used to recognize, analyze, and categorize mutations and transcriptomic data from cutaneous squamous cell carcinomas (Pickering et al., 2014; Li et al., 2015). Analysis of the squamous cell carcinoma samples was done at (http://geneontology.org/) powered by Protein ANalysis THrough Evolutionary Relationships (PANTHER) (The Gene Ontology Resourc, 2019; Ashburner et al., 2000).

5.3. H2CB recovery assay

6-well format: Cells were counted, then either 1.5×10^5 HFK or 5×10^4 *TERT*-HFK cells were seeded on a 6 well tissue culture plate and grown for 24 h. Cells were then treated with 4 μM H2CB, refreshing the H2CB media every 2 days. After 6 days, the cells were washed with PBS and given fresh EpiLife. Once cells reached 90% confluency, they were counted then moved to new 6 wells. This process was continued until cells were no longer able to be passaged or cells could be moved to a 10 cm plate.

10 cm format: Cells were counted, then 3.0×10^5 cells were seeded on a 10 cm tissue culture plate and grown for 24 h. Cells were then treated with 4 μM H2CB, refreshing the H2CB media every 2 days. After 6 days, the cells were washed with PBS and given fresh EpiLife. Once cells reached 90% confluency they were counted, then 9.0×10^4 cells were reseeded. This process was continued until cells were no longer able to be passaged or for 28 days.

5.4. RT-qPCR

Cells were lysed, isolated, reverse transcribed, and then RT-qPCR was performed as previously described (Dacus et al., 2020). The following probes (Thermo Scientific) were used: ACTB (Hs01060665_g1), STK4 (Hs00178979_m1), LATS2 (Referred to as LATS in the text) (Hs01059009_m1), YAP1 (Hs00902712_g1), CTGF (Hs00170014_m1), CYR61 (Hs00155479_m1), TEAD1 (Hs00173359_m1), CCND1 (Hs00765553_m1), AXL (Hs01064444_m1), SERPINE1 (Hs00167155_m1).

5.5. Immunoblotting

Cells were washed and lysed, then lysates were run, transferred, probed, and visualized as previously described (Dacus et al., 2020). The following antibodies were used: GAPDH (Santa Cruz Biotechnologies sc-47724), LATS2 (Referred to as LATS in the text, Cell Signaling Technologies D83D6), Phospho-LATS1/2 (Ser909) (Referred to as pLATS in the text) (Cell Signaling Technologies #9157), YAP (Cell Signaling Technologies 4912S), Phospho-YAP (Ser127) (Referred to pYAP in the text) (Cell Signaling Technologies 4911S), AXL (Cell Signaling Technologies 8661S, p300 (Santa Cruz Biotechnologies sc-584).

5.6. Senescence-associated β-galactosidase staining

Cells were seeded onto three 6-well plates and treated with H2CB then stained as previously described (Dacus et al., 2020).

5.7. Chromosome counts via metaphase spread

'Before' and after cells recovered from H2CB exposure *TERT*-immortalized HFK cells were grown to 80% confluency then chromosomes were detected and counted as previously described (Howe et al., 2014).

5.8. Statistical analysis

Unless otherwise noted, statistical significance was determined by a paired Student *t*-test and was confirmed when appropriate by a two-way analysis of variance (ANOVA) with Turkey's correction. Only *P* values less than 0.05 were reported as significant.

CRediT authorship contribution statement

Dalton Dacus: Conceptualization, Methodology, Validation, Formal analysis, Investigation, Writing - original draft, Writing - review & editing, Visualization, Project administration. **Elizabeth Riforgiate:** Validation, Writing - original draft, Writing - review & editing, Investigation. **Nicholas A. Wallace:** Conceptualization, Methodology, Validation, Investigation, Resources, Writing - original draft, Writing - review & editing, Supervision, Project administration, Funding acquisition.

Declaration of competing interest

The authors declare that they have no conflicts of interests related to the work described in our manuscript.

Acknowledgments:

We thank and acknowledge Jocelyn A. McDonald for assisting with our metaphase spread imaging. Michael Underbrink for providing the *TERT*-immortalized-HFK. Jazmine A. Snow and Emily Burghardt for constructive criticism of the manuscript.

This work was supported by the Department of Defense CMDRP PRCRP CA160224 (NW) and made possible through generous support from the Les Clow family and the Johnson Cancer Research Center at Kansas State University. Declarations of interest: none.

Appendix A. Supplementary data

Supplementary data to this article can be found online at https://doi.org/10.1016/j.virol.2020.07.016.

References

Alam, M., Ratner, D., 2001. Cutaneous squamous-cell carcinoma. N. Engl. J. Med. 344, 975–983.

Aldabagh, B., Angeles, J.G.C., Cardones, A.R., Arron, S.T., 2013. Cutaneous squamous cell carcinoma and human papillomavirus: is there an association? Dermatol. Surg. Off. Publ. Am. Soc. Dermatol. Surg. Al. 39, 1–23.

Alonso-Lecue, P., de Pedro, I., Coulon, V., Molinuevo, R., Lorz, C., Segrelles, C., Ceballos, L., López-Aventín, D., García-Valtuille, A., Bernal, J.M., Mazorra, F., Pujol, R.M., Paramio, J., Ramón Sanz, J., Freije, A., Toll, A., Gandarillas, A., 2017. Inefficient differentiation response to cell cycle stress leads to genomic instability and malignant progression of squamous carcinoma cells. 6. Cell Death Dis. 8, e2901 e2901.

Ashburner, M., Ball, C.A., Blake, J.A., Botstein, D., Butler, H., Cherry, J.M., Davis, A.P., Dolinski, K., Dwight, S.S., Eppig, J.T., Harris, M.A., Hill, D.P., Issel-Tarver, L., Kasarskis, A., Lewis, S., Matese, J.C., Richardson, J.E., Ringwald, M., Rubin, G.M., Sherlock, G., 2000. Gene Ontology: tool for the unification of biology. Nat. Genet. 25, 25–29.

Boxman, I.L.A., Berkhout, R.J.M., Mulder, L.H.C., Wolkers, M.C., Bavinck, J.N.B., Vermeer, B.J., ter Schegget, J., 1997. Detection of human papillomavirus DNA in plucked hairs from renal transplant recipients and healthy volunteers. J. Invest. Dermatol. 108, 712–715.

Boyle, J., Briggs, J.D., RonaM, Mackie, Junor, B.J.R., Aitchison, T.C., 1984. CANCER, warts, and sunshine IN renal transplant patients: a case-control study. Lancet 323, 702–705.

Cerami, E., Gao, J., Dogrusoz, U., Gross, B.E., Sumer, S.O., Aksoy, B.A., Jacobsen, A., Byrne, C.J., Heuer, M.L., Larsson, E., Antipin, Y., Reva, B., Goldberg, A.P., Sander, C., Schultz, N., 2012. The cBio cancer genomics portal: an open platform for exploring multidimensional cancer genomics data. Cancer Discov 2, 401–404.

Chahoud, J., Semaan, A., Chen, Y., Cao, M., Rieber, A.G., Rady, P., Tyring, S.K., 2016. Association between β-genus human papillomavirus and cutaneous squamous cell carcinoma in immunocompetent individuals—a meta-analysis. JAMA Dermatol 152, 1354–1364.

Cheng, K.A., Kurtis, B., Babayeva, S., Zhuge, J., Tantchou, I., Cai, D., Lafaro, R.J., Fallon, J.T., Zhong, M., 2015. Heterogeneity of TERT promoter mutations status in squamous cell carcinomas of different anatomical sites. Ann. Diagn. Pathol. 19, 146–148.

Dacus, D., Cotton, C., McCallister, T.X., Wallace, N.A., 2020. Beta Human Papillomavirus 8E6 Attenuates LATS Phosphorylation after Failed Cytokinesis. Journal of Virology 94. https://doi.org/10.1128/JVI.02184-19.

Davoli, T., Denchi, E.L., de Lange, T., 2010. Persistent telomere damage induces bypass of mitosis and tetraploidy. Cell 141, 81–93.

de Koning, M.N.C., Struijk, L., Bavinck, J.N.B., Kleter, B., ter Schegget, J., Quint, W.G.V., Feltkamp, M.C.W., 2007. Betapapillomaviruses frequently persist in the skin of healthy individuals. J. Gen. Virol. 88, 1489–1495.

Deady, S., Sharp, L., Comber, H., 2014. Increasing skin cancer incidence in young, affluent, urban populations: a challenge for prevention. Br. J. Dermatol. 171, 324–331.

Dickson, M.A., Hahn, W.C., Ino, Y., Ronfard, V., Wu, J.Y., Weinberg, R.A., Louis, D.N., Li, F.P., Rheinwald, J.G., 2000. Human keratinocytes that express hTERT and also bypass a p16INK4a-enforced mechanism that limits life span become immortal yet retain normal growth and differentiation characteristics. Mol. Cell Biol. 20, 1436–1447.

Fahradyan, A., Howell, A.C., Wolfswinkel, E.M., Tsuha, M., Sheth, P., Wong, A.K., 2017. Updates on the management of non-melanoma skin cancer (NMSC). Healthcare 5.

Gabet, A.-S., Accardi, R., Bellopede, A., Popp, S., Boukamp, P., Sylla, B.S., Londoño-Vallejo, J.A., Tommasino, M., 2008. Impairment of the telomere/telomerase system and genomic instability are associated with keratinocyte immortalization induced by the skin human papillomavirus type 38. FASEB J 22, 622–632.

Ganem, N.J., Storchova, Z., Pellman, D., 2007. Tetraploidy, aneuploidy and cancer. Curr. Opin. Genet. Dev. 17, 157–162.

Ganem, N.J., Cornils, H., Chiu, S.-Y., O'Rourke, K.P., Arnaud, J., Yimlamai, D., Théry, M., Camargo, F.D., Pellman, D., 2014. Cytokinesis failure triggers Hippo tumor suppressor pathway activation. Cell 158, 833–848.

Gao, J., Aksoy, B.A., Dogrusoz, U., Dresdner, G., Gross, B., Sumer, S.O., Sun, Y., Jacobsen, A., Sinha, R., Larsson, E., Cerami, E., Sander, C., Schultz, N., 2013. Integrative analysis of complex cancer genomics and clinical profiles using the cBioPortal. Sci. Signal. 6, pl1.

Genders, R.E., Mazlom, H., Michel, A., Plasmeijer, E.I., Quint, K.D., Pawlita, M., van der Meijden, E., Waterboer, T., de Fijter, H., Claas, F.H., Wolterbeek, R., Feltkamp, M.C.W., Bouwes Bavinck, J.N., 2015. The presence of betapapillomavirus antibodies around transplantation predicts the development of keratinocyte carcinoma in organ transplant recipients: a cohort study. J. Invest. Dermatol. 135, 1275–1282.

Griewank, K.G., Murali, R., Schilling, B., Schimming, T., Möller, I., Moll, I., Schwamborn, M., Sucker, A., Zimmer, L., Schadendorf, D., Hillen, U., 2013. TERT promoter mutations are frequent in cutaneous basal cell carcinoma and squamous cell carcinoma. PLoS ONE 8.

Hampras, S.S., Giuliano, A.R., Lin, H.-Y., Fisher, K.J., Abrahamsen, M.E., Sirak, B.A., Iannacone, M.R., Gheit, T., Tommasino, M., Rollison, D.E., 2014. Natural history of cutaneous human papillomavirus (HPV) infection in men: the HIM study. PLOS ONE 9, e104843.

Hampras, S.S., Rollison, D.E., Giuliano, A.R., McKay-Chopin, S., Minoni, L., Sereday, K., Gheit, T., Tommasino, M., 2017. Prevalence and concordance of cutaneous beta human papillomavirus infection at mucosal and cutaneous sites. J. Infect. Dis. 216, 92–96.

Hasche, D., Vinzón, S.E., Rösl, F., 2018. Cutaneous papillomaviruses and non-melanoma skin cancer: causal agents or innocent bystanders? Front. Microbiol. 9.

Hayashi, M.T., Karlseder, J., 2013. DNA damage associated with mitosis and cytokinesis failure. Oncogene 32, 4593–4601.

Hollestein, L.M., de Vries, E., Aarts, M.J., Schroten, C., Nijsten, T.E.C., 2014. Burden of disease caused by keratinocyte cancer has increased in The Netherlands since 1989. J. Am. Acad. Dermatol. 71, 896–903.

Howe, B., Umrigar, A., Tsien, F., 2014. Chromosome preparation from cultured cells. J Vis Exp. https://doi.org/10.3791/50203. e50203.

Howie, H.L., Koop, J.I., Weese, J., Robinson, K., Wipf, G., Kim, L., Galloway, D.A., 2011. Beta-HPV 5 and 8 E6 promote p300 degradation by blocking AKT/p300 association. PLoS Pathog. 7.

Howley, P.M., Pfister, H.J., 2015a. Beta genus papillomaviruses and skin cancer. Virology 290–296 0.

Howley, P.M., Pfister, H.J., 2015b. Beta genus papillomaviruses and skin cancer. Virology 290–296 0.

Hufbauer, M., Akgül, B., 2017. Molecular mechanisms of human papillomavirus induced skin carcinogenesis. Viruses 9.

Lens, S.M.A., Medema, R.H., 2019. Cytokinesis defects and cancer. Nat Rev Cancer 19, 32–45.

Li, Y.Y., Hanna, G.J., Laga, A.C., Haddad, R.I., Lorch, J.H., Hammerman, P.S., 2015. Genomic analysis of metastatic cutaneous squamous cell carcinoma. Clin Cancer Res Off J Am Assoc Cancer Res 21, 1447–1456.

Lomas, A., Leonardi-Bee, J., Bath-Hextall, F., 2012. A systematic review of worldwide incidence of nonmelanoma skin cancer. Br. J. Dermatol. 166, 1069–1080.

Martincorena, I., Roshan, A., Gerstung, M., Ellis, P., Loo, P.V., McLaren, S., Wedge, D.C., Fullam, A., Alexandrov, L.B., Tubio, J.M., Stebbings, L., Menzies, A., Widaa, S., Stratton, M.R., Jones, P.H., Campbell, P.J., 2015. High burden and pervasive positive selection of somatic mutations in normal human skin. Science 348, 880–886.

McLaughlin-Drubin, M.E., 2015. Human papillomaviruses and non-melanoma skin cancer. Semin. Oncol. 42, 284–290.

Meyers, J.M., Uberoi, A., Grace, M., Lambert, P.F., Munger, K., 2017. Cutaneous HPV8 and MmuPV1 E6 proteins target the NOTCH and TGF-β tumor suppressors to inhibit differentiation and sustain keratinocyte proliferation. PLoS Pathog. 13.

Mi, H., Huang, X., Muruganujan, A., Tang, H., Mills, C., Kang, D., Thomas, P.D., 2017. PANTHER version 11: expanded annotation data from Gene Ontology and Reactome pathways, and data analysis tool enhancements. Nucleic Acids Res. 45, D183–D189.

Nunes, E.M., Talpe-Nunes, V., Sichero, L., 2018. Epidemiology and biology of cutaneous human papillomavirus. Clinics 73.

Orth, G., 2008. Host defenses against human papillomaviruses: lessons from epidermodysplasia verruciformis. Curr. Top. Microbiol. Immunol. 321, 59–83.

Patel, A.S., Karagas, M.R., Perry, A.E., Nelson, H.H., 2008. Exposure profiles and human papillomavirus infection in skin cancer: an analysis of 25 genus β-types in a population-based study. J. Invest. Dermatol. 128, 2888–2893.

Pickering, C.R., Zhou, J.H., Lee, J.J., Drummond, J.A., Peng, S.A., Saade, R.E., Tsai, K.Y., Curry, J.L., Tetzlaff, M.T., Lai, S.Y., Yu, J., Muzny, D.M., Doddapaneni, H., Shinbrot, E., Covington, K.R., Zhang, J., Seth, S., Caulin, C., Clayman, G.L., El-Naggar, A.K., Gibbs, R.A., Weber, R.S., Myers, J.N., Wheeler, D.A., Frederick, M.J., 2014. Mutational landscape of aggressive cutaneous squamous cell carcinoma. Clin. Cancer Res. Off. J. Am. Assoc. Cancer Res. 20, 6582–6592.

Pópulo, H., Boaventura, P., Vinagre, J., Batista, R., Mendes, A., Caldas, R., Pardal, J., Azevedo, F., Honavar, M., Guimarães, I., Manuel Lopes, J., Sobrinho-Simões, M., Soares, P., 2014. TERT promoter mutations in skin cancer: the effects of sun exposure and X-irradiation. J. Invest. Dermatol. 134, 2251–2257.

Rollison, D.E., Viarisio, D., Amorrortu, R.P., Gheit, T., Tommasino, M., 2019. An emerging issue in oncogenic virology: the role of beta human papillomavirus types in the development of cutaneous squamous cell carcinoma. J. Virol. 93, e01003–e01018.

Scott, G.A., Laughlin, T.S., Rothberg, P.G., 2014. Mutations of the *TERT* promoter are common in basal cell carcinoma and squamous cell carcinoma. Mod. Pathol. 27, 516–523.

Storchova, Z., Kuffer, C., 2008. The consequences of tetraploidy and aneuploidy. J. Cell Sci. 121, 3859–3866.

Strickley, J.D., Messerschmidt, J.L., Awad, M.E., Li, T., Hasegawa, T., Ha, D.T., Nabeta, H.W., Bevins, P.A., Ngo, K.H., Asgari, M.M., Nazarian, R.M., Neel, V.A., Jenson, A.B., Joh, J., Demehri, S., 2019. Immunity to commensal papillomaviruses protects against skin cancer. Nature 575, 519–522.

The gene ontology resource: 20 years and still GOing strong. Nucleic. Acids Res. 47, D330–D338.

Tommasino, M., 2017. The biology of beta human papillomaviruses. Virus Res. 231, 128–138.

Underbrink, M.P., Howie, H.L., Bedard, K.M., Koop, J.I., Galloway, D.A., 2008. E6 proteins from multiple human betapapillomavirus types degrade Bak and protect keratinocytes from apoptosis after UVB irradiation. J. Virol. 82, 10408–10417.

Urquidi, V., Tarin, D., Goodison, S., 2000. Role of telomerase in cell senescence and oncogenesis. Annu. Rev. Med. 51, 65–79.

Victorelli, S., Passos, J.F., 2017. Telomeres and cell senescence - size matters not. EBioMedicine 21, 14–20.

Wallace, N.A., Robinson, K., Galloway, D.A., 2014. Beta human papillomavirus E6 expression inhibits stabilization of p53 and increases tolerance of genomic instability. J. Virol. 88, 6112–6127.

Wang, J., Dupuis, C., Tyring, S.K., Underbrink, M.P., 2016. Sterile α motif domain containing 9 is a novel cellular interacting partner to low-risk type human papillomavirus E6 proteins. PLoS ONE 11.

Weissenborn, S.J., Nindl, I., Purdie, K., Harwood, C., Proby, C., Breuer, J., Majewski, S.,

Pfister, H., Wieland, U., 2005. Human papillomavirus-DNA loads in actinic keratoses exceed those in non-melanoma skin cancers. J. Invest. Dermatol. 125, 93–97.
Weissenborn, S.J., De Koning, M.N.C., Wieland, U., Quint, W.G.V., Pfister, H.J., 2009. Intrafamilial transmission and family-specific spectra of cutaneous betapapillomaviruses. J. Virol. 83, 811–816.
Wendel, S.O., Wallace, N.A., 2017. Loss of genome fidelity: beta HPVs and the DNA damage response. Front. Microbiol. 8.
White, E.A., Kramer, R.E., Tan, M.J.A., Hayes, S.D., Harper, J.W., Howley, P.M., 2012. Comprehensive analysis of host cellular interactions with human papillomavirus E6 proteins identifies new E6 binding partners and reflects viral diversity. J. Virol. 86, 13174–13186.
Winer, R.L., Gheit, T., Cherne, S., Lin, J., Stern, J.E., Poljak, M., Feng, Q., Tommasino, M., 2017. Prevalence and correlates of beta human papillomavirus detection in fingernail samples from mid-adult women. Papillomavirus Res 5, 1–5.

Virology 548 (2020) 174–181

Contents lists available at ScienceDirect

Virology

journal homepage: www.elsevier.com/locate/virology

DNA repair gene expression is increased in HPV positive head and neck squamous cell carcinomas

Andrew J. Holcomb[a], Laura Brown[b], Ossama Tawfik[b], Rashna Madan[b], Yelizaveta Shnayder[a], Sufi Mary Thomas[a], Nicholas A. Wallace[c,*]

[a] The University of Kansas Medical Center, Department of Otolaryngology, Head and Neck Surgery, 3901 Rainbow Boulevard, Kansas City, KS, 66160, USA
[b] The University of Kansas Medical Center, Department of Pathology and Lab Medicine, 3901 Rainbow Boulevard, Kansas City, KS 66160, USA
[c] Kansas State University, Department of Biology, 116 Ackert Hall, Manhattan, KS, 66506, USA

A B S T R A C T

The incidence of head and neck squamous cell carcinomas (HNSCCs) is rising in developed countries. This is driven by an increase in HNSCCs caused by high-risk human papillomavirus (HPV) infections or HPV + HNSCCs. Compared to HNSCCs not caused by HPV (HPV– HNSCCs), HPV + HNSCCs are more responsive to therapy and associated with better oncologic outcomes. As a result, the HPV status of an HNSCC is an important determinant in medical management. One method to determine the HPV status of an HNSCC is increased expression of p16 caused by the HPV E7 oncogene. We identified novel expression changes in HPV + HNSCCs. A comparison of gene expression among HPV+ and HPV- HNSCCs in The Cancer Genome Atlas demonstrated increased DNA repair gene expression in HPV + HNSCCs. Further, DNA repair gene expression correlated with HNSCC survival. Immunohistochemical analysis of a novel HNSCC microarray confirmed that DNA repair protein abundance is elevated in HPV + HNSCCs.

1. Introduction

Human papillomaviruses (HPVs) are a family of over 200 different viruses that are grouped into five genera (alpha-, beta-, gamma-, mu-, and nu-papillomaviruses) (Bernard et al., 2010). This large family of viruses causes a wide array of maladies by infecting human mucosal and epithelial tissue (Doorbar et al., 2012). The diseases associated with HPV infections range from relatively benign warts to deadly carcinomas (Doorbar et al., 2015). Oncogenicity has been most clearly demonstrated for a subset of the alpha-papillomavirus genus, termed high-risk alpha-papillomaviruses. For simplicity, we refer to high-risk alpha-papillomaviruses as HPVs in this report. HPVs cause nearly all cervical cancers through the expression of two viral oncogenes (HPV E6 and E7) that disrupt tumor suppressor pathways (Bosch et al., 2002). HPV E6 promotes p53 degradation and activates telomerase, while HPV E7 destabilizes Rb (Boyer et al., 1996, p. 53; Dyson et al., 1989; Huibregtse et al., 1991; Münger et al., 1989a, 1989b, p. 6). Both HPV E6 and E7 also manipulate the host DNA repair responses such that viral replication is promoted at the expense of host genome fidelity (Anacker et al., 2016, 2014; Chappell et al., 2015; Gillespie et al., 2012; Hong and Laimins, 2013; Mehta and Laimins, 2018; Wallace, 2020; Wallace and Galloway, 2014).

In addition to their role in cervical cancers, HPVs cause a growing subset of head and neck squamous cell carcinomas (HNSCCs) (Kobayashi et al., 2018). These HPV positive HNSCCs (HPV + HNSCCs) are an increasing proportion of malignancies in developed countries (Chaturvedi and Zumsteg, 2018; Marur et al., 2010). This increase is occurring as efforts to combat the abuse of tobacco and alcohol have decreased the number of HNSCCs that are not related to HPV infections (HPV– HNSCCs). There are notable differences in HPV+ and HPV- HNSCCs. Clinically, HPV + HNSCCs are typically less aggressive and more responsive to care (Ang et al., 2010; Ang and Sturgis, 2012). At the molecular level, HPV- HNSCC tend to have p53 mutations, while HPV + HNSCCs more often have wild type p53 and notably higher p16 abundance (Blons and Laurent-Puig, 2003; Maruyama et al., 2014; Westra et al., 2008).

We hypothesize that HPV oncogenes cause other gene expression differences in HNSCCs. To test this hypothesis and identify host gene changes associated with HPV, we used a combination of computational and standard pathology analyses. This mixed-method approach identified increased expression of DNA repair genes in HPV + HNSCCs compared to HPV- HNSCCs. More specifically, this examination of a publicly available dataset from The Cancer Genome Atlas (TCGA) shows genes from two repair pathways (homologous recombination (HR) and translesion synthesis (TLS)) are more robustly expressed in HPV + HNSCCs (Cancer Genome Atlas Network, 2015). Differential expression of three of these genes were associated with changes in HNSCC survival. We generated a novel tissue microarray (TMA) of HPV

* Corresponding author.
E-mail address: nwallac@ksu.edu (N.A. Wallace).

https://doi.org/10.1016/j.virol.2020.07.004
Received 24 April 2020; Received in revised form 1 July 2020; Accepted 3 July 2020
Available online 22 July 2020
0042-6822/

+ and HPV- HNSCCs to further probe this relationship. TMA immunohistochemical staining confirmed our *in silico* data, showing increased DNA repair protein abundance in HPV + HNSCCs. The most specific increase was seen for the homologous recombination protein, RAD51.

2. Results

2.1. DNA repair gene expression was increased in HPV positive HNSCCs compared to HPV negative HNSCCs

To understand how gene expression differed between HPV+ and HPV- HNSCCs, we segregated the TCGA dataset on HNSCCs by the clinical designation of HPV status as originally reported (Cancer Genome Atlas Network, 2015). There were data from 21 HPV + HNSCCs and 65 HPV- HNSCCs. We ranked genes that were differentially expressed in HPV + versus HPV- HNSCCs based on the statistical significance of the differences. We then used the Gene Ontology enRIchment anaLysis and visuaLizAtion tool (GOrilla) to determine if these differentially expressed genes were involved in any shared cellular processes (Eden et al., 2009) GOrilla analysis demonstrated that the genes that were differentially expressed in HPV + versus HPV- HNSCCs were frequently involved in the cellular stress response (Fig. 1 and Supplemental Data 1). More specifically, there was a striking enrichment for changes in DNA damage repair (DDR) gene expression ($p < 10^{-7}$).

These data demonstrate clear differences in DDR gene expression in HNSCCs based on HPV status, but they do not indicate whether repair gene expression is more often higher or lower in HPV + HNSCCs compared to HPV- HNSCCs. Therefore, we quantified the expression of 137 DDR genes in HPV+ and HPV- HNSCCs. DNA repair genes were chosen using unbiased definitions of six established repair pathways (nucleotide excision repair (NER), Fanconi Anemia repair (FA), base excision repair (BER), TLS, HR and non-homologous end joining (NHEJ)) (Alan and D'Andrea, 2010; Bult et al., 2019; Cooper, 2000; Davis and Chen, 2013; Kanehisa and Goto, 2000; Laat and Hoeijmakers, 1999; Prakash et al., 2005; Whitaker et al., 2017). The ratio of the expression difference and the significance of these changes was determined for each gene (Fig. 2A). This analysis demonstrated that DDR gene expression was commonly increased in HPV + HNSCCs relative to HPV- HNSCCs. We dissected this data further by defining the frequency of increased gene expression among the DDR pathways. Increased DDR gene expression in HPV + HNSCCs was evident across all DDR pathways, ranging from 81.8% of NER genes to 100% of the significant changes in TLS and FA genes (Fig. 2B).

Based on these findings and our laboratory's *in* vitro studies demonstrating HPV oncogenes manipulation of HR and TLS, we focused our analysis on genes from these two pathways [Wendel et al. submitted, 40]. Specifically, we chose four representative TLS genes (PCNA, RAD18, UBE2A and UBE2B) and four representative HR genes (BRCA1, BRCA2, RPA1, RAD51). These analyses included few genes and thus were more amenable to manipulation, so we moved from the clinical definition of HPV status to one defined by molecular signatures and also used in the original report from TCGA (Cancer Genome Atlas Network, 2015). When comparing the expression of these genes, all eight had increased expression in HPV + HNSCCs (Fig. 3A–H). Because the prognosis for HPV + HNSCCs is significantly better than HPV- HNSCCs, we evaluated whether expression of these eight genes was associated with differences in median survival. For this analysis, we included the complete TCGA dataset (Fig. 4). When analyzed together, increased expression of the eight representative TLS and HR genes was not associated with a significant difference in survival (Data Not Shown). However, when analyzed individually, the expression of three of these eight genes was associated changes in survival. Increased expression of two HR genes (BRCA1 and RPA1) was associated with increased HNSCC survival, while increased UBE2A expression correlated with decreased survival (Fig. 4).

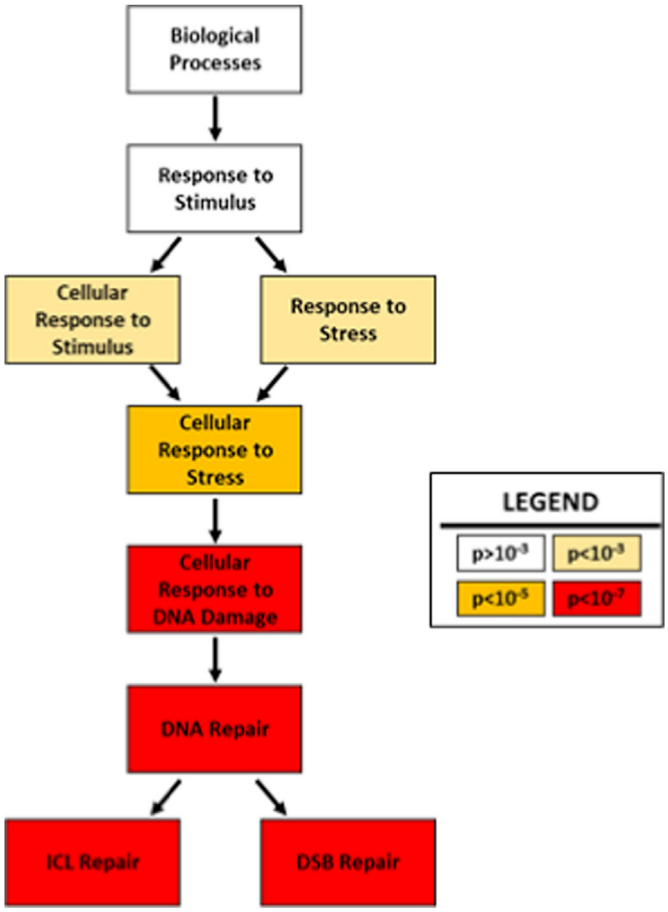

Fig. 1. Gene Ontology Analysis of Differential Gene Expression in HPV + versus HPV- HNSCCs. Results for gene ontology (GO) analysis of gene expression differences in HPV + compared to HPV- HNSCCs. Boxes show cellular functions in hierarchical order, descending from general to specific functions. Darker colors indicate greater statistical significance of enrichment.

2.2. Differences in homologous recombination and translesion synthesis protein abundance were detected in HNSCCs

Our data suggested that increased HR and TLS gene expression has the potential to serve as a biomarker for HPV status in HNSCCs. Unfortunately, detecting differences in gene transcripts is not practical clinically. However, immunohistochemical staining (IHC) is frequently used to distinguish tumors from margins and among different types of tumors. This includes the detections of increased p16 levels as a marker of HPV status in HNSCCs. An obvious and preliminary step in developing biomarkers for detection by IHC is confirming that there are detectable differences from control tissue. Based on our computational data, we hypothesized that elevated HR and TLS protein abundance would be detectable by IHC in a subset of HNSCCs. Specifically, we hypothesized that these increases would be seen more often in HPV + HNSCC. We began testing the first part of our hypothesis by comparing TLS and HR protein abundance in HNSCC and untransformed oral mucosa using the Human Protein Atlas (HPA) (Uhlén et al., 2015, 2005). This resource provided histology data for these tissue that had been scored by independent pathologists. As a positive control, we observed p16 staining (Fig. 5). There were detectable differences in p16 between control and transformed oral epithelial cells. P16 abundance was at times higher in HNSCCs than control tissue. However, to our surprise, p16 levels were most often reduced compared to control tissue. Because the HPV status of these samples was

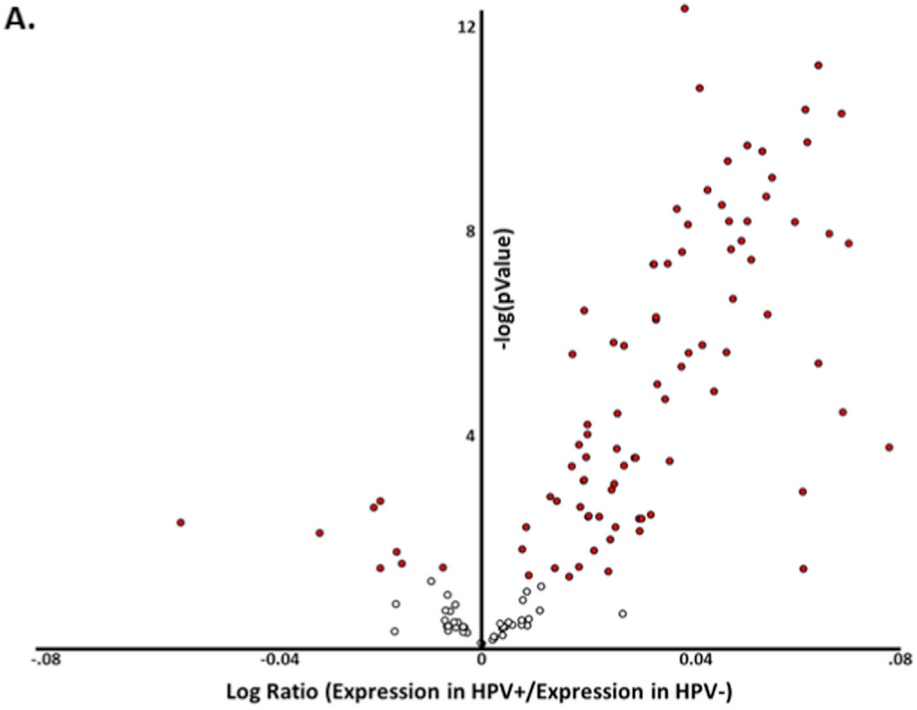

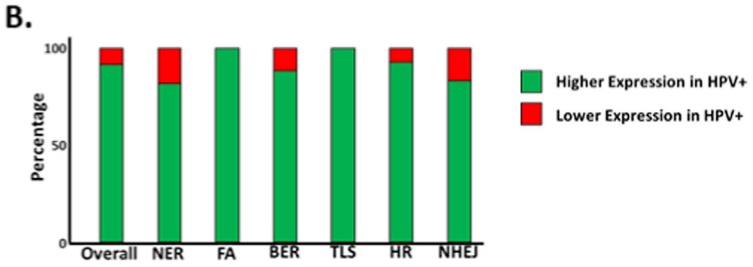

Fig. 2. Differences in DNA Repair Gene Expression Between HPV- and HPV + HNSCCs. A. Volcano plot of DNA repair gene expression compared between HPV+ and HPV- HNSCCs. Statistical significance is shown on the Y-axis, plotted as the negative log of the p-value. The log ratio of gene expression in HPV + HNSCCs compared to HPV- HNSCCs are shown on the X-axis. Red circles denote significant changes in expression ($p < 0.05$), while clear dots indicate points below this statistical cutoff. Data points to the left of the Y-axis have decreased expression in HPV + HNSCCs. Data points to the right of the Y-axis have increased expression in HPV + HNSCCs. B. Bar graph showing the ratio of differnces in DNA repair gene expression in HNSCCs based on HPV status. Red indicates the percentage of genes with lower expression in HPV + HNSCCs. Green indicates the percentage of genes with higher expression in HPV + HNSCCs. Data is shown for genes "overall" and grouped into six pathways (NER = nucleotide excision repair, FA = Fanconi anemia repair, BER = base excision repair, TLS = translesion synthesis, HR = homologous recombination, NHEJ = non-homologous end joining).

undetermined, this could indicate that most HNSCCs in the HPA are HPV negative. We used a housekeeping gene (nucleolin) as a negative control. There was no differential nucleolin staining between transformed or control tissue.

Having confirmed the utility of this resource, our next step was to use data contained in the HPA to conduct a preliminary analysis of TLS and HR proteins as biomarkers for HPV status in HNSCCs. Specifically, our goal was to determine if any of the gene products of BRCA1, RAD18, PCNA, UBE2A/B (RAD6), RAD51 and RPA1 (RPA70) could be detected at higher levels in HNSCCs compared to normal oral mucosa. These data were promising as a proportion of HNSCCs had BRCA1, RAD51, RAD18, and PCNA levels higher than control tissue. Notably, the frequency of their increase was at least as high as the frequency of increased p16 (Fig. 5).

While these data were encouraging, the inability to compare repair protein staining levels among HPV+ and HPV- HNSCC represented a significant shortcoming. To address this gap in our analysis, we generated a novel tissue microarray (TMA) to determine if the abundance of these seven representative DDR proteins differed between HPV+ and HPV- HNSCCs. The TMA consisted of 27 HPV+ and 9 HPV- HNSCCs. Patient demographic and tumor variables were compared between HPV positive and negative groups (Table 1). Significant differences in mean age existed between groups (58.7 in HPV+, 69.7 in HPV-, $p < 0.01$), consistent with the younger demographic of people with HPV + HNSCCs (Chaturvedi and Zumsteg, 2018). In addition, HPV + tumors were more likely to be poorly differentiated, though not statistically significant ($p = 0.11$). This reflects an established tendency for HPV + tumors to present with de-differentiated histopathology (Dahlstrom et al., 2003). Individuals with HPV- tumors were more likely to be recurrent or previously treated, though again not statistically significant ($p = 0.06$). This was consistent with the recognized tendency for HPV- HNSCCs to recur more frequently (Faraji et al., 2017). No other clinical or tumor characteristics were notably different between groups, including gender, tumor stage, perineural invasion and lymphovascular invasion status.

We used a composite scoring approach for the analysis of the TMA. This took into account percentage of the tumor stained and the intensity of the staining. Inter-rater reliability between pathologists was excellent with an intra-class correlation coefficient of 0.90. Computer assisted analysis was compared to pathologist analysis and demonstrated similar results (Pearson correlation coefficient = 0.68). While no differences were seen in four of queried proteins (RPA70, BRCA2, PCNA and RAD18), there was greater IHC staining for two HR proteins, RAD51 and BRCA1 (Fig. 6 and Supplemental Fig. 1). Mean composite scores in BRCA1 analysis for HPV+ and HPV- HNSCCs were 1.04 and 0.63 respectively, which approached significance ($p = 0.07$). Mean composite scores for RAD51 significantly differed between HPV+ and HPV- HNSCCs (2.06 and 0.76, respectively, $p < 0.01$, Fig. 6).

3. Conclusions

The incidence of HPV + HNSCC is rising rapidly (Chaturvedi and Zumsteg, 2018; Marur et al., 2010). Given the known differences between HPV+ and HPV- HNSCCs with respect to their epidemiology, clinical behavior, response to treatment, and prognosis, biomarkers capable of distinguishing between the two types of HNSCCs are useful

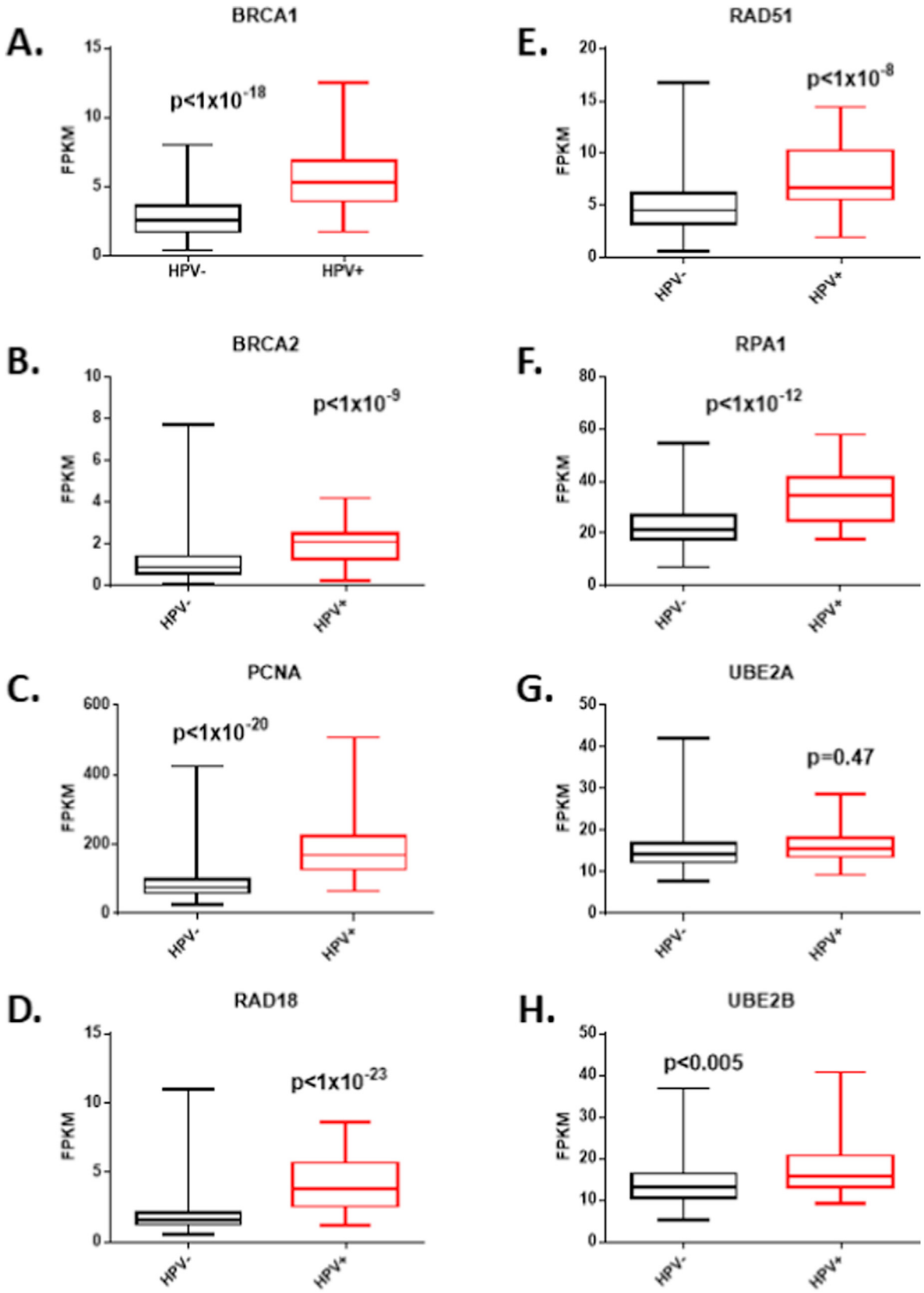

Fig. 3. Expression of Representative Translesion Synthesis and Homologous Recombination Genes is Higher in HPV + HNSCCs. Box plots depict the expression of A. BRCA1, B. BRCA2, C. PCNA, D. RAD18, E. RAD51, F. RPA1, G. UBE2A, and H. UBE2B gene expression in HPV + (red) and HPV- (black) HNSCCs. Expression is plotted as FPKM (fragments per kilobase of exon model per million reads mapped), a standard normalization of gene expression based on RNA-seq data found in the TCGA database.

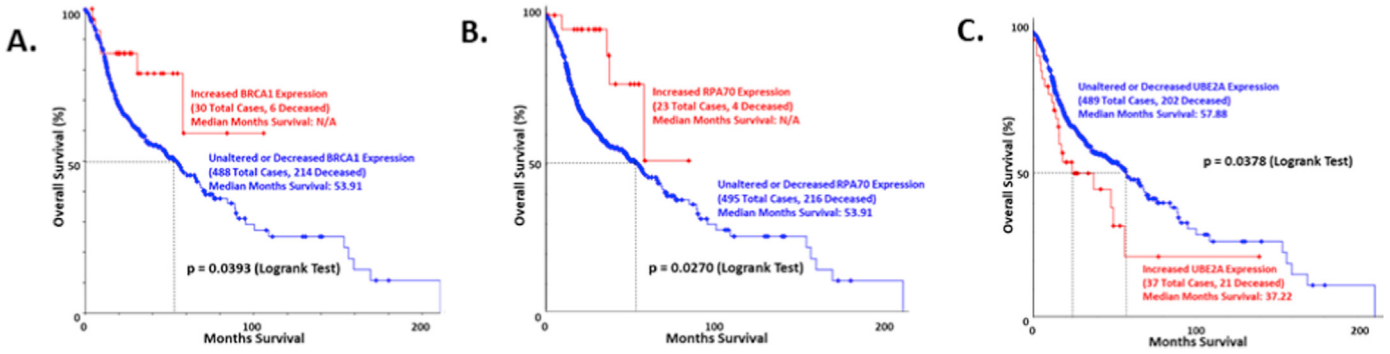

Fig. 4. Prognostic Value of DNA Repair Gene Expression in HNSCCs. Kaplan Meier curves for HNSCCs differentiated by expression of A. BRCA1, B. RPA70, and C. UBE2A. These plots were generated using data from the Cancer Genome Atlas. Patients who had cancers with significantly high expression (z score ≥ 2) are shown in red. All other patients are shown in blue. The dotted black line provides visualization of the median survival calculation. P-values denoting significant difference (log-rank test) in the two populations are indicated along with the population sizes.

(Ang et al., 2010; Ang and Sturgis, 2012; Gillison et al., 2008). While direct detection of HPV is an attractive option, it is more expensive than tradition pathologic approaches. This gap in clinical diagnostic tests merits new investigations of expression changes associated with HPV + HNSCCs. We took a multipronged approach to objectively identify genes that were differentially expressed in HPV + compared to HPV- HNSCCS. Our computational analysis of the TCGA database demonstrated that the expression of genes involved in DNA repair was higher in HPV + HNSCCs (Figs. 1–3). We also found that expression of three of these genes (UBE2A, BRCA1, and RPA1) significantly correlated with survival (Fig. 4). Importantly, increased UBE2A expression was a negative prognostic factor. This indicates that the relationship between DDR gene expression is nuanced and that all repair genes cannot be treated as indirect indicators of HPV status. Our transcriptomic analysis support this assertion as we found UBE2A expression did not significantly differ between HPV+ and HPV- HNSCCs. Our analysis of HNSCC tissues from the HPA demonstrated that it was possible to detect differences in DDR protein abundance in HNSCCs compared to control tissue. Moreover, these differences were similar to the differences detected when the same comparison was made using an established biomarker of HPV status, p16 (Fig. 5). Generating a TMA with HPV+ and HPV- HNSCCs allowed us to show that increased repair gene transcripts translated to increased protein that was detectable by IHC (Fig. 6). In summary, we found that DDR gene expression in HPV + HNSCC was similar to the alterations observed with tissue culture systems (Wallace, 2020; Wallace and Galloway, 2014). Further, these results are similar with another recent effort to understand if DNA repair protein abundance mirrored HPV status in HNSCCs (Kono et al., 2020). This supports the value and validity of *in vitro* characterization of HPV oncogene biology.

Currently, p16 is used as a surrogate marker of HPV in HNSCCs (Liang et al., 2012). p16 levels are higher in HPV + HNSCCs and much of the biology driving this change is understood. HPV E7 deregulates the cell cycle by disrupting Rb-E2F complexes (Dyson et al., 1989, p. 7).

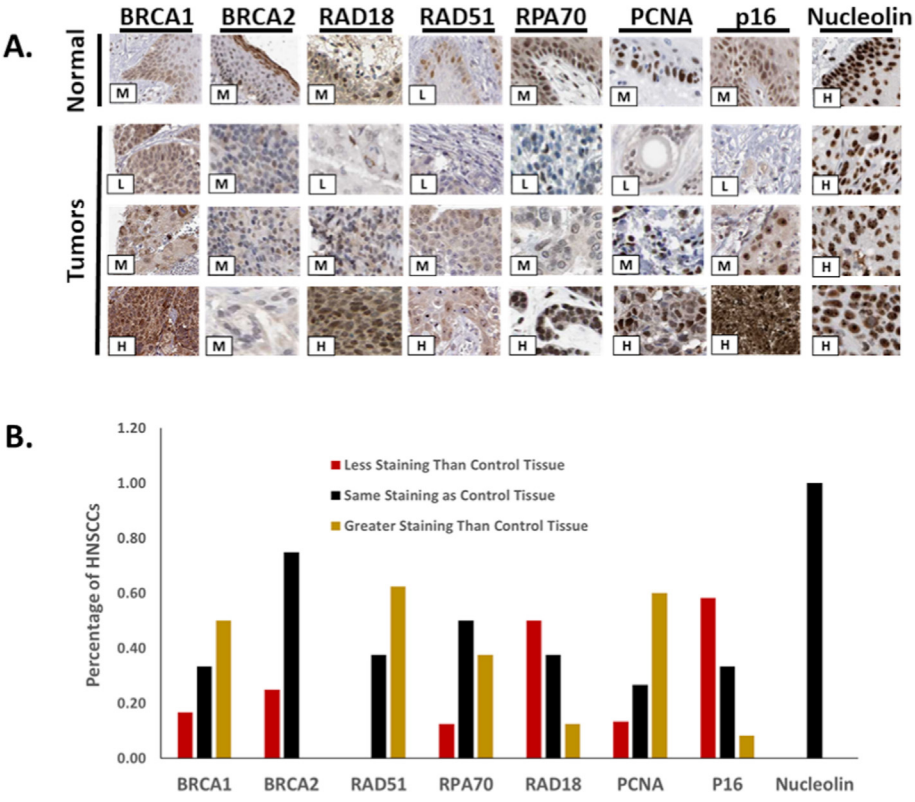

Fig. 5. DNA Repair Protein Abundance Varies Among HNSCCs and Compared to Normal Oral Epithelia. A. Representative IHC staining of DNA repair proteins in untransformed oral epithelia (normal) and HNSCCs (tumors) from the Human Protein Atlas (top). Letters in the lower left of each image indicate the composite score of the tissue shown. (H = High, M = Medium, L = Low) For normal tissue, the representative image corresponds to the knowledge-based annotation provided by Human Protein Atlas. B. The distribution of composite scores compared to control tissue. Red bars denote the percentage of tumors with a composite score lower than control tissue. Black bars denote the percentage of tumors with the same composite score as control tissue. Brown bars denote the percentage of tumors with a composite score higher than control tissue. P16 is included as an established biomarker of HPV status with more than half of its composite scores higher or lower than control tissue. Nucleolin is included as a negative control with composite scores that match control tissue.

Table 1
Tumor Microarray Demographic Data. Patient and tumor characteristics are compared between HPV+ and HPV- HNSCC groups.

		HPV Positive n = 26	HPV Negative n = 9	p =
Age (mean (SD))		58.7 (10.1)	69.7 (9.4)	0.0069
Sex (n (%))	Male	19 (73.1)	6 (66.7)	0.6936
	Female	7 (26.9)	3 (33.3)	
Tumor Site (n (%))	Tonsil	17 (65.4)	3 (33.3)	0.3241
	Base of tongue	9 (34.6)	5 (55.6)	
	Soft palate	0 (0)	1 (11.1)	
Perineural Invasion (n (%))		5 (19.2)	1 (11.1)	1
Lymphovascular Invasion (n (%))		4 (15.4)	2 (22.2)	0.6353
Recurrence/Prior Treatment (n (%))		0 (0)	2 (22.2)	0.0605
Histologic Grade (n (%))	1–2	12 (46.2)	1 (11.1)	0.1094
	3–4	14 (53.8)	8 (88.9%)	
T Stage (n (%))	1–2	22 (84.6)	7 (77.8)	0.6353
	3–4	4 (15.4)	2 (22.2)	

This causes replication stress and increased p16 expression. As a surrogate marker of HPV, p16 is notably sensitive. However, p16 is also influenced by stimuli other than HPV E7 (e.g., B-RAF activation) (Mackiewicz-Wysocka et al., 2017). Because differences in RAD51 abundance between HPV+ and HPV- are detectable by IHC, changes in RAD51 (and potentially other DDR protein levels) may be able to complement existing biomarkers. For instance, combining p16 with RAD51 could decrease the risk of false positives and more accurately triage HNSCCs by HPV status.

Expression of UBE2A, BRCA1 and RPA1 each significantly correlated with HNSCC survival. HPV oncogenes cause increased expression of both BRCA1 and RPA1 in cell culture systems (Wallace et al., 2017). This observation combined with the positive prognostic value of their expression suggests that they may also be acting as surrogate markers of HPV status. Our TMA data support this position. It is more difficult to explain the correlation of increased UBE2A expression with decreased survival. UBE2A expression did not significantly vary between HPV- and HPV + HNSCCs. An attractive explanation is that high UBE2A expression promotes Cisplatin resistance. Both HPV+ and HPV- HNSCCs are frequently treated with the drug and UBE2A is an essential component of TLS, a pathway that promotes Cisplatin resistance when over-activated (Albertella et al., 2005; Srivastava et al., 2015).

In summary, our data support the development of TLS and HR proteins as biomarkers of HPV status in HNSCCs. However, they also require further investigation and substantiation. Our future studies will focus on the expansion of our TMA. While the data presented here is interesting, expanding our TMA to include additional HPV+ and HPV- HNSCC samples as well as non-tumor control tissues would be an improvement. Further, determining HPV status by more definitive methods than p16 would also improve our analysis.

4. Materials and methods

Human Protein Atlas: Representative IHC and staining information was obtained from the HPA (Uhlén et al., 2005). Composite gene marker IHC scores were determined by evaluating staining intensity and frequency. These were then converted to categories corresponding to the knowledge-based annotation used by the HPA for control tissue.

The Cancer Genome Atlas (TCGA) Analysis: HNSCC TCGA data were analyzed to define mRNA expression (Uhlén et al., 2015, 2005). Expression levels were normalized to control tissues. For the analysis found in Figs. 1 and 2, HPV status was based on clinical criteria as reported to TCGA. To be considered "clinically positive" for HPV, the tumor had to be located in an oropharyngeal subsite and be accompanied by a positive assay for HPV that was reported in the electronic case report. Tumors where HPV status were not determined excluded from this analysis.

For the analysis of gene expression found in Fig. 3, the HPV status was based on molecular signatures that include microRNA, DNA methylation, gene expression (cellular and viral) as reported in TCGA manuscript (Cancer Genome Atlas Network, 2015). These approaches are similar, but identical to more recent efforts to analyze HPV status in HNSCCs (Johnson et al., 2018; Pérez Sayáns et al., 2019)

The web-based analysis tools at www.cbioportal.com were used to examine RNAseq data from these tumors (Cerami et al., 2012; Gao et al., 2013).

Protein and Gene Designations: When the gene and protein names differ, we show both in this format: GENE (PROTEIN).

Tissue Microarray Creation: De-identified archival formalin fixed, paraffin embedded patient tissue was obtained from the University of Kansas Medical Center, Biospecimen Repository Core Facility using an Institutional Review Board approved protocol. p16 IHC served as a marker of HPV positive samples. Tumors were considered p16 positive when there was strong and diffuse staining in at least 75% of tumor cells. Surgical specimens from HPV+ and HPV- HNSCCs were selected. Thirty-six total specimens were included in the TMA (27 HPV+ and nine HPV- specimens). Representative areas were marked on hematoxylin and eosin stained slides by a board certified pathologist for use. Using the marked slide as a map, 2-mm thick core punches were taken from the corresponding donor paraffin block and transferred to a recipient paraffin block using the TMArrayer instrument (Pathology Devices). The block containing unique donor cores were sectioned at 4um, mounted on adhesive slides, and dried prior to staining procedures.

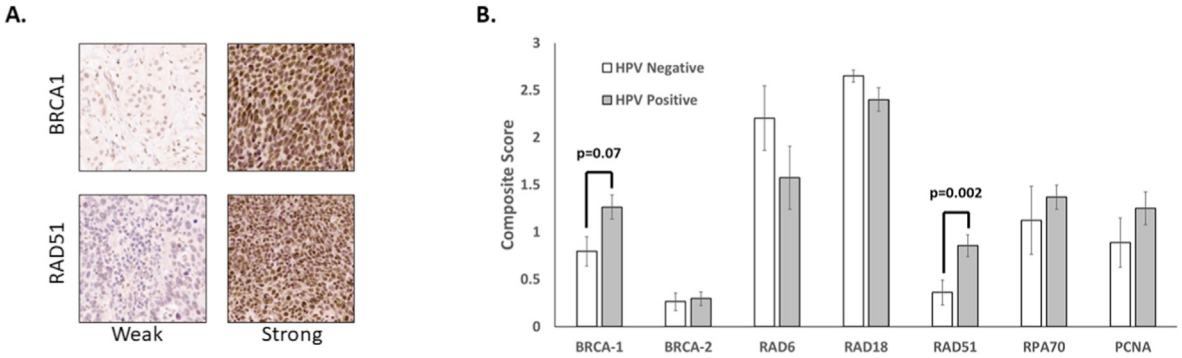

Fig. 6. Immunohistochemical analysis of DNA repair proteins in HPV positive and negative HNSCC. A. Representative images of tumor sections considered to have weak or strong staining for RAD51 or BRCA1 as indicated. B. Immunohistochemical analysis was performed for seven DNA repair proteins using a tissue microarray derived from 27 HPV positive and nine HPV negative HNSCC specimens. Staining intensity and percentage of nuclear staining were measured to derive composite scores that were compared between groups using Mann-Whitney U-test. P values are indicated for comparisons that approached or exceeded cutoffs for statistically significance. All other comparisons did not approach significance.

Immunohistochemistry: Slides were baked at 60 °C for 1 h. After deparaffinization and rehydration, tissue sections were treated with either citrate buffer or Borg Decloaker for 5 min in a pressure cooker for antigen retrieval. Hydrogen peroxide (3%) was applied to the sections for 10 min. Sections were incubated with primary antibodies against BRCA1 (Biocare Medical), BRCA2 (Proteintech), PCNA, RAD51 (Abcam), RAD6, RAD18 or RPA1/RPA70 (Abcam) for 30 min. After buffer rinsing, sections were incubated with anti-mouse HRP-labeled polymer (EnVision) or anti-HRP-labeled polymer (Mach2) for 30 min and buffer rinsed twice. Finally, the staining was visualized by DAB+ (Dako). IHC staining was performed using the IntelliPATH FLX Automated Stainer at room temperature. A light hematoxylin counterstain was performed, then slides were dehydrated, cleared, and mounted using permanent mounting media.

Immunohistochemical Analysis: TMA slides were analyzed independently by two board-certified pathologists who were blinded to the sample's HPV status. Tumors were scored for intensity of staining on a scale of zero to four and on the percentage of tumor cells that were positive. A composite score between zero and four was derived by multiplying the intensity by percent staining. Aperio ImageScope (Version 12.3.0) was used for a secondary computer-based analysis to validate pathologist's assessments. An algorithm was created within the program to capture staining intensity and percentage. This was optimized for accuracy on a series of sample slides.

Clinical Data Analysis: De-identified clinical data were received from the University of Kansas Medical Center's Biospecimen Repository Core Facility. Age was provided in five-year ranges and the median range was used for data analysis.

Statistical Analysis: SPSS software was used for statistical analyses of the TMA (version 22; IBM Corp). Fishers Exact and Analysis of Variance tests were applied to categorical variables and Mann-Whitney U tests were applied to continuous variables. Significance was only reported for p-values < 0.05. Kaplan-Meier curves display survival data, and the logrank test assessed survival differences. TCGA data were analyzed using the analysis tools at www.cbioportal.org (Cerami et al., 2012; Gao et al., 2013).

Pathway and Gene Ontology Analysis: The Kyoto Encyclopedia of Genes and Genomes and The Mouse Genome Informatics (MGI) were used to identify gene subsets specific to the following pathways: TLS, HR, NER, FA, BER, NHEJ (Bult et al., 2019; Kanehisa and Goto, 2000). MGI was used to define genes in the translesion synthesis pathway because this pathway was not included in the Kyoto Encyclopedia of Genes and Genomes. We compared differences in gene expression between HPV+ and HPV- HNSCC tumors and used p-value data to rank genes. Gene ontology analysis of this ranked list was conducted using the Gene Ontology enrichment anaLysisand visualizAtion (GOrilla) online tool. A threshold of $p < 10^{-5}$ was chosen.

CRediT authorship contribution statement

Andrew J. Holcomb: Conceptualization, Methodology, Validation, Writing - original draft, Writing - review & editing, Investigation. **Laura Brown:** Conceptualization, Methodology, Validation, Writing - original draft, Writing - review & editing, Investigation. **Ossama Tawfik:** Conceptualization, Methodology, Validation, Writing - original draft, Writing - review & editing, Investigation, Supervision, Funding acquisition. **Rashna Madan:** Conceptualization, Methodology, Validation, Writing - original draft, Writing - review & editing, Investigation, Supervision. **Yelizaveta Shnayder:** Conceptualization, Writing - original draft, Writing - review & editing, Resources, Supervision, Funding acquisition. **Sufi Mary Thomas:** Conceptualization, Writing - original draft, Writing - review & editing, Supervision, Funding acquisition. **Nicholas A. Wallace:** Conceptualization, Software, Methodology, Validation, Writing - original draft, Writing - review & editing, Investigation, Supervision, Funding acquisition.

Declaration of competing interest

The authors declare that they have no conflicts of interests related to the work described in our manuscript.

Acknowledgements

We acknowledge the University of Kansas Cancer Center's Biospecimen Repository Core Facility for helping obtain human specimens. This work was supported by the National Institutes of Health (P20-GM103418; YS and NAW and R01 CA227838; SMT), and the University of Kansas Cancer Center (CCSG P30CA168524; SMT).

Appendix A. Supplementary data

Supplementary data to this article can be found online at https://doi.org/10.1016/j.virol.2020.07.004.

References

Alan, D., D'Andrea, M.D., 2010. The Fanconi anemia and breast cancer susceptibility pathways. N. Engl. J. Med. 362, 1909–1919. https://doi.org/10.1056/NEJMra0809889.

Albertella, M.R., Green, C.M., Lehmann, A.R., O'Connor, M.J., 2005. A role for polymerase η in the cellular tolerance to cisplatin-induced damage. Canc. Res. 65, 9799–9806. https://doi.org/10.1158/0008-5472.CAN-05-1095.

Anacker, D.C., Aloor, H.L., Shepard, C.N., Lenzi, G.M., Johnson, B.A., Kim, B., Moody, C.A., 2016. HPV31 utilizes the ATR-chk1 pathway to maintain elevated RRM2 levels and a replication-competent environment in differentiating keratinocytes. Virology 499, 383–396. https://doi.org/10.1016/j.virol.2016.09.028.

Anacker, D.C., Gautam, D., Gillespie, K.A., Chappell, W.H., Moody, C.A., 2014. Productive replication of human papillomavirus 31 requires DNA repair factor Nbs1. J. Virol. 88, 8528–8544. https://doi.org/10.1128/JVI.00517-14.

Ang, K.K., Harris, J., Wheeler, R., Weber, R., Rosenthal, D.I., Nguyen-Tân, P.F., Westra, W.H., Chung, C.H., Jordan, R.C., Lu, C., Kim, H., Axelrod, R., Silverman, C.C., Redmond, K.P., Gillison, M.L., 2010. Human papillomavirus and survival of patients with oropharyngeal cancer. N. Engl. J. Med. 363, 24–35. https://doi.org/10.1056/NEJMoa0912217.

Ang, K.K., Sturgis, E.M., 2012. Human papillomavirus as a marker of the natural history and response to therapy of head and neck squamous cell carcinoma. Semin. Radiat. Oncol. 22, 128–142. https://doi.org/10.1016/j.semradonc.2011.12.004.

Bernard, H.-U., Burk, R.D., Chen, Z., van Doorslaer, K., Hausen, H. zur, de Villiers, E.-M., 2010. Classification of papillomaviruses (PVs) based on 189 PV types and proposal of taxonomic amendments. Virology 401, 70–79. https://doi.org/10.1016/j.virol.2010.02.002.

Blons, H., Laurent-Puig, P., 2003. TP53 and head and neck neoplasms. Hum. Mutat. 21, 252–257. https://doi.org/10.1002/humu.10171.

Bosch, F.X., Lorincz, A., Muñoz, N., Meijer, C.J.L.M., Shah, K.V., 2002. The causal relation between human papillomavirus and cervical cancer. J. Clin. Pathol. 55, 244–265.

Boyer, S.N., Wazer, D.E., Band, V., 1996. E7 protein of human papilloma virus-16 induces degradation of retinoblastoma protein through the ubiquitin-proteasome pathway. Canc. Res. 56, 4620–4624.

Bult, C.J., Blake, J.A., Smith, C.L., Kadin, J.A., Richardson, J.E., Mouse Genome Database Group, 2019. Mouse genome database (MGD) 2019. Nucleic Acids Res. 47, D801–D806. https://doi.org/10.1093/nar/gky1056.

Cancer Genome Atlas Network, 2015. Comprehensive genomic characterization of head and neck squamous cell carcinomas. Nature 517, 576–582. https://doi.org/10.1038/nature14129.

Cerami, E., Gao, J., Dogrusoz, U., Gross, B.E., Sumer, S.O., Aksoy, B.A., Jacobsen, A., Byrne, C.J., Heuer, M.L., Larsson, E., Antipin, Y., Reva, B., Goldberg, A.P., Sander, C., Schultz, N., 2012. The cBio cancer genomics portal: an open platform for exploring multidimensional cancer genomics data. Canc. Discov. 2, 401–404. https://doi.org/10.1158/2159-8290.CD-12-0095.

Chappell, W.H., Gautam, D., Ok, S.T., Johnson, B.A., Anacker, D.C., Moody, C.A., 2015. Homologous recombination repair factors Rad51 and BRCA1 are necessary for productive replication of human papillomavirus 31. J. Virol. 90, 2639–2652. https://doi.org/10.1128/JVI.02495-15.

Chaturvedi, A.K., Zumsteg, Z.S., 2018. A snapshot of the evolving epidemiology of oropharynx cancers. Cancer 124, 2893–2896. https://doi.org/10.1002/cncr.31383.

Cooper, G.M., 2000. Recombination between Homologous DNA Sequences.

Dahlstrom, K.R., Adler-Storthz, K., Etzel, C.J., Liu, Z., Dillon, L., El-Naggar, A.K., Spitz, M.R., Schiller, J.T., Wei, Q., Sturgis, E.M., 2003. Human papillomavirus type 16 infection and squamous cell carcinoma of the head and neck in never-smokers: a matched pair analysis. Clin. Canc. Res. 9, 2620–2626.

Davis, A.J., Chen, D.J., 2013. DNA double strand break repair via non-homologous end-joining. Transl. Cancer Res. 2, 130–143. https://doi.org/10.3978/j.issn.2218-676X.2013.04.02.

Doorbar, J., Egawa, N., Griffin, H., Kranjec, C., Murakami, I., 2015. Human papillomavirus molecular biology and disease association. Rev. Med. Virol. 25, 2–23. https://

doi.org/10.1002/rmv.1822.
Doorbar, J., Quint, W., Banks, L., Bravo, I.G., Stoler, M., Broker, T.R., Stanley, M.A., 2012. The biology and life-cycle of human papillomaviruses. Vaccine 30 (5), F55–F70. https://doi.org/10.1016/j.vaccine.2012.06.083.
Dyson, N., Howley, P.M., Münger, K., Harlow, E., 1989. The human papilloma virus-16 E7 oncoprotein is able to bind to the retinoblastoma gene product. Science 243, 934–937.
Eden, E., Navon, R., Steinfeld, I., Lipson, D., Yakhini, Z., 2009. GOrilla: a tool for discovery and visualization of enriched GO terms in ranked gene lists. BMC Bioinf. 10, 48. https://doi.org/10.1186/1471-2105-10-48.
Faraji, F., Eisele, D.W., Fakhry, C., 2017. Emerging insights into recurrent and metastatic human papillomavirus-related oropharyngeal squamous cell carcinoma. Laryngoscope Investig. Otolaryngol. 2, 10–18. https://doi.org/10.1002/lio2.37.
Gao, J., Aksoy, B.A., Dogrusoz, U., Dresdner, G., Gross, B., Sumer, S.O., Sun, Y., Jacobsen, A., Sinha, R., Larsson, E., Cerami, E., Sander, C., Schultz, N., 2013. Integrative analysis of complex cancer genomics and clinical profiles using the cBioPortal. Sci. Signal. 6, pl1. https://doi.org/10.1126/scisignal.2004088.
Gillespie, K.A., Mehta, K.P., Laimins, L.A., Moody, C.A., 2012. Human papillomaviruses recruit cellular DNA repair and homologous recombination factors to viral replication centers. J. Virol. 86, 9520–9526. https://doi.org/10.1128/JVI.00247-12.
Gillison, M.L., D'Souza, G., Westra, W., Sugar, E., Xiao, W., Begum, S., Viscidi, R., 2008. Distinct risk factor profiles for human papillomavirus type 16-positive and human papillomavirus type 16-negative head and neck cancers. J. Natl. Cancer Inst. 100, 407–420. https://doi.org/10.1093/jnci/djn025.
Hong, S., Laimins, L.A., 2013. The JAK-STAT transcriptional regulator, STAT-5, activates the ATM DNA damage pathway to induce HPV 31 genome amplification upon epithelial differentiation. PLoS Pathog. 9, e1003295. https://doi.org/10.1371/journal.ppat.1003295.
Huibregtse, J.M., Scheffner, M., Howley, P.M., 1991. A cellular protein mediates association of p53 with the E6 oncoprotein of human papillomavirus types 16 or 18. EMBO J. 10, 4129–4135.
Johnson, M.E., Cantalupo, P.G., Pipas, J.M., 2018. Identification of head and neck cancer subtypes based on human papillomavirus presence and E2F-regulated gene expression. mSphere 3. https://doi.org/10.1128/mSphere.00580-17.
Kanehisa, M., Goto, S., 2000. KEGG: Kyoto Encyclopedia of genes and genomes. Nucleic Acids Res. 28, 27.
Kobayashi, K., Hisamatsu, K., Suzui, N., Hara, A., Tomita, H., Miyazaki, T., 2018. A review of HPV-related head and neck cancer. J. Clin. Med. 7, 241. https://doi.org/10.3390/jcm7090241.
Kono, T., Hoover, P., Poropatich, K., Paunesku, T., Mittal, B.B., Samant, S., Laimins, L.A., 2020. Activation of DNA damage repair factors in HPV positive oropharyngeal cancers. Virology 547, 27–34. https://doi.org/10.1016/j.virol.2020.05.003.
Laat, W.L.de, Jaspers, N.G.J., Hoeijmakers, J.H.J., 1999. Molecular mechanism of nucleotide excision repair. Genes Dev. 13, 768–785.
Liang, C., Marsit, C.J., McClean, M.D., Nelson, H.H., Christensen, B.C., Haddad, R.I., Clark, J.R., Wein, R.O., Grillone, G.A., Houseman, E.A., Halec, G., Waterboer, T., Pawlita, M., Krane, J.F., Kelsey, K.T., 2012. Biomarkers of HPV in head and neck squamous cell carcinoma. Canc. Res. 72, 5004–5013. https://doi.org/10.1158/0008-5472.CAN-11-3277.
Mackiewicz-Wysocka, M., Czerwińska, P., Filas, V., Bogajewska, E., Kubicka, A., Przybyła, A., Dondajewska, E., Kolenda, T., Marszałek, A., Mackiewicz, A., 2017. Oncogenic BRAF mutations and p16 expression in melanocytic nevi and melanoma in the Polish population. Postepy Dermatol. Alergol. 34, 490–498. https://doi.org/10.5114/ada.2017.71119.
Marur, S., D'Souza, G., Westra, W.H., Forastiere, A.A., 2010. HPV-associated head and neck cancer: a virus-related cancer epidemic. Lancet Oncol. 11, 781–789. https://doi.org/10.1016/S1470-2045(10)70017-6.
Maruyama, H., Yasui, T., Ishikawa-Fujiwara, T., Morii, E., Yamamoto, Y., Yoshii, T., Takenaka, Y., Nakahara, S., Todo, T., Hongyo, T., Inohara, H., 2014. Human papillomavirus and p53 mutations in head and neck squamous cell carcinoma among Japanese population. Canc. Sci. 105, 409–417. https://doi.org/10.1111/cas.12369.
Mehta, K., Laimins, L., 2018. Human papillomaviruses preferentially recruit DNA repair factors to viral genomes for rapid repair and amplification. mBio 9https://doi.org/10.1128/mBio.00064-18. e00064-18.
Münger, K., Werness, B.A., Dyson, N., Phelps, W.C., Harlow, E., Howley, P.M., 1989a. Complex formation of human papillomavirus E7 proteins with the retinoblastoma tumor suppressor gene product. EMBO J. 8, 4099–4105.
Münger, K., Werness, B.A., Dyson, N., Phelps, W.C., Harlow, E., Howley, P.M., 1989b. Complex formation of human papillomavirus E7 proteins with the retinoblastoma tumor suppressor gene product. EMBO J. 8, 4099–4105.
Pérez Sayáns, M., Chamorro Petronacci, C.M., Lorenzo Pouso, A.I., Padín Iruegas, E., Blanco Carrión, A., Suárez Peñaranda, J.M., García García, A., 2019. Comprehensive genomic review of TCGA head and neck squamous cell carcinomas (HNSCC). J. Clin. Med. 8. https://doi.org/10.3390/jcm8111896.
Prakash, S., Johnson, R.E., Prakash, L., 2005. Eukaryotic translesion synthesis DNA polymerases: specificity of structure and function. Annu. Rev. Biochem. 74, 317–353. https://doi.org/10.1146/annurev.biochem.74.082803.133250.
Srivastava, A.K., Han, C., Zhao, R., Cui, T., Dai, Y., Mao, C., Zhao, W., Zhang, X., Yu, J., Wang, Q.-E., 2015. Enhanced expression of DNA polymerase eta contributes to cisplatin resistance of ovarian cancer stem cells. Proc. Natl. Acad. Sci. U.S.A. 112, 4411–4416. https://doi.org/10.1073/pnas.1421365112.
Uhlén, M., Björling, E., Agaton, C., Szigyarto, C.A.-K., Amini, B., Andersen, E., Andersson, A.-C., Angelidou, P., Asplund, A., Asplund, C., Berglund, L., Bergström, K., Brumer, H., Cerjan, D., Ekström, M., Elobeid, A., Eriksson, C., Fagerberg, L., Falk, R., Fall, J., Forsberg, M., Björklund, M.G., Gumbel, K., Halimi, A., Hallin, I., Hamsten, C., Hansson, M., Hedhammar, M., Hercules, G., Kampf, C., Larsson, K., Lindskog, M., Lodewyckx, W., Lund, J., Lundeberg, J., Magnusson, K., Malm, E., Nilsson, P., Odling, J., Oksvold, P., Olsson, I., Oster, E., Ottosson, J., Paavilainen, L., Persson, A., Rimini, R., Rockberg, J., Runeson, M., Sivertsson, A., Sköllermo, A., Steen, J., Stenvall, M., Sterky, F., Strömberg, S., Sundberg, M., Tegel, H., Tourle, S., Wahlund, E., Waldén, A., Wan, J., Wernérus, H., Westberg, J., Wester, K., Wrethagen, U., Xu, L.L., Hober, S., Pontén, F., 2005. A human protein atlas for normal and cancer tissues based on antibody proteomics. Mol. Cell. Proteomics 4, 1920–1932. https://doi.org/10.1074/mcp.M500279-MCP200.
Uhlén, M., Fagerberg, L., Hallström, B.M., Lindskog, C., Oksvold, P., Mardinoglu, A., Sivertsson, Å., Kampf, C., Sjöstedt, E., Asplund, A., Olsson, I., Edlund, K., Lundberg, E., Navani, S., Szigyarto, C.A.-K., Odeberg, J., Djureinovic, D., Takanen, J.O., Hober, S., Alm, T., Edqvist, P.-H., Berling, H., Tegel, H., Mulder, J., Rockberg, J., Nilsson, P., Schwenk, J.M., Hamsten, M., von Feilitzen, K., Forsberg, M., Persson, L., Johansson, F., Zwahlen, M., von Heijne, G., Nielsen, J., Pontén, F., 2015. Proteomics. Tissue-based map of the human proteome. Science 347, 1260419. https://doi.org/10.1126/science.1260419.
Wallace, N.A., 2020. Catching HPV in the homologous recombination cookie jar. Trends Microbiol. 28, 191–201. https://doi.org/10.1016/j.tim.2019.10.008.
Wallace, N.A., Galloway, D.A., 2014. Manipulation of cellular DNA damage repair machinery facilitates propagation of human papillomaviruses. Semin. Canc. Biol. 26, 30–42. https://doi.org/10.1016/j.semcancer.2013.12.003.
Wallace, N.A., Khanal, S., Robinson, K.L., Wendel, S.O., Messer, J.J., Galloway, D.A., 2017. High risk alpha papillomavirus oncogenes impair the homologous recombination pathway. J. Virol. JVI. https://doi.org/10.1128/JVI.01084-17. 01084-17.
Westra, W.H., Taube, J.M., Poeta, M.L., Begum, S., Sidransky, D., Koch, W.M., 2008. Inverse relationship between human papillomavirus-16 infection and disruptive p53 gene mutations in squamous cell carcinoma of the head and neck. Clin. Canc. Res. 14, 366–369. https://doi.org/10.1158/1078-0432.CCR-07-1402.
Whitaker, A.M., Schaich, M.A., Smith, M.S., Flynn, T.S., Freudenthal, BretD., 2017. Base excision repair of oxidative DNA damage: from mechanism to disease. Front. Biosci. (Landmark Ed) 22, 1493–1522.

Journal of Virology®

TRANSFORMATION AND ONCOGENESIS

Beta Human Papillomavirus 8E6 Attenuates LATS Phosphorylation after Failed Cytokinesis

Dalton Dacus,[a] Celeste Cotton,[a,b] Tristan X. McCallister,[a] Nicholas A. Wallace[a]

[a]Division of Biology, Kansas State University, Manhattan, Kansas, USA
[b]Langston University, Langston, Oklahoma, USA

ABSTRACT Beta genus human papillomaviruses (β-HPVs) cause cutaneous squamous cell carcinomas (cSCCs) in a subset of immunocompromised patients. However, β-HPVs are not necessary for tumor maintenance in the general population. Instead, they may destabilize the genome in the early stages of cancer development. Supporting this idea, β-HPV's 8E6 protein attenuates p53 accumulation after failed cytokinesis. This paper offers mechanistic insight into how β-HPV E6 causes this change in cell signaling. An *in silico* screen and characterization of HCT 116 cells lacking p300 suggested that the histone acetyltransferase is a negative regulator of Hippo pathway (HP) gene expression. HP activation restricts growth in response to stimuli, including failed cytokinesis. Loss of p300 resulted in increased HP gene expression, including proproliferative genes associated with HP inactivation. β-HPV 8E6 expression recapitulates some of these phenotypes. We used a chemical inhibitor of cytokinesis (dihydrocytochalasin B [H2CB]) to induce failed cytokinesis. This system allowed us to show that β-HPV 8E6 reduced activation of large tumor suppressor kinase (LATS), an HP kinase. LATS is required for p53 accumulation following failed cytokinesis. These phenotypes were dependent on β-HPV 8E6 destabilizing p300 and did not completely attenuate the HP. It did not alter H2CB-induced nuclear exclusion of the transcription factor YAP. β-HPV 8E6 also did not decrease HP activation in cells grown to a high density. Although our group and others have previously described inhibition of DNA repair, to the best of our knowledge, this marks the first time that a β-HPV E6 protein has been shown to hinder HP signaling.

IMPORTANCE β-HPVs contribute to cSCC development in immunocompromised populations. However, it is unclear if these common cutaneous viruses are tumorigenic in the general population. Thus, a more thorough investigation of β-HPV biology is warranted. If β-HPV infections do promote cSCCs, they are hypothesized to destabilize the cellular genome. *In vitro* data support this idea by demonstrating the ability of the β-HPV E6 protein to disrupt DNA repair signaling events following UV exposure. We show that β-HPV E6 more broadly impairs cellular signaling, indicating that the viral protein dysregulates the HP. The HP protects genome fidelity by regulating cell growth and apoptosis in response to a myriad of deleterious stimuli, including failed cytokinesis. After failed cytokinesis, β-HPV 8E6 attenuates phosphorylation of the HP kinase (LATS). This decreases some, but not all, HP signaling events. Notably, β-HPV 8E6 does not limit senescence associated with failed cytokinesis.

KEYWORDS cancer, cytokinesis, Hippo signaling pathway, human papillomavirus, skin cancer, apoptosis, senescence

The human papillomavirus (HPV) family includes over 200 double-stranded DNA viruses that are divided into five genera, all of which infect human epithelia (1). Upon infecting mucosal or cutaneous tissue, members of each genus can cause a broad array of pathologies. Of these, the most prominent diseases are the anogenital and

Citation Dacus D, Cotton C, McCallister TX, Wallace NA. 2020. Beta human papillomavirus 8E6 attenuates LATS phosphorylation after failed cytokinesis. J Virol 94:e02184-19. https://doi.org/10.1128/JVI.02184-19.

Editor Lawrence Banks, International Centre for Genetic Engineering and Biotechnology

Address correspondence to Nicholas A. Wallace, nwallac@ksu.edu.

Received 2 January 2020
Accepted 19 March 2020
Accepted manuscript posted online 1 April 2020
Published 1 June 2020

oropharyngeal carcinomas caused by alpha genus HPVs (2, 3). Cutaneous beta genus HPVs (β-HPVs) have also been linked to tumorigenesis via high viral DNA loads in cutaneous squamous cell carcinomas (cSCCs) of immunocompromised patients, primarily in sun-exposed skin (4–6).

While β-HPV infections are common in immunocompetent individuals, their contribution to cSCCs is less clear. The main etiological factor in skin cancer pathogenesis is UV. Further, the characterizations of cSCCs in the general population do not include continued β-HPV expression (7–9). Viral loads decrease as lesions progress from precancerous actinic keratosis (AK) to cSCC (10–12). These data have led to the hypothesized "hit-and-run" mechanism of oncogenesis, where β-HPVs cooperate with UV to enhance genomic instability in the early stages of carcinogenesis (10, 13, 14). This elevated mutational load then increases the chances of tumor progression independent of continued viral gene expression.

While it is hard to prove the role of a transient viral infection in persistent cancer, β-HPVs are also a common resident of our skin and are frequently found in AKs. Despite the billions of dollars spent on sun care products annually, 58 million Americans still have one or more AKs. Moreover, over $1 billion is spent during 5.2 million outpatient visits each year for AK treatment (15, 16). The cost of these AKs for the patient, both financial and emotional, increases if these lesions develop into malignancies. Within 1 year of diagnosis, an estimated 0.6% of AKs progress to cSCCs. This progression expands to 2.6% of AKs 5 years after diagnosis (17). Because β-HPV infections are quite common, even a mild increase in cancer risk would be notable. Thus, it is important to understand their potential contribution to the genome instability that drives cSCC progression.

A great deal is known about the tumorigenic potential of β-HPV proteins, particularly the E6 protein. The presence of the putative oncogene E6 from β-HPV 8 (β-HPV 8E6) is enough to cause cancers in mice without UV exposure (18, 19). β-HPV 8E6 inhibits differentiation and promotes proliferation by targeting the NOTCH and TGF-β signaling pathways (20). Another central theme of β-HPV E6 proteins is their ability to bind the cellular histone acetyltransferase p300 (21–24). β-HPV 8E6 and the E6 from β-HPV 5 bind p300 strongly, leading to its destabilization and decreasing DNA damage repair (DDR) gene expression (22, 25, 26). β-HPV type 38's E6 protein has a lower p300-binding affinity and cannot destabilize the cellular protein (27). Nevertheless, binding p300 is essential for HPV38-induced immortalization of human foreskin keratinocytes (HFKs) (28). This suggests that p300 binding may be a shared factor in β-HPV-promoted oncogenesis. Because p300 is a master regulator of gene expression (29, 30), other signaling pathways are likely to be altered by β-HPV 8E6's destabilization of the histone acetyltransferase.

Approximately 10% of skin cells do not divide after entering mitosis (25, 31). β-HPV 8E6 allows these cells to divide by preventing p53 stabilization in a p300-dependent manner (25). p53 accumulation requires the activation of large tumor suppressor kinase (LATS), a kinase in the Hippo signaling pathway (HP) (32). This suggests that β-HPV 8E6 may attenuate LATS activity. The HP also prevents growth by inhibiting the proproliferative activity of YAP/TAZ (32–34). Our analysis of transcriptomic data from cell lines segregated by their relative p300 expression was consistent with p300 acting as a negative regulator of HP and HP-responsive gene expression. We confirm that p300 modulates HP gene expression using HCT 116 cells with and without the p300 gene locus. Expressing β-HPV 8E6 in HFKs recapitulated some, but not all, of these effects. p300 is also important for responding to dihydrocytochalasin B (H2CB)-induced failed cytokinesis. HCT 116 cells without p300 had reduced LATS activation and p53 accumulation. β-HPV 8E6's destabilization of p300 similarly hindered LATS phosphorylation and p53 accumulation. Despite p53's role in apoptosis, elevated p53 levels did not correlate with increased apoptosis until the drug was washed off and the cells were allowed to recover. During this recovery period, β-HPV 8E6 displayed some ability to reduce markers of apoptosis. β-HPV 8E6 did not completely abrogate the HP's response

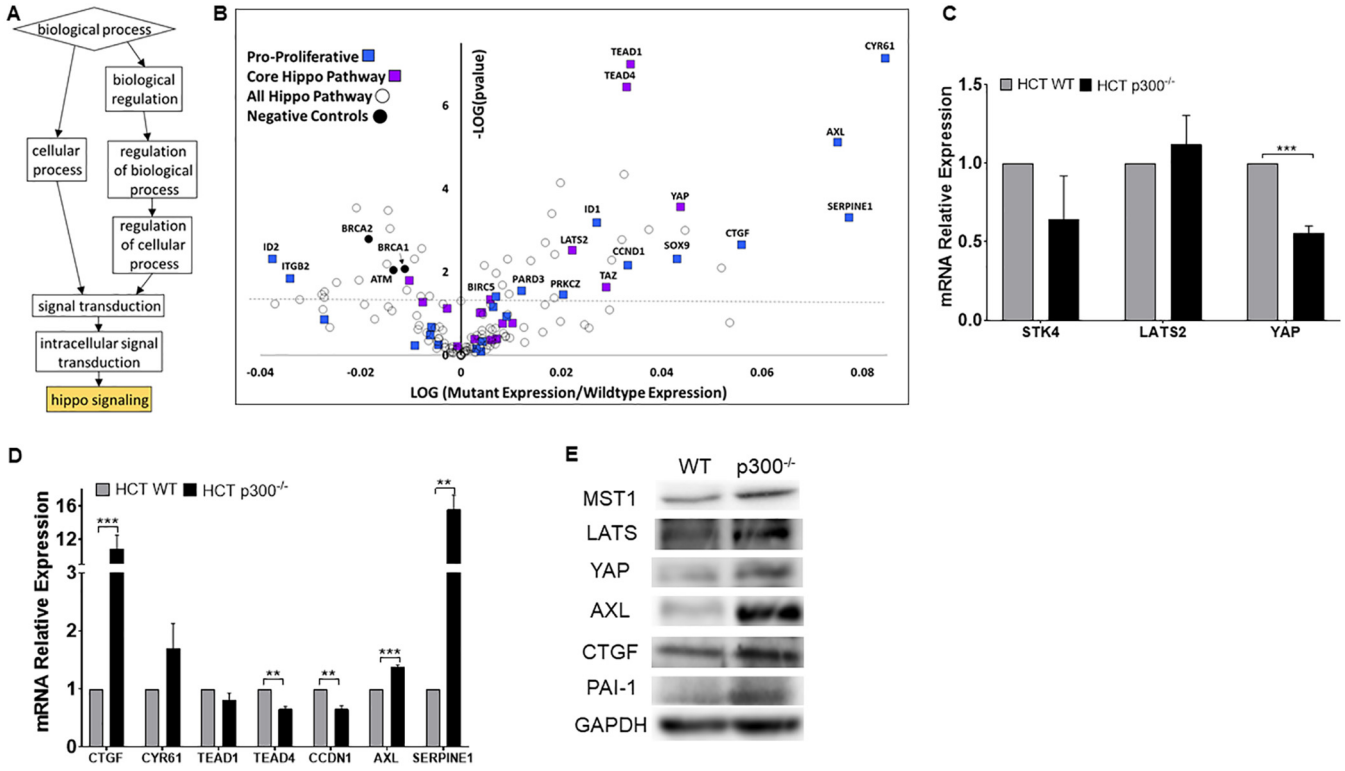

FIG 1 Loss of p300 leads to changes in Hippo pathway gene expression. (A) Gene ontology of 1,020 cancer cell lines via GOrilla. Boxes show GO biological process terms. Boxes descend from general to specific functions. Gold color indicates $P \leq 0.001$. (B) Volcano plot of 154 HP genes in 1,020 cancer cell lines with decreased EP300 expression. The colors blue, purple, and black represent proproliferative TEAD targets, core HP genes, and p300-negative controls, respectively. The horizontal line denotes $P = 0.05$. (C and D) Canonical HP genes (C) and TEAD-regulated mRNA expression (D) in HCT 116 WT and -p300$^{-/-}$ measured by RT-qPCR and normalized to β-actin mRNA. (E) Representative immunoblots of HP and TEAD-regulated proteins in HCT 116 WT and -p300$^{-/-}$. Figures depict the mean ± the standard error of the mean; $n \geq 3$. *, significant difference between indicated samples; *, $P \leq 0.05$; **, $P \leq 0.01$; ***, $P \leq 0.001$ (Student's *t* test).

to failed cytokinesis, as YAP was still excluded from the nucleus. β-HPV 8E6 also did not impede the HP induction in cells grown to a high density.

RESULTS

Loss of p300 alters Hippo pathway gene expression. Animal models show that certain β-HPV E6 genes can contribute to UV-associated carcinogenesis (18, 19, 23). *In vitro* studies from our group and others have added molecular details by describing β-HPV E6's ability to impair the DDR by destabilizing p300 (18, 22, 27, 28, 35, 36). Despite this focus on repair, there are DDR-independent pathways that protect genome fidelity (37–39). To identify p300-regulated pathways that could contribute to β-HPV E6-associated genome destabilization, we performed an *in silico* screen comparing RNA sequencing data among 1,020 cancer cell lines grouped by their relative p300 expression levels (Data Set S1 in the supplemental material) (40–42). The rationale for this approach is based on our prior observations that reducing p300 expression via RNA interference (RNAi) phenocopies β-HPV 8E6's p300-dependent reduction of gene expression (22, 26). We compared expression in cell lines with and without low p300 expression (Z scores of less than −1.64 and greater than −1.64, respectively). Of the cell lines screened, 71 had low p300 expression. The remaining 949 cell lines were considered as not having low p300 expression. This identified 4,211 genes that had altered expression in cells with lower p300 expression. Next, gene ontology (GO) analysis was performed using Gene Ontology enRIchment anaLysis and visuaLizAtion tool (GOrilla) to identify pathways that were significantly altered when p300 expression was reduced (43, 44). Notably, HP was the only pathway identified by GOrilla as significantly changed (Fig. 1A). We then performed a more detailed analysis of HP, using the Kyoto Encyclopedia of Genes and Genomes (KEGG) to provide an unbiased definition of the path-

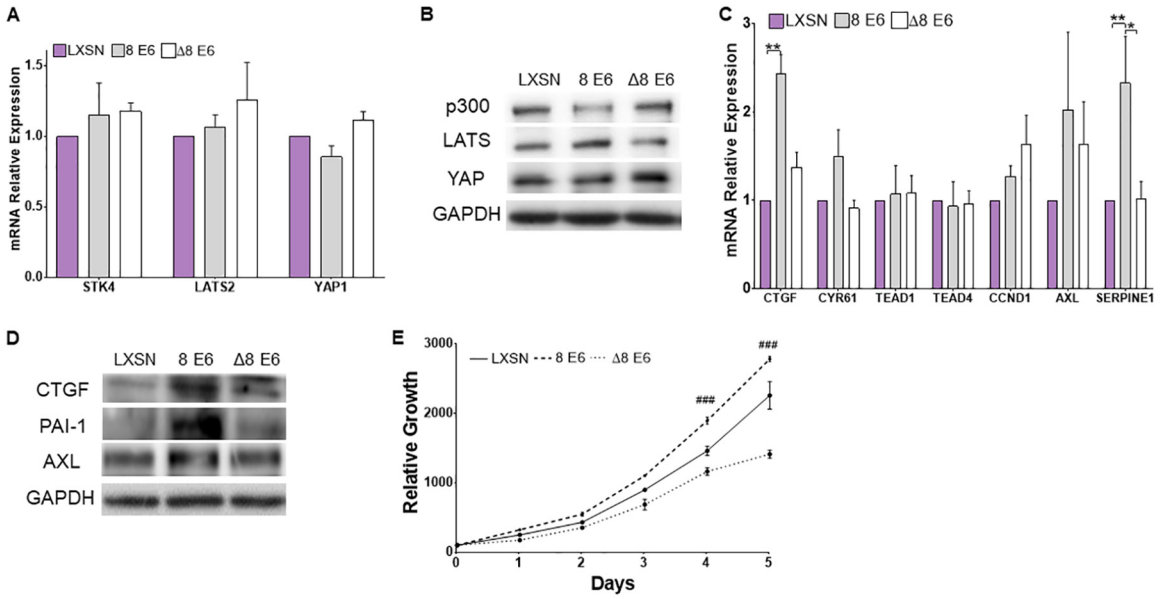

FIG 2 β-HPV 8E6 alters Hippo pathway gene expression. Canonical HP genes (A) and TEAD-regulated mRNA expression (C) in HFKs LXSN, β-HPV 8E6, and β-HPV Δ8E6 measured by RT-qPCR and normalized to β-actin mRNA. Representative immunoblots of HP (B) and TEAD-regulated proteins (D) in HFKs LXSN, β-HPV 8E6, and β-HPV Δ8E6. (E) Relative growth recorded over a 5-day period. Figures depict mean ± standard error of the mean; $n \geq 3$. *, significant difference between indicated samples; #, significant difference from LXSN; one symbol (* or #), $P \leq 0.05$; two symbols (** or ##), $P \leq 0.01$; three symbols (*** or ###), $P \leq 0.001$ (Student's *t* test). In β-HPV Δ8E6, residues 132 to 136 were deleted.

way's members. When p300 expression was reduced, many canonical HP genes were upregulated. However, the most striking changes occurred in proproliferative TEAD-responsive genes (e.g., CYR61, CTGF, AXL, and SERPINE1) (Fig. 1B). As expected, there was a significant reduction in the expression of genes (ATM, BRCA1, and BRCA2) that are dependent on p300 for robust transcription (26, 45, 46).

We used isogenic HCT 116 cells with (WT) or without the p300 gene ($p300^{-/-}$) deleted to confirm our *in silico* analysis (47). The p300 status of these cells was verified by immunoblot (data not shown) before the expression of canonical HP genes (LATS2, STK4, and YAP1) was measured by quantitative real-time PCR (RT-qPCR). Note, STK4 is the gene that encodes the HP kinase, MST1. Of the three HP genes analyzed, the expression of YAP was significantly decreased by p300 loss (Fig. 1C). Next, we defined the abundance of TEAD and TEAD-responsive gene transcripts by RT-qPCR. Seven genes (CTGF, CYR61, TEAD1, TEAD4, CCND1, AXL, and SERPINE1) were chosen based on indications that they were negatively regulated by p300 in our computational screen. Some of these transcripts were more abundant in HCT 116 cells that lacked p300, with increased expression of CTGF, AXL, and SERPINE1 reaching statistical significance (Fig. 1D). Next, we turned to immunoblots to determine if p300 loss leads to changes at the protein level. These data show that increased canonical HP proteins are increased in the absence of p300 (Fig. 1E). The elevated levels extended to AXL, CTGF, and PAI-1 (the protein encoded by the SERPINE1 gene).

***β*-HPV E6 expression alters Hippo pathway gene expression.** β-HPV 8E6 destabilizes p300, but this does not result in complete loss of the histone acetyltransferase. We questioned if this decrease in p300 was enough to dysregulate the HP. To determine the extent that the reduction of p300 by β-HPV 8E6 increased HP gene expression, we defined the expression of canonical HP genes using RT-qPCR. β-HPV 8E6 did not increase expression of the canonical HP genes in human foreskin keratinocytes or HFKs (Fig. 2A). Immunoblots of these cells were consistent with these results except for LATS, which was more abundant when β-HPV 8E6 was expressed (Fig. 2B). We continued this analysis by defining the amount of TEAD and TEAD-responsive genes in HFKs expressing β-HPV 8E6. RT-qPCR comparing expression between vector control

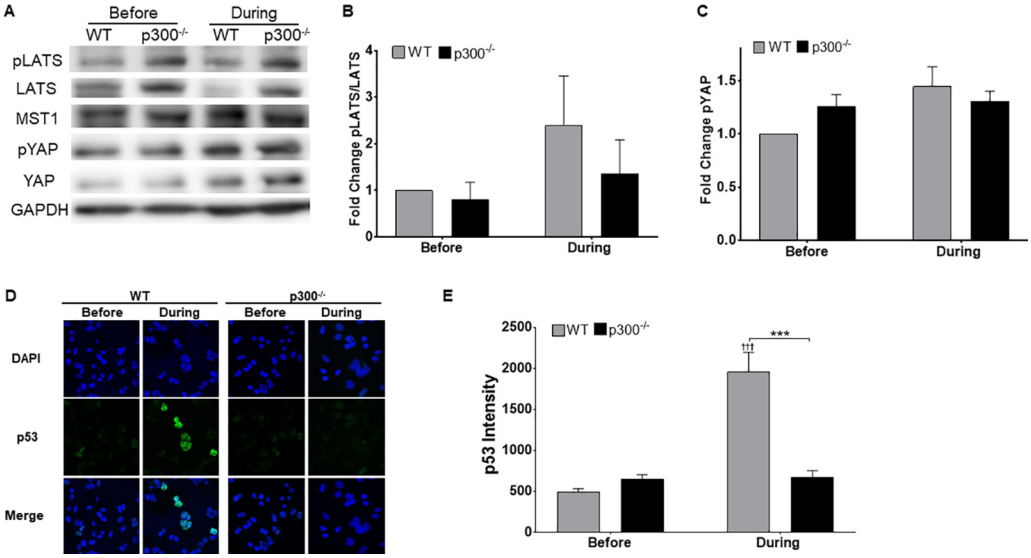

FIG 3 Loss of p300 impedes the Hippo pathway's response to failed cytokinesis. (A) Representative immunoblot of HP proteins before and during H2CB treatment. (B and C) Densitometry of immunoblots described in panel A. GAPDH was used as a loading control. (D) Representative images of p53 (green)- and DAPI (blue)-stained HCT 116 cells before and during H2CB exposure. (E) Relative p53 intensity in HCT 116 cells. At least 150 cells/line were image across three independent experiments. Figures depict mean ± standard error of the mean; $n \geq 3$. *, significant difference between indicated samples; †, significant difference relative to before H2CB; one symbol (* or †), $P \leq 0.05$; two symbols (** or ††), $P \leq 0.01$; three symbols (*** or †††), $P \leq 0.001$ (Student's *t* test). In β-HPV Δ8E6, residues 132 to 136 were deleted.

(LXSN) and β-HPV E6-expressing HFKs found β-HPV E6 increased expression of some TEAD-responsive genes (CTGF, CYR61, CCND1, AXL, and SERPINE1) (Fig. 2C). This was similar to our results in HCT 116 cells except for CCND1. Immunoblots were used to compare protein levels for TEAD-responsive genes, with elevated expression in HFKs expression in β-HPV 8E6. This demonstrated that β-HPV 8E6 increases CTGF, PAI-1, and AXL protein (Fig. 2D). A luciferase reporter assay showed a small but reproducible increase in luciferase expression driven from a TEAD-responsive promoter (data not shown). The increased expression of proproliferative TEAD-responsive genes correlated with increased proliferation (Fig. 2E). Consistent with a p300-dependent mechanism, β-HPV 8E6-driven changes in the HP were abrogated by the deletion of the p300-binding domain in a previously characterized mutant, β-HPV Δ8E6 (Fig. 2).

p300 is necessary for a robust Hippo pathway response to failed cytokinesis. The HP typically restricts growth in response to adverse conditions. This includes failed cytokinesis, induced by dihydrocytochalasin B (H2CB), an inhibitor of actin polymerization (48). Because the loss of p300 promoted proliferation gene expression and dysregulated the HP, we hypothesized that p300 was required for the cellular response to H2CB exposure. Confirming previous data, LATS phosphorylation increased in HCT 116 cells with exposure to 4 μM H2CB (Fig. 3A and B). YAP phosphorylation was similarly elevated by H2CB treatment (Fig. 3A and C). Loss of p300 in HCT 116 cells reduced LATS in response to H2CB (Fig. 3A and B). When cells are treated with H2CB, LATS activation leads to p53 accumulation (32). To determine if p300 was necessary for this response, we used immunofluorescence microscopy to detect p53 in wild-type (WT) and p300 knockout ($p300^{-/-}$) HCT 116 cells grown in H2CB-containing media. We were able to confirm previous reports of p53 buildup in response to the drug in WT HCT 116 cells (Fig. 3D and E). However, p53 did not accumulate in HCT 116 cells lacking p300.

***β*-HPV 8E6 attenuates LATS2 phosphorylation but does not impede nuclear exclusion of YAP.** These data suggest that β-HPV 8E6 alters H2CB induction of the HP. Before evaluating this possibility, we needed to confirm that β-HPV 8E6 did not impede H2CB-induced failed cytokinesis. The visualization of cells with more than one nucleus provides a straightforward measure of failed cytokinesis. We used bright-field and immunofluorescence microscopy to detect the presence of two or more nuclei in cells

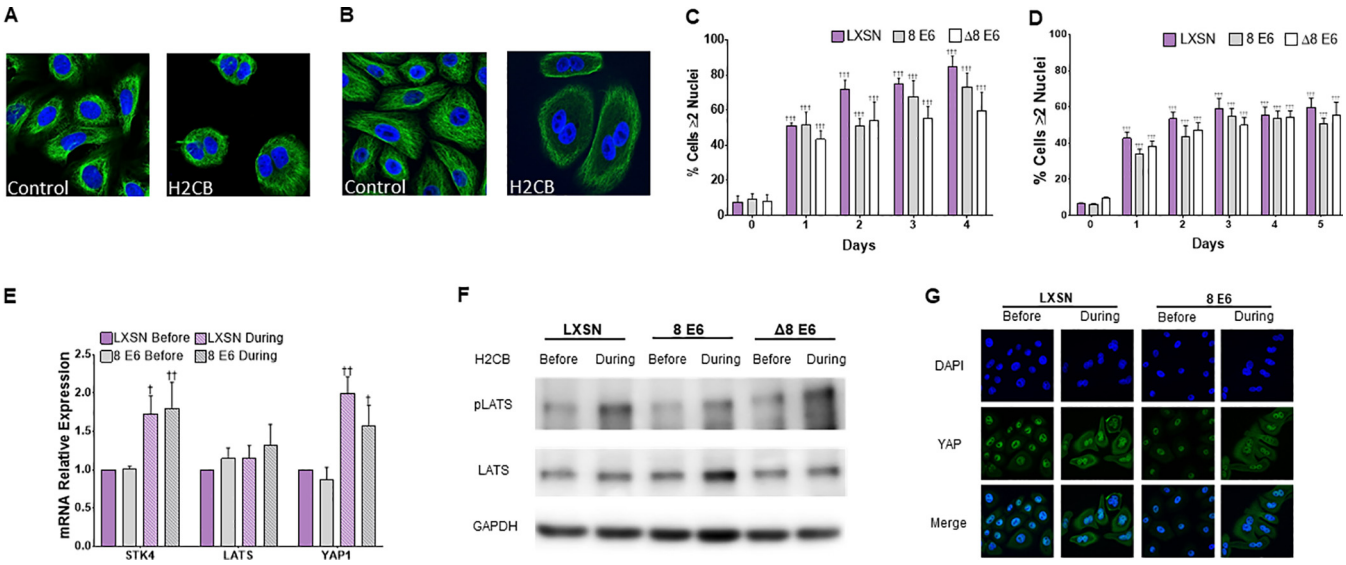

FIG 4 β-HPV 8E6 diminishes LATS phosphorylation during failed cytokinesis. Representative images of U2OS (A) and HFK (B) cells before and during H2CB exposure. Green and blue represent α-tubulin and DAPI, respectively. Quantification of U2OS (C) and HFK (D) cells with 2 or more nuclei as a function of time in H2CB. (E) STK4, LATS, and YAP1 expression before and after H2CB exposure measured by RT-qPCR; $n = 2$. (F) Representative immunoblot of pLATS and totals LATS protein levels in HFK cells before and during H2CB exposure. (G) Representative images of YAP (green)- and DAPI (blue)-stained HFK cells before and during H2CB treatment. At least 200 cells/line were imaged from three independent experiments. Figures depict mean ± standard error of the mean; $n \geq 3$. †, significant difference relative to before H2CB; †, $P \leq 0.05$; ††, $P \leq 0.01$; †††, $P \leq 0.001$ (Student's *t* test). In β-HPV Δ8E6, residues 132 to 136 were deleted.

grown in media containing H2CB (Fig. 4A to D). The percentage of cells with supernumerary nuclei increased as a function of time in H2CB. This was true in both HFK and U2OS cells. The frequency of these abnormal cells was also not notably altered by β-HPV 8E6 or β-HPV Δ8E6. H2CB increased STK4 and YAP1 gene expression. Neither β-HPV 8E6 nor β-HPV Δ8E6 changed this (Fig. 4E). Consistent with our observations in HCT 116 cells, β-HPV 8E6 reduced LATS phosphorylation in cells exposed to H2CB (Fig. 4F). β-HPV Δ8E6 did not attenuate LATS phosphorylation. β-HPV 8E6's restriction of HP signaling may be limited to reducing LATS phosphorylation. β-HPV 8E6 did not change YAP phosphorylation or the abundance of other HP proteins (data not shown). Moreover, immunofluorescence microscopy of YAP shows that β-HPV 8E6 did not hinder the nuclear exclusion of YAP associated with the protein's phosphorylation (Fig. 4G) (49). As expected from these results, H2CB reduced TEAD-responsive promoter activity. β-HPV 8E6 did not prevent this decrease (data not shown).

***β*-HPV 8E6 attenuates p53 accumulation after failed cytokinesis.** Seeing β-HPV 8E6 reduce LATS phosphorylation led us to hypothesize that β-HPV 8E6 would also reduce p53 accumulation in response to H2CB. To test this, we used immunofluorescence microscopy to detect p53 in U2OS grown in media containing H2CB. Consistent with our previous observations, H2CB increased the frequency of cells with more than one nucleus. H2CB increased p53 levels in vector control cells but not in cells expressing β-HPV E6 (Fig. 5A and B). This abrogation of p53 accumulation is likely dependent on p300 degradation, as β-HPV Δ8E6 expressing U2OS and vector control had a similar frequency of p53-stained cells. To validate these results, we used immunoblotting to detect p53 levels in cells grown in H2CB. These experiments also demonstrated that β-HPV 8E6 can repress p53 buildup in response to H2CB. Again, vector control U2OS and β-HPV Δ8E6-expressing U2OS behaved similarly in this assay (Fig. 5C and D). We speculated that the additional p53 found in cells grown with H2CB would result in apoptosis. Fluorescence-based detection of two apoptosis markers (propidium iodide and annexin V) were used to test this idea (50, 51). Surprisingly, we did not see exposure to H2CB associated with an increase in either of these apoptosis markers (Fig. 5E and F). There were also no differences in staining among vector control HFKs and HFKs expressing β-HPV 8E6 or β-HPV Δ8E6.

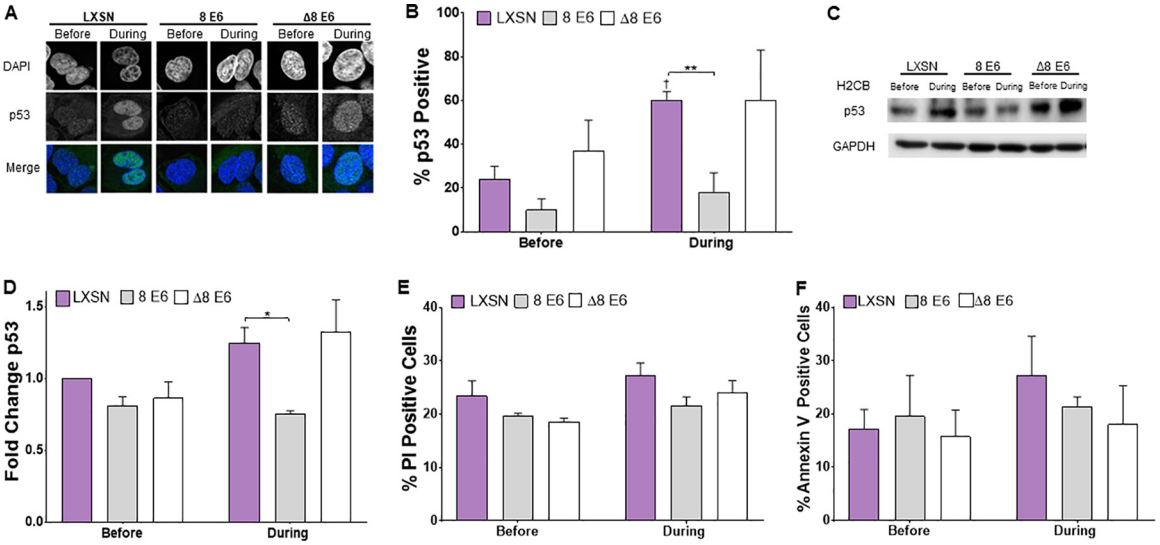

FIG 5 β-HPV 8E6 attenuates p53 accumulation upon H2CB-induced failed cytokinesis. (A) Representative images of p53 and DAPI staining in cells before and during H2CB treatment. (B) Percent of p53-positive U2OS cells. (C) Representative immunoblot of p53 before and during H2CB exposure. (D) Densitometry of immunoblots described in panel C. GAPDH was used as a loading control. Data were normalized to p53 levels in untreated LXSN cells (set to 1). (E) Percent of propidium iodide-stained HFK cells before and during H2CB exposure. (F) Percent of annexin V-stained HFK cells before and during H2CB treatment. At least 200 cells/line were imaged from three independent experiments. Figures depict mean ± standard error of the mean; $n \geq 3$. *, significant difference between indicated samples; †, significant difference relative to before H2CB; one symbol (* or †), $P \leq 0.05$; two symbols (** or ††), $P \leq 0.01$; three symbols (*** or †††), $P \leq 0.001$ (Student's *t* test). In β-HPV Δ8E6, residues 132 to 136 were deleted.

H2CB stalls cytokinesis. It was important to understand if/how those cells recover once the drug is removed and cytokinesis is again possible. To this end, we compared HFKs grown in three conditions: without H2CB (before), grown with 4 days of continual H2CB (during), and grown in H2CB for 4 days followed by 3 additional days without H2CB (after). Figure 6A depicts our experimental setup. We used microscopy to determine the frequency of HFKs with supernumerary nuclei (two or more) in each of these conditions. β-HPV 8E6 did not make supernumerary nuclei less prevalent before or during H2CB exposure (Fig. 6B). However, β-HPV 8E6 decrease supernumerary nuclei after H2CB. This appears to be dependent on p300 destabilization, as supernumerary nuclei were similarly prevalent in HFKs with β-HPV Δ8E6 or vector control. We next used immunoblots to determine if β-HPV 8E6 maintained its ability to attenuate LATS phosphorylation after H2CB. While LATS phosphorylation was elevated in vector control HFKs after H2CB, they remained low in HFKs expressing β-HPV 8E6. This phenotype was not seen in HFKs expressing β-HPV Δ8E6. We used immunofluorescence microscopy as an additional way of detecting p53. These experiments complement the results from immunoblotting, as p53-positive cells were more frequent after H2CB in the vector control but not β-HPV 8E6-expressing HFKs (Fig. 6D and E). We repeated the detection of propidium iodide (PI) and annexin described in Fig. 5 after H2CB. β-HPV 8E6 reduced the percentage of PI-positive HFKs after H2CB compared to vector control and β-HPV Δ8E6-expressing HFKs (Fig. 6F). Annexin V staining was also reduced, but this change did not reach statistical significance (Fig. 6G).

***β*-HPV 8E6 does not completely abrogate the Hippo pathway.** Having seen diminished LATS activation, we queried whether β-HPV 8E6 prevented the HP from restricting growth after H2CB was removed. We used immunofluorescence microscopy to detect Ki67, an established marker of proliferation. While we readily detected Ki67 in both vector control and β-HPV 8E6-expressing HFKs before H2CB, Ki67 was notably less abundant during and after H2CB (Fig. 7A). Ki67 staining intensity was also lower in HFKs expressing β-HPV 8E6 (Fig. 7B). Consistent with these results, HFKs were not capable of long-term proliferation with or without β-HPV 8E6 (data not shown). To understand what was happening to HFKs after H2CB, we stained for senescence-associated beta-

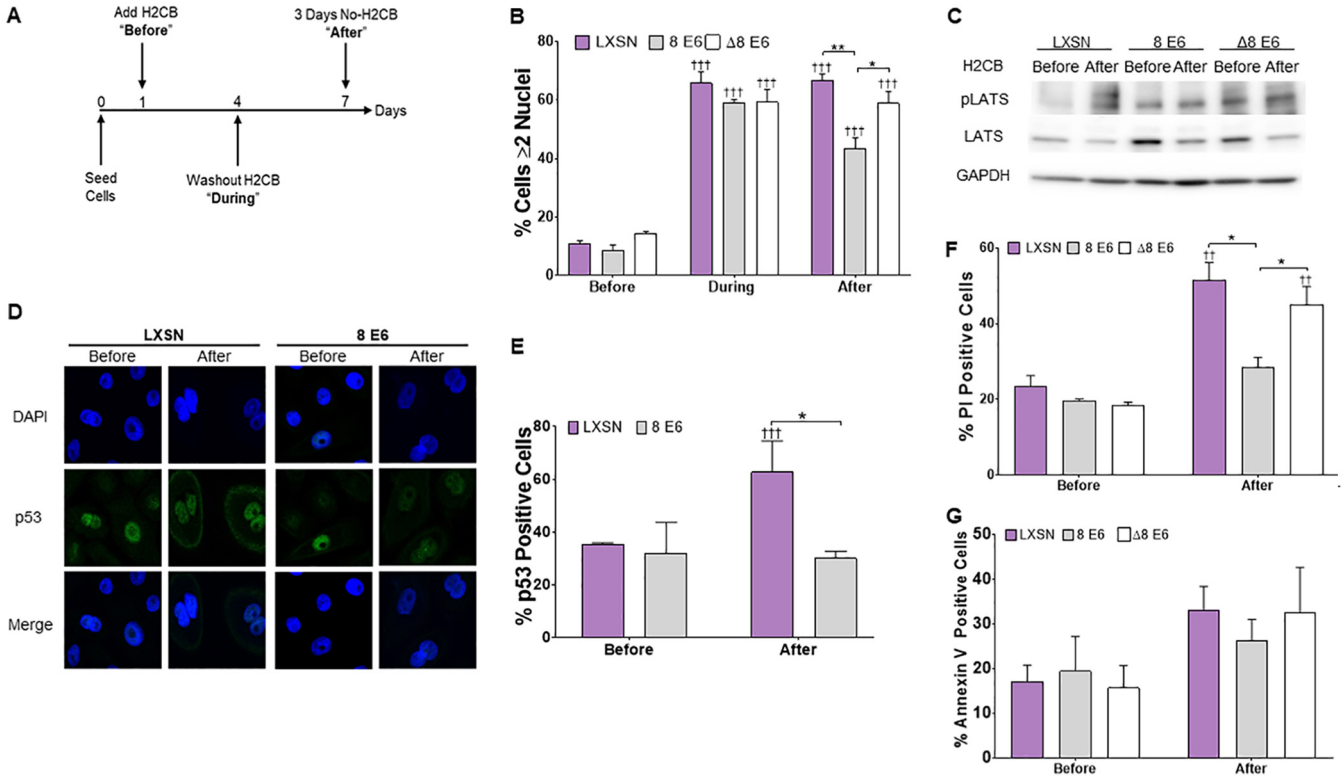

FIG 6 β-HPV 8E6 hinders LATS phosphorylation and p53 accumulation after failed cytokinesis. (A) Timeline for administration and removal of H2CB. (B) Percent of HFK cells with ≥ 2 nuclei per cell before, during, and after H2CB treatment. (C) Representative immunoblots of pLATS and totals LATS in HFKs before and after H2CB exposure. (D) Representative images of p53 and DAPI staining in cells before and after H2CB exposure. (E) Percent of p53-stained HFK cells before and after H2CB exposure. At least 200 cells/line were imaged across three independent experiments. (F) Percent of propidium iodide-stained HFK cells before and after H2CB exposure. (G) Percent of annexin V-stained HFK cells before and after H2CB treatment. Figures depict mean ± standard error of the mean; $n \geq 3$. *, significant difference between indicated samples; †, significant difference relative to before H2CB; one symbol (* or †), $P \leq 0.05$; two symbols (** or ††), $P \leq 0.01$; three symbols (*** or †††), $P \leq 0.001$ (Student's *t* test). In β-HPV Δ8E6, residues 132 to 136 were deleted.

galactosidase (SA β-Gal) activity as an indicator of cellular senescence. These data were consistent with our Ki67 staining experiments (Fig. 7C and D). HFKs were more likely to have SA β-Gal activity after H2CB, and β-HPV 8E6 expression amplified this phenotype.

The HP restricts growth by relocating YAP from the nucleus to the cytoplasm. We used immunofluorescence microscopy to define the subcellular localization of YAP in HFKs before, during, and after H2CB (Fig. 7E and F). Cytoplasmic YAP increased in HFKs during and after H2CB as expected. β-HPV 8E6 attenuated this only after H2CB exposure (Fig. 7F). Additionally, we saw a nominal decrease in nuclear-located YAP in HFKs expressing β-HPV 8E6 alone after H2CB treatment. To more precisely define YAP localization, we performed subcellular fractionation on HFKs before and after H2CB (Fig. 7G). Immunoblotting demonstrated that phosphorylated YAP was more abundant in the cytoplasm, particularly after H2CB. This was also true for phosphorylated LATS. After H2CB, β-HPV 8E6 decreased the amount of total YAP in the nuclear fraction, despite reducing total and cytoplasmic phospho-LATS1/2 (pLATS).

We wanted to determine the extent that β-HPV 8E6 could attenuate LATS phosphorylation in response to other stimuli. Because cell density is a commonly used activator of the HP, we compared LATS and YAP phosphorylation in confluent and subconfluent HFKs (Fig. 8A and B). Immunoblots of these cells demonstrate increased YAP phosphorylation in confluent HFKs compared to subconfluent HFKs. The phosphorylation of LATS did not increase under these conditions. Next, we used immunofluorescence microscopy to determine if HFKs increased p53 levels when grown to high confluence (Fig. 8C and D). As expected, p53 staining was more intense in confluent compared to subconfluent HFKs. In general, neither β-HPV 8E6 nor β-HPV Δ8E6 changed these responses. However, β-HPV Δ8E6 decreased p53 staining. We have no

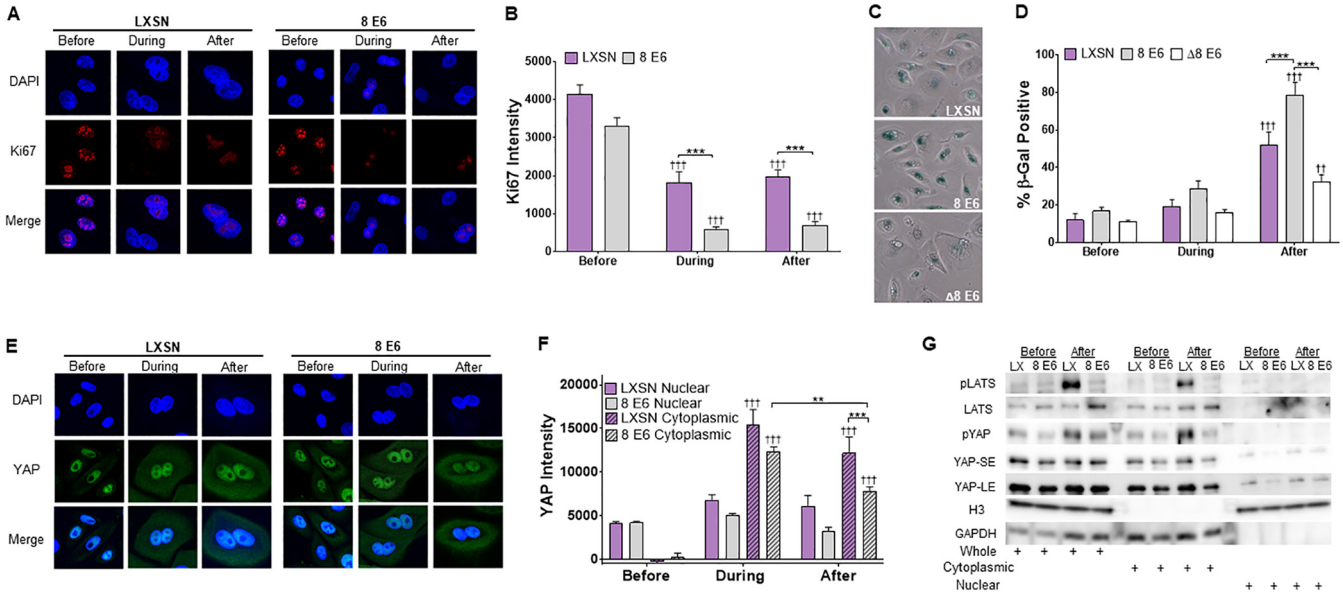

FIG 7 β-HPV 8E6 increases SA β-Gal staining and reduces YAP abundance after failed cytokinesis. (A) Representative images of Ki67 (red) and DAPI (blue) staining in HFK cells before, during, and after H2CB treatment. (B) Relative KI67 intensity in HFK cells before, during, and after H2CB treatment. At least 150 cells/line were imaged across three independent experiments. (C) Representative images of HFK cells stained for SA β-Gal activity (blue). (D) Percent of SA β-Gal-positive HFK cells before, during, and after H2CB exposure. (E) Representative images of HFK cells stained for YAP (green) and DAPI (blue). (F) Cytoplasmic and nuclear YAP intensity in HFK cells before, during, and after H2CB treatment. At least 205 images were imaged across three independent experiments. (G) Subcellular fractionation of HFKs harvested before and after H2CB treatment. Hippo pathway proteins were probed via immunoblotting. GAPDH and histone H3 serve as cytoplasmic and nuclear loading controls, respectively. YAP-SE and YAP-LE indicate short- and long-term exposure of YAP, respectively. Figures depict mean ± standard error of the mean; $n \geq 3$. *, significant difference between indicated samples; †, significant difference relative to before H2CB; one symbol (* or †), $P \leq 0.05$, two symbols (** or ††), $P \leq 0.01$; three symbols (*** or †††), $P \leq 0.001$ (Student's *t* test). In β-HPV Δ8E6, residues 132 to 136 were deleted.

explanation of this observation, but it does demonstrate that β-HPV Δ8E6 is not universally inactive.

DISCUSSION

Tumorigenesis is among the grave consequences associated with changes in ploidy. HP activation is one of the cellular mechanisms that prevents polyploidy by halting the proliferation of cells that do not divide after replication (32, 52). Despite the high stakes, cytokinesis fails in approximately 10% of skin cells that enter mitosis (25, 31). As a result, the HP may play an important role in preventing cSCCs. The growth arrest associated with HP activation is likely refractory to β-HPV replication, as HPV replicates in actively proliferating cells (53). Our work suggests that β-HPV 8E6 helps binucleated cells survive by mitigating HP activation. Presumably limiting HP signaling is beneficial to papillomaviruses in general, as genus α HPV oncogenes also dysregulate the Hippo pathway (54, 55).

The "evolutionary motivation" behind this could stem from the modest growth advantage that we report. However, this weak phenotype seems unlikely to drive convergent evolution toward HP dysregulation. Given the HP's role in immunity, it is more enticing to speculate that targeting the HP helps HPVs avoid an immune response (56, 57). Indeed, an MST1 deficiency increased β-HPV infections (58). Since the HP was only discovered 14 years ago (59), there could also be other currently unknown advantages to be gained by disrupting the pathway.

Less speculatively, we extend the understanding of β-HPV 8E6 biology. β-HPV E6 disrupts multiple cell signaling pathways necessary for DNA repair and regulating differentiation. Much of β-HPV E6's ability to disrupt DNA repair is linked to p300 destabilization. We demonstrate that changes in signaling associated with reduced p300 extend to the HP, as LATS phosphorylation is attenuated following failed cytokinesis. β-HPV 8E6 also displays some antiapoptotic properties in response to H2CB-

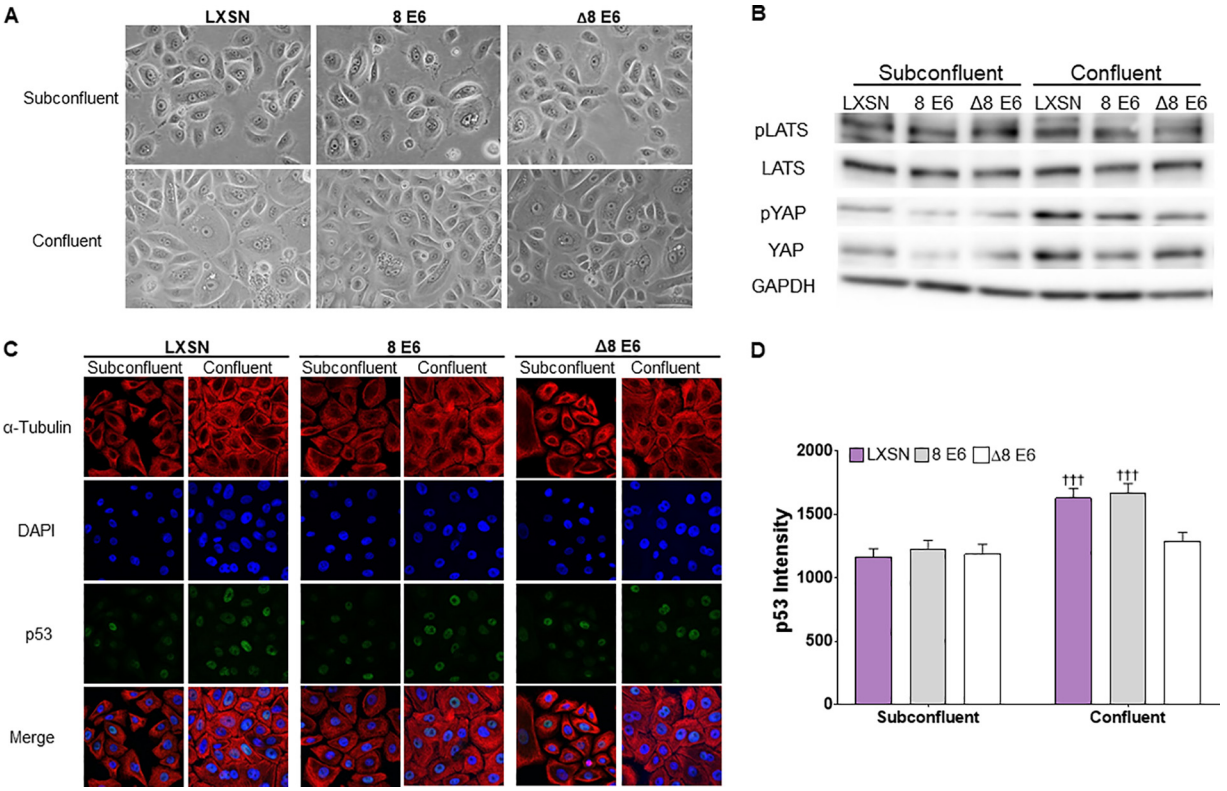

FIG 8 β-HPV 8E6 does not inhibit the Hippo pathway's response to cellular density. (A) Representative images of subconfluent and confluent HFKs. (B) Representative immunoblot of HP proteins in confluent and subconfluent HFKs. (C) Representative images of α-tubulin (red)-, p53 (green)-, and DAPI (blue)-stained subconfluent and confluent HFK cells. (D) Mean p53 intensity in HFK cells before and after confluence. At least 200 cells/line were imaged across 3 independent experiments; $n = 2$ for β-HPV Δ8E6. Figures depict mean ± standard error of the mean; $n \geq 3$. †, significant difference relative to before H2CB; †, $P \leq 0.05$; ††, $P \leq 0.01$; †††, $P \leq 0.001$ (Student's *t* test). In β-HPV Δ8E6, residues 132 to 136 were deleted.

induced failed cytokinesis. Together, these data demonstrate that β-HPV 8E6 is a versatile protein capable of a striking reprogramming of cellular signaling. We also extend the long history of using viral oncogenes to learn about cell biology by linking p300 to the HP- and TEAD-responsive gene expression.

The fact that most people get infected with β-HPV but a significantly lower number of those infections become cSCCs causes many to doubt that the virus is tumorigenic. β-HPV 8E6 may be more mutagenic in certain genetic backgrounds. For instance, β-HPV 8E6 reduces LATS phosphorylation after failed cytokinesis, but the cells still senesce. This suggests that mutations that help cells avoid senescence would augment β-HPVs tumorigenic potential. One could imagine any number of additional mutations that might synergize with β-HPV 8E6 to promote mutagenesis. Genetic landscapes where the opposite is true seem equally likely. Moreover, β-HPV E6 could also be more or less harmful when coexpressed with other β-HPV genes. Future studies are needed to evaluate these complexities.

MATERIALS AND METHODS

Cell cultures. U2OS and HCT 116 cells were maintained in Dulbecco modified Eagle medium (DMEM) supplemented with 10% fetal bovine serum (FBS) and penicillin-streptomycin. Primary HFKs were derived from neonatal human foreskins. HFKs were grown in EpiLife medium supplemented with calcium chloride (60 μM), human keratinocyte growth supplement (Thermo Fisher Scientific), and penicillin-streptomycin. HPV genes were cloned, transfected, and confirmed as previously described (25). We carefully monitored cell density in all experiments. To avoid confounding our experiments by activating the Hippo pathway via contact inhibition, experiments were aborted if unintended differences in seeding resulted in cell densities that were more than 10% different among cell lines at the beginning of an experiment.

Proliferation assays and H2CB cell viability assays. Cells were counted, and 4.0×10^4 cells were plated into 6 wells per cell line of 6-well tissue culture dishes. One well was trypsinized, resuspended, and

counted 3 times via hemocytometer with trypan blue. For dihydrocytochalasin B (H2CB) cell viability assays, cells were grown for 24 h and then treated with 2/4 μM H2CB, and fresh H2CB was readministered every 2 days while cells were trypsinized and counted 3 times via hemocytometer with trypan blue.

RT-qPCR. Cell were lysed using TRIzol (Invitrogen) and RNA isolated with the RNeasy kit (Qiagen). Two micrograms of RNA were reverse transcribed using the iScript cDNA synthesis kit (Bio-Rad). Quantitative real-time PCR (RT-qPCR) was performed in triplicate with the TaqMan FAM-MGB gene expression assay (Applied Biosystems) and C1000 touch thermal cycler (Bio-Rad). The following probes (Thermo Scientific) were used: ACTB (Hs01060665_g1), STK4 (Hs00178979_m1), LATS2 (referred to as LATS in the text) (Hs01059009_m1), YAP1 (Hs00902712_g1), CTGF (Hs00170014_m1), CYR61 (Hs00155479_m1), TEAD4 (Hs01125032_m1), TEAD1 (Hs00173359_m1), CCND1 (Hs00765553_m1), AXL (Hs01064444_m1), and SERPINE1 (Hs00167155_m1).

Immunoblotting. After being washed with ice-cold phosphate-buffered saline (PBS), cells were lysed with radioimmunoprecipitation assay (RIPA) lysis buffer (VWR Life Science) supplemented with Phosphatase inhibitor cocktail 2 (Sigma) and protease inhibitor cocktail (Bimake). The Pierce bicinchoninic acid (BCA) protein assay kit (Thermo Scientific) was used to determine protein concentration. Equal protein lysates were run on Novex 4-12% Tris-Glycine WedgeWell mini gels (Invitrogen) and transferred to Immobilon-P membranes (Millipore). Membranes were then probed with the following primary antibodies: glyceraldehyde-3-phosphate dehydrogenase (GAPDH) (Santa Cruz Biotechnologies; catalog no. sc-47724), LATS2 (Cell Signaling Technologies; clone D83D6), phospho-LATS1/2 (Ser909) (referred to as pLATS in the text) (Cell Signaling Technologies; product no. 9157), YAP (Cell Signaling Technologies; product no. 4912S), phospho-YAP (Ser127) (Referred to pYAP in the text) (Cell Signaling Technologies; product no. 4911S), MST1 (Cell Signaling Technologies; product no. 3682S), AXL (Cell Signaling Technologies; product no. 8661S), CTGF (Abcam; catalog no. ab6692), PAI-1 (Cell Signaling Technologies; product no. 11907S), p53 (Calbiochem; catalog no. OP43; 100 μg), p300 (Santa Cruz Biotechnologies; catalog no. sc-584), and histone H3 (Abcam; catalog no. ab1791). After exposure to the matching horseradish peroxidase (HRP)-conjugated secondary antibody, cells were visualized using SuperSignal West Femto maximum sensitivity substrate (Thermo Scientific).

cBioPortal and gene ontology analysis. Software from www.cbioportal.org was used to recognize, analyze, and categorize mutations and transcriptomic data from over 1,000 cancer cell lines (40–42) and cutaneous squamous cell carcinomas (60, 61). Gene Ontology enRIchment anaLysis and visuaLizAtion tool (GOrilla) identified and visualized enriched GO terms from these data (43, 44). The Kyoto Encyclopedia of Genes and Genomes (KEGG) was used to identify genes specific to the Hippo signaling pathway (hsa04390).

Senescence-associated β-galactosidase staining. Cells were seeded onto three 6-well plates and were grown for 24 h. Then, they were treated with 4 μM H2CB for stated times, after which cells were fixed and stained for senescence-associated β-galactosidase (β-Gal) expression according to the manufacturer's protocol (Cell Signaling Technologies).

Immunofluorescence microscopy. Cells were seeded onto either 96-well glass-bottom plates (Cellvis) or coverslips and grown overnight. Cells treated with H2CB for a specified time and concentration were fixed with 4% formaldehyde. Then, 0.1% Triton-X solution in PBS was used to permeabilize the cells, followed by blocking with 3% bovine serum albumin in PBS for 30 min. Cells were then incubated with the following: p53 (Cell Signaling Technologies; clone 1C12), YAP (Cell Signaling Technologies; product no. 4912S), Ki67 (Abcam; catalog no. ab15580), alpha-tubulin (Abcam; catalog no. ab18251), and α-tubulin (Cell Signaling Technologies; product no. 3873S). The cells were washed and stained with the appropriate secondary antibodies: Alexa Fluor 594 goat anti-rabbit (Thermo Scientific; catalog no. A11012) and Alexa Fluor 488 goat anti-mouse (Thermo Scientific A11001). After washing, the cells were stained with 28 μM 4′,6-diamidino-2-phenylindole (DAPI) in PBS and visualized with the Zeiss LSM 770 microscope. Images were analyzed using ImageJ techniques previously described in reference 62.

Apoptosis assay. After H2CB treatment, HFKs were harvested via trypsinization and then counted while incubating at 37°C for 30 min. After incubation, cells were resuspended to 1×10^6 cells/ml. Next, cells were stained with 100 μg/ml of propidium iodide (PI) and 1× annexin-binding buffer following the protocol from Dead Cell apoptosis kit (Invitrogen; catalog no. V13242). Stained cells were imaged with the Countess II FL automated cell counter (Invitrogen). Images were processed using ImageJ software.

Subcellular fractionation. Cells were seeded at 5.0×10^5 cells/10 cm^2 plate and grown for 24 h. Cells were then treated with 4 μM H2CB for 3 days, washed with PBS, and recovered in fresh EpiLife for 3 days (after H2CB treatment). Before and after H2CB exposure, cells were washed with ice-cold PBS and divided into cytosolic and nuclear fractions via Abcam's subcellular fractionation protocol. Afterward, lysates were treated the same as in the Immunoblotting section.

Statistical analysis. Unless otherwise noted, statistical significance was determined by an unpaired Student's *t* test and was confirmed when appropriate by two-way analysis of variance (ANOVA) with Turkey's correction. Only *P* values of less than 0.05 were reported as significant.

SUPPLEMENTAL MATERIAL

Supplemental material is available online only.

SUPPLEMENTAL FILE 1, XLSX file, 0.9 MB.

ACKNOWLEDGMENTS

We thank and acknowledge the Kansas State University College of Veterinary Medicine (KSU-CVM) Confocal Core, especially Joel Sanneman, for assisting with our

immunofluorescence imaging, Michael Underbrink for providing the telomerase reverse transcriptase (TERT)-immortalized HFKs, Stefano Piccolo for gifting the 8×GTIIC plasmid, along with Emily Burghardt and Jazmine Snow for their constructive criticism of the manuscript. Also, we thank members of the Zhilong Yang lab for their support.

This work was supported by Department of Defense grant CMDRP PRCRP CA160224 (to N.A.W.) and was made possible by generous support from the Les Clow family and the Johnson Cancer Research Center at Kansas State University.

REFERENCES

1. Van Doorslaer K, Li Z, Xirasagar S, Maes P, Kaminsky D, Liou D, Sun Q, Kaur R, Huyen Y, McBride AA. 2017. The Papillomavirus Episteme: a major update to the papillomavirus sequence database. Nucleic Acids Res 45:D499–D506. https://doi.org/10.1093/nar/gkw879.
2. Zur Hausen H. 2002. Papillomaviruses and cancer: from basic studies to clinical application. Nat Rev Cancer 2:342–350. https://doi.org/10.1038/nrc798.
3. Cogliano V, Baan R, Straif K, Grosse Y, Secretan B, El Ghissassi F, WHO International Agency for Research on Cancer. 2005. Carcinogenicity of human papillomaviruses. Lancet Oncol 6:204. https://doi.org/10.1016/S1470-2045(05)70086-3.
4. Orth G, Jablonska S, Favre M, Croissant O, Jarzabek-Chorzelska M, Rzesa G. 1978. Characterization of two types of human papillomaviruses in lesions of Epidermodysplasia verruciformis. Proc Natl Acad Sci U S A 75:1537–1541. https://doi.org/10.1073/pnas.75.3.1537.
5. Purdie KJ, Surentheran T, Sterling JC, Bell L, McGregor JM, Proby CM, Harwood CA, Breuer J. 2005. Human papillomavirus gene expression in cutaneous squamous cell carcinomas from immunosuppressed and immunocompetent individuals. J Invest Dermatol 125:98–107. https://doi.org/10.1111/j.0022-202X.2005.23635.x.
6. Harwood CA, McGregor JM, Proby CM, Breuer J. 1999. Human papillomavirus and the development of non-melanoma skin cancer. J Clin Pathol 52:249–253. https://doi.org/10.1136/jcp.52.4.249.
7. Chahoud J, Semaan A, Chen Y, Cao M, Rieber AG, Rady P, Tyring SK. 2016. Association between β-genus human papillomavirus and cutaneous squamous cell carcinoma in immunocompetent individuals—a meta-analysis. JAMA Dermatol 152:1354–1364. https://doi.org/10.1001/jamadermatol.2015.4530.
8. Masini C, Fuchs PG, Gabrielli F, Stark S, Sera F, Ploner M, Melchi CF, Primavera G, Pirchio G, Picconi O, Petasecca P, Cattaruzza MS, Pfister HJ, Abeni D. 2003. Evidence for the association of human papillomavirus infection and cutaneous squamous cell carcinoma in immunocompetent individuals. Arch Dermatol 139:890–894. https://doi.org/10.1001/archderm.139.7.890.
9. Chitsazzadeh V, Coarfa C, Drummond JA, Nguyen T, Joseph A, Chilukuri S, Charpiot E, Adelmann CH, Ching G, Nguyen TN, Nicholas C, Thomas VD, Migden M, MacFarlane D, Thompson E, Shen J, Takata Y, McNiece K, Polansky MA, Abbas HA, Rajapakshe K, Gower A, Spira A, Covington KR, Xiao W, Gunaratne P, Pickering C, Frederick M, Myers JN, Shen L, Yao H, Su X, Rapini RP, Wheeler DA, Hawk ET, Flores ER, Tsai KY. 2016. Cross-species identification of genomic drivers of squamous cell carcinoma development across preneoplastic intermediates. Nat Commun 7:12601. https://doi.org/10.1038/ncomms12601.
10. Weissenborn SJ, Nindl I, Purdie K, Harwood C, Proby C, Breuer J, Majewski S, Pfister H, Wieland U. 2005. Human papillomavirus-DNA loads in actinic keratoses exceed those in non-melanoma skin cancers. J Invest Dermatol 125:93–97. https://doi.org/10.1111/j.0022-202X.2005.23733.x.
11. Howley PM, Pfister HJ. 2015. Beta genus papillomaviruses and skin cancer. Virology 479–480:290–296. https://doi.org/10.1016/j.virol.2015.02.004.
12. Weissenborn SJ, De Koning MNC, Wieland U, Quint WGV, Pfister HJ. 2009. Intrafamilial transmission and family-specific spectra of cutaneous betapapillomaviruses. J Virol 83:811–816. https://doi.org/10.1128/JVI.01338-08.
13. Akgül B, Cooke JC, Storey A. 2006. HPV-associated skin disease. J Pathol 208:165–175. https://doi.org/10.1002/path.1893.
14. Aldabagh B, Angeles JGC, Cardones AR, Arron ST. 2013. Cutaneous squamous cell carcinoma and human papillomavirus: is there an association? Dermatol Surg 39:1–23. https://doi.org/10.1111/j.1524-4725.2012.02558.x.
15. Rosen T, Lebwohl MG. 2013. Prevalence and awareness of actinic keratosis: barriers and opportunities. J Am Acad Dermatol 68:S2–9. https://doi.org/10.1016/j.jaad.2012.09.052.
16. Warino L, Tusa M, Camacho F, Teuschler H, Fleischer AB, Feldman SR. 2006. Frequency and cost of actinic keratosis treatment. Dermatol Surg 32:1045–1049. https://doi.org/10.1111/j.1524-4725.2006.32228.x.
17. Criscione VD, Weinstock MA, Naylor MF, Luque C, Eide MJ, Bingham SF, Department of Veteran Affairs Topical Tretinoin Chemoprevention Trial Group. 2009. Actinic keratoses: natural history and risk of malignant transformation in the Veterans Affairs Topical Tretinoin Chemoprevention Trial. Cancer 115:2523–2530. https://doi.org/10.1002/cncr.24284.
18. Marcuzzi GP, Hufbauer M, Kasper HU, Weißenborn SJ, Smola S, Pfister H. 2009. Spontaneous tumour development in human papillomavirus type 8 E6 transgenic mice and rapid induction by UV-light exposure and wounding. J Gen Virol 90:2855–2864. https://doi.org/10.1099/vir.0.012872-0.
19. Schaper ID, Marcuzzi GP, Weissenborn SJ, Kasper HU, Dries V, Smyth N, Fuchs P, Pfister H. 2005. Development of skin tumors in mice transgenic for early genes of human papillomavirus type 8. Cancer Res 65:1394–1400. https://doi.org/10.1158/0008-5472.CAN-04-3263.
20. Meyers JM, Uberoi A, Grace M, Lambert PF, Munger K. 2017. Cutaneous HPV8 and MmuPV1 E6 proteins target the NOTCH and TGF-β tumor suppressors to inhibit differentiation and sustain keratinocyte proliferation. PLoS Pathog 13:e1006171. https://doi.org/10.1371/journal.ppat.1006171.
21. Underbrink MP, Howie HL, Bedard KM, Koop JI, Galloway DA. 2008. E6 proteins from multiple human betapapillomavirus types degrade Bak and protect keratinocytes from apoptosis after UVB irradiation. J Virol 82:10408–10417. https://doi.org/10.1128/JVI.00902-08.
22. Wallace NA, Robinson K, Howie HL, Galloway DA. 2012. HPV 5 and 8 E6 abrogate ATR activity resulting in increased persistence of UVB induced DNA damage. PLoS Pathog 8:e1002807. https://doi.org/10.1371/journal.ppat.1002807.
23. Viarisio D, Mueller-Decker K, Kloz U, Aengeneyndt B, Kopp-Schneider A, Gröne H-J, Gheit T, Flechtenmacher C, Gissmann L, Tommasino M. 2011. E6 and E7 from beta HPV38 cooperate with ultraviolet light in the development of actinic keratosis-like lesions and squamous cell carcinoma in mice. PLoS Pathog 7:e1002125. https://doi.org/10.1371/journal.ppat.1002125.
24. Deshmukh J, Pofahl R, Pfister H, Haase I. 2016. Deletion of epidermal Rac1 inhibits HPV-8 induced skin papilloma formation and facilitates HPV-8- and UV-light induced skin carcinogenesis. Oncotarget 7:57841–57850. https://doi.org/10.18632/oncotarget.11069.
25. Wallace NA, Robinson K, Galloway DA. 2014. Beta human papillomavirus E6 expression inhibits stabilization of p53 and increases tolerance of genomic instability. J Virol 88:6112–6127. https://doi.org/10.1128/JVI.03808-13.
26. Wallace NA, Gasior SL, Faber ZJ, Howie HL, Deininger PL, Galloway DA. 2013. HPV 5 and 8 E6 expression reduces ATM protein levels and attenuates LINE-1 retrotransposition. Virology 443:69–79. https://doi.org/10.1016/j.virol.2013.04.022.
27. Howie HL, Koop JI, Weese J, Robinson K, Wipf G, Kim L, Galloway DA. 2011. Beta-HPV 5 and 8 E6 promote p300 degradation by blocking AKT/p300 association. PLoS Pathog 7:e1002211. https://doi.org/10.1371/journal.ppat.1002211.
28. Muench P, Probst S, Schuetz J, Leiprecht N, Busch M, Wesselborg S, Stubenrauch F, Iftner T. 2010. Cutaneous papillomavirus E6 proteins must interact with p300 and block p53-mediated apoptosis for cellular immortalization and tumorigenesis. Cancer Res 70:6913–6924. https://doi.org/10.1158/0008-5472.CAN-10-1307.
29. Dancy BM, Cole PA. 2015. Protein lysine acetylation by p300/CBP. Chem Rev 115:2419–2452. https://doi.org/10.1021/cr500452k.

30. Chan HM, Thangue N. 2001. p300/CBP proteins: HATs for transcriptional bridges and scaffolds. J Cell Sci 114:2363–2373.
31. Soto M, García-Santisteban I, Krenning L, Medema RH, Raaijmakers JA. 2018. Chromosomes trapped in micronuclei are liable to segregation errors. J Cell Sci 131:jcs214742. https://doi.org/10.1242/jcs.214742.
32. Ganem NJ, Cornils H, Chiu S-Y, O'Rourke KP, Arnaud J, Yimlamai D, Théry M, Camargo FD, Pellman D. 2014. Cytokinesis failure triggers Hippo tumor suppressor pathway activation. Cell 158:833–848. https://doi.org/10.1016/j.cell.2014.06.029.
33. Stukenberg PT. 2004. Triggering p53 after cytokinesis failure. J Cell Biol 165:607–608. https://doi.org/10.1083/jcb.200405089.
34. Shinmura K, Bennett RA, Tarapore P, Fukasawa K. 2007. Direct evidence for the role of centrosomally localized p53 in the regulation of centrosome duplication. Oncogene 26:2939–2944. https://doi.org/10.1038/sj.onc.1210085.
35. Wallace NA, Robinson K, Howie HL, Galloway DA. 2015. β-HPV 5 and 8 E6 disrupt homology dependent double strand break repair by attenuating BRCA1 and BRCA2 expression and foci formation. PLoS Pathog 11:e1004687. https://doi.org/10.1371/journal.ppat.1004687.
36. Snow JA, Murthy V, Dacus D, Hu C, Wallace NA. 2019. β-HPV 8E6 attenuates ATM and ATR signaling in response to UV damage. Pathogens 8:267. https://doi.org/10.3390/pathogens8040267.
37. Ganem NJ, Storchova Z, Pellman D. 2007. Tetraploidy, aneuploidy and cancer. Curr Opin Genet Dev 17:157–162. https://doi.org/10.1016/j.gde.2007.02.011.
38. Sen S. 2000. Aneuploidy and cancer. Curr Opin Oncol 12:82–88. https://doi.org/10.1016/j.gde.2007.02.011.
39. Meyers JM, Spangle JM, Munger K. 2013. The human papillomavirus type 8 E6 protein interferes with NOTCH activation during keratinocyte differentiation. J Virol 87:4762–4767. https://doi.org/10.1128/JVI.02527-12.
40. Barretina J, Caponigro G, Stransky N, Venkatesan K, Margolin AA, Kim S, Wilson CJ, Lehár J, Kryukov GV, Sonkin D, Reddy A, Liu M, Murray L, Berger MF, Monahan JE, Morais P, Meltzer J, Korejwa A, Jané-Valbuena J, Mapa FA, Thibault J, Bric-Furlong E, Raman P, Shipway A, Engels IH, Cheng J, Yu GK, Yu J, Aspesi P, de Silva M, Jagtap K, Jones MD, Wang L, Hatton C, Palescandolo E, Gupta S, Mahan S, Sougnez C, Onofrio RC, Liefeld T, MacConaill L, Winckler W, Reich M, Li N, Mesirov JP, Gabriel SB, Getz G, Ardlie K, Chan V, Myer VE, et al. 2012. The Cancer Cell Line Encyclopedia enables predictive modelling of anticancer drug sensitivity. Nature 483:603–607. https://doi.org/10.1038/nature11003.
41. Gao J, Aksoy BA, Dogrusoz U, Dresdner G, Gross B, Sumer SO, Sun Y, Jacobsen A, Sinha R, Larsson E, Cerami E, Sander C, Schultz N. 2013. Integrative analysis of complex cancer genomics and clinical profiles using the cBioPortal. Sci Signal 6:pl1. https://doi.org/10.1126/scisignal.2004088.
42. Cerami E, Gao J, Dogrusoz U, Gross BE, Sumer SO, Aksoy BA, Jacobsen A, Byrne CJ, Heuer ML, Larsson E, Antipin Y, Reva B, Goldberg AP, Sander C, Schultz N. 2012. The cBio Cancer Genomics Portal: an open platform for exploring multidimensional cancer genomics data. Cancer Discov 2:401–404. https://doi.org/10.1158/2159-8290.CD-12-0095.
43. Eden E, Navon R, Steinfeld I, Lipson D, Yakhini Z. 2009. GOrilla: a tool for discovery and visualization of enriched GO terms in ranked gene lists. BMC Bioinformatics 10:48. https://doi.org/10.1186/1471-2105-10-48.
44. Eden E, Lipson D, Yogev S, Yakhini Z. 2007. Discovering motifs in ranked lists of DNA sequences. PLoS Comput Biol 3:e39. https://doi.org/10.1371/journal.pcbi.0030039.
45. Stauffer D, Chang B, Huang J, Dunn A, Thayer M. 2007. p300/CREB-binding protein interacts with ATR and is required for the DNA replication checkpoint. J Biol Chem 282:9678–9687. https://doi.org/10.1074/jbc.M609261200.
46. Ogiwara H, Kohno T. 2012. CBP and p300 histone acetyltransferases contribute to homologous recombination by transcriptionally activating the BRCA1 and RAD51 genes. PLoS One 7:e52810. https://doi.org/10.1371/journal.pone.0052810.
47. Iyer NG, Chin S-F, Ozdag H, Daigo Y, Hu D-E, Cariati M, Brindle K, Aparicio S, Caldas C. 2004. p300 regulates p53-dependent apoptosis after DNA damage in colorectal cancer cells by modulation of PUMA/p21 levels. Proc Natl Acad Sci U S A 101:7386–7391. https://doi.org/10.1073/pnas.0401002101.
48. Maness PF, Walsh RC. Jr., 1982. Dihydrocytochalasin B disorganizes actin cytoarchitecture and inhibits initiation of DNA synthesis in 3T3 cells. Cell 30:253–262. https://doi.org/10.1016/0092-8674(82)90031-9.
49. Zhao B, Li L, Tumaneng K, Wang C-Y, Guan K-L. 2010. A coordinated phosphorylation by Lats and CK1 regulates YAP stability through SCFβ-TRCP. Genes Dev 24:72–85. https://doi.org/10.1101/gad.1843810.
50. Cornelissen M, Philippé J, De Sitter S, De Ridder L. 2002. Annexin V expression in apoptotic peripheral blood lymphocytes: an electron microscopic evaluation. Apoptosis 7:41–47. https://doi.org/10.1023/a:1013560828090.
51. Riccardi C, Nicoletti I. 2006. Analysis of apoptosis by propidium iodide staining and flow cytometry. Nat Protoc 1:1458–1461. https://doi.org/10.1038/nprot.2006.238.
52. Senovilla L, Vitale I, Martins I, Tailler M, Pailleret C, Michaud M, Galluzzi L, Adjemian S, Kepp O, Niso-Santano M, Shen S, Marino G, Criollo A, Boileve A, Job B, Ladoire S, Ghiringhelli F, Sistigu A, Yamazaki T, Rello-Varona S, Locher C, Poirier-Colame V, Talbot M, Valent A, Berardinelli F, Antoccia A, Ciccosanti F, Fimia GM, Piacentini M, Fueyo A, Messina NL, Li M, Chan CJ, Sigl V, Pourcher G, Ruckenstuhl C, Carmona-Gutierrez D, Lazar V, Penninger JM, Madeo F, Lopez-Otin C, Smyth MJ, Zitvogel L, Castedo M, Kroemer G. 2012. An immunosurveillance mechanism controls cancer cell ploidy. Science 337:1678–1684. https://doi.org/10.1126/science.1224922.
53. McBride AA. 2008. Replication and Partitioning of Papillomavirus Genomes. Adv Virus Res 72:155–205. https://doi.org/10.1016/S0065-3527(08)00404-1.
54. He C, Mao D, Hua G, Lv X, Chen X, Angeletti PC, Dong J, Remmenga SW, Rodabaugh KJ, Zhou J, Lambert PF, Yang P, Davis JS, Wang C. 2015. The Hippo/YAP pathway interacts with EGFR signaling and HPV oncoproteins to regulate cervical cancer progression. EMBO Mol Med 7:1426–1449. https://doi.org/10.15252/emmm.201404976.
55. Morgan E, Patterson M, Lee SY, Wasson C, Macdonald A. 2018 High-risk human papillomaviruses down-regulate expression of the Ste20 family kinase MST1 to inhibit the Hippo pathway and promote transformation. bioRxiv https://doi.org/10.1101/369447.
56. Cheng J, Jing Y, Kang D, Yang L, Li J, Yu Z, Peng Z, Li X, Wei Y, Gong Q, Miron RJ, Zhang Y, Liu C. 2018. The role of Mstl in lymphocyte homeostasis and function. Front Immunol 9:149. https://doi.org/10.3389/fimmu.2018.00149.
57. Zhang Y, Zhang H, Zhao B. 2018. Hippo signaling in the immune system. Trends Biochem Sci 43:77–80. https://doi.org/10.1016/j.tibs.2017.11.009.
58. Crequer A, Picard C, Patin E, D'Amico A, Abhyankar A, Munzer M, Debré M, Zhang S-Y, Saint-Basile G. d, Fischer A, Abel L, Orth G, Casanova J-L, Jouanguy E. 2012. Inherited MST1 deficiency underlies susceptibility to EV-HPV infections. PLoS One 7:e44010. https://doi.org/10.1371/journal.pone.0044010.
59. Pan D. 2010. The Hippo signaling pathway in development and cancer. Dev Cell 19:491–505. https://doi.org/10.1016/j.devcel.2010.09.011.
60. Li YY, Hanna GJ, Laga AC, Haddad RI, Lorch JH, Hammerman PS. 2015. Genomic analysis of metastatic cutaneous squamous cell carcinoma. Clin Cancer Res off J Am Assoc Cancer Res 21:1447–1456. https://doi.org/10.1158/1078-0432.CCR-14-1773.
61. Pickering CR, Zhou JH, Lee JJ, Drummond JA, Peng SA, Saade RE, Tsai KY, Curry JL, Tetzlaff MT, Lai SY, Yu J, Muzny DM, Doddapaneni H, Shinbrot E, Covington KR, Zhang J, Seth S, Caulin C, Clayman GL, El-Naggar AK, Gibbs RA, Weber RS, Myers JN, Wheeler DA, Frederick MJ. 2014. Mutational landscape of aggressive cutaneous squamous cell carcinoma. Clin Cancer Res off J Am Assoc Cancer Res 20:6582–6592. https://doi.org/10.1158/1078-0432.CCR-14-1768.
62. Murthy V, Dacus D, Gamez M, Hu C, Wendel SO, Snow J, Kahn A, Walterhouse SH, Wallace NA. 2018. Characterizing DNA repair processes at transient and long-lasting double-strand DNA breaks by immunofluorescence microscopy. JoVE e57653. https://doi.org/10.3791/57653.

CellPress
REVIEWS

Review

Catching HPV in the Homologous Recombination Cookie Jar

Nicholas A. Wallace[1,*]

To replicate, the human papillomaviruses (HPVs) that cause anogenital and oropharyngeal malignancies must simultaneously activate DNA repair pathways and avoid the cell cycle arrest that normally accompanies DNA repair. For years it seemed that HPV oncogenes activated the homologous recombination pathway to facilitate the HPV lifecycle. However, recent developments show that, although homologous recombination gene expression and markers of pathway activation are increased, homologous recombination itself is attenuated. This review provides an overview of the diverse ways that HPV oncogenes manipulate homologous recombination and ideas on how the resulting dysregulation and inhibition offer opportunities for improved therapies and biomarkers.

Highlights

HPV exploits the homologous recombination pathway to promote faithful replication of their genome.

Failure to address HPV E7 induced replication stress makes homologous recombination proteins available for HPV replication, but jeopardizes host genome integrity.

Despite notably mechanistic differences, homologous recombination attenuation is shared among HPV genera.

Manipulation of homologous recombination by HPV oncogenes is apparent in tumors associated with the virus.

Increased homologous recombination gene expression and attenuation of the pathway offer opportunities for biomarker development and improved therapeutic approaches, respectively.

Understanding Human Papillomaviruses and Host DNA Machinery to Combat Disease

According to the World Health Organization, human papillomavirus (HPV) infections cause cancers that kill someone about every 90 s. HPV transforms tissues throughout the anogenital tract and oral cavity [1]. There are several formulations of prophylactic vaccines against these infections, each with an admirable safety profile, that provide immunity against the deadliest HPV infections [2]. In the developed world, their primary limitation is under-utilization resulting from vaccine hesitancy and misconceptions about increased promiscuity associated with their protection. Despite nascent attempts to determine if HPV vaccination can benefit infected individuals, there is no evidence of therapeutic benefit [3–5]. Thus, the millions of HPV infections that occur each year remain a tremendous health hazard [6]. Because HPV-associated tumors often take decades to develop, universal vaccination would not immediately reduce HPV-associated malignancies [7,8]. Rather, the frequency of HPV-positive head and neck cancers grows at a staggering rate [9] and the United States' National Cancer Institute reports that 5-year survival rates for cervical cancer prognosis have not improved in decades. In low- and middle-income countries, where HPV is most deadly, additional barriers prevent full utilization of these vaccines. In these regions, vaccine-based intervention efforts also face financial and logistic limitations.

This has motivated researchers to interrogate HPV biology in the hope of improving these grim statistics. The relationship between HPV replication and the host DNA repair has gained significant interest because repair defects result in acute sensitivity to genotoxic chemotherapeutics. Each cell in our bodies repairs an estimated 10 000 lesions every day [10]. This bombardment is quite diverse and addressed by a complex and interwoven series of signaling cascades, collectively known as the **DNA damage response** (**DDR**; see Glossary). Whether DDR promotes or restricts viral propagation differs among viruses, but interplay between viral replication and host DDR is common [11,12]. For HPV, DDR activation is critical. However, HPV must also avoid the cell cycle arrest that accompanies DDR. While decoupling arrest and repair is advantageous for the virus, host genome integrity suffers, leading to an accumulation of tumorigenic mutations.

DDR is subdivided into pathways that fix specific types of lesion during particular portions of the cell cycle [13]. **Double-strand breaks** (**DSBs**) in DNA are arguably the most important type of lesion, both for HPV and the cell. DSBs are by far the worst type of damage faced by cells [10]. Improperly repaired DSBs result in large-scale deletions and rearrangements [10], such that a single unrepaired DSB can cause cell death [14]. As a result, there are overlapping pathways to fix these lesions. **Homologous recombination** (Figure 1A) is the best pathway for avoiding mutations and maintaining genome stability, but its use of the sister chromatid as a repair template restricts it to the S and G2 phases of the

[1]Division of Biology, Kansas State University, Manhattan, KS, USA

*Correspondence: nwallac@ksu.edu

cell cycle [15]. HPV replication is reliant on upregulating homologous recombination genes and recruiting these proteins to viral replication centers (Figure 1B).

This review offers a summary of recent revelations about the relationship between homologous recombination and HPV, with apologies for omission of the seminal earlier discoveries that made these breakthroughs possible. We focus mostly on the 'high risk' human papillomaviruses that are the most oncogenic and are referred to simply as HPV (see Box 1 for a discussion of diversity among genus α human papillomaviruses, or reference [16] for a more complete discussion of HPV diversity). There is also a brief discussion of homologous recombination and cutaneous genus β HPV infections.

HPV's Reliance on Host Homologous Recombination Proteins

HPV replication is not uniformly dependent on homologous recombination proteins. The HPV life cycle has two distinct phases (Figure 2A). The first begins with the virus infecting epithelial cells, gaining access to basal keratinocytes through microabrasions. When these cells divide laterally, the viral genome replicates along with the cell, keeping a steady number of genomes. This is the virus's maintenance phase [17]. Homologous recombination proteins are not necessary for maintenance. As basal cells divide and differentiate towards the skin's surface, HPV enters the second phase of its life cycle, known as amplification [17]. As the name suggests, HPV intensifies its replication efforts during amplification, reaching several hundred copies per cell (Figure 2B). A map of the major HPV gene products and genome features can be found in Figure 2C.

Amplification requires activation of **ataxia-telangiectasia mutated** (**ATM**) signaling [18]. ATM is a pinnacle DDR kinase that initiates DSB repair [19]. While its targets include cell cycle checkpoints and proteins in other repair pathways, ATM's role in amplification appears to be linked to its induction of homologous recombination. ATM phosphorylates SMC1, a known facilitator of homologous recombination [20,21]. During this period of the viral lifecycle, ATM also phosphorylates at least two homologous recombination proteins, **BRCA1** and **NBS1** [22]. Both of these proteins, and another homologous recombination factor, **RAD51**, are essential for amplification [22,23]. While a complete understanding of how ATM is activated by HPV is lacking, a cellular histone acetyltransferase, TIP60, is involved [24]. Signal transducer and activator of transcription 5 (**STAT5**), a member of the JAK/STAT signaling cascade, is necessary for HPV to activate ATM [25]. **HPV E7** is also the primary viral factor for inducing ATM during replication.

Activation of the DDR is not limited to the **HPV E6** and E7 oncogenes. HPV E1 and HPV E2 proteins directly facilitate HPV replication by activating DSB repair signaling. HPV E2 induces an ATM response [26], while HPV E1's helicase activity results in DDR machinery localizing to viral replication foci [27]. HPV E1 and E2 remain active in the face of exogenous DNA damage synthesizing DNA, albeit with loss of fidelity, suggesting that homologous recombination protects viral genome integrity [28]. Homologous recombination machinery's role in HPV replication is pervasive. Although the details of the advantage gained by this activation have not been fully delineated, homologous recombination may help to resolve replication errors as HPV rapidly and exponentially expands its copy number [11]. Inhibiting individual members of this pathway restricts HPV amplification *in vitro*, making HPV's interaction with these proteins attractive targets for antiviral drug development.

Taking Full Advantage of Host Homologous Recombination Factors

Because HPV is so dependent on the pathway, the virus has an array of tools for increasing its access to homologous recombination machinery. By binding and destabilizing the retinoblastoma protein (RB), HPV E7 increases homologous recombination protein abundance [29]. This is accomplished in part by raising RAD51 and BRCA1 stability. HPV E6 can cooperate with HPV E7 to further induce homologous recombination gene expression, increase the amount of RAD51, **RPA70**, BRCA1 and **BRCA2** in cells [30]. Some of the expression changes are the result of chromatin modifications. **SIRT1**, a deacetylase, remodels the host and viral DNA facilitating the recruitment of NBS1 and RAD51 to the HPV genome [31]. SIRT1 is also localized to the HPV origin of replication, where it regulates HPV E1- and E2-dependent replication via acetylation and stabilization of HPV E2 [32].

Glossary

ATM: an apical DNA repair kinase that typically responds to double-strand DNA breaks. It is activated during amplification and is necessary for the HPV lifecycle.
ATR: major DNA repair kinase. ATR most often responds to replication stress. HPV must activate ATR during amplification.
BRCA1/2: these two repair proteins are critical for homologous recombination and DNA crosslink repair. Both are induced by HPV oncogene expression, and BRCA1 is necessary for viral replication.
DDR: DNA damage repair; catch-all phrase encompassing any cell signaling process that responds to the ~10 000 DNA lesions per cell each day. HPV oncogenes activate and impair DDR.
DSB: double-strand break in DNA; a single DSB can result in cell death. HPV causes and delays their repair.
Homologous recombination: the least mutagenic means a cell has of repairing DSBs. This pathway is activated and subverted by HPV oncogenes to promote viral replication.
HPV E6: staves off apoptosis by degrading p53, impairing host genome fidelity in the process.
HPV E7: causes replication stress by promoting unregulated growth; it is responsible for most of the elevated DDR gene expression associated with HPV.
MCM helicase: cellular replicative polymerase responsible for unwinding DNA. It will continuing unwinding DNA when replicative polymerase stalls, exposing unstable single-stranded DNA.
NBS1: MRN complex member, with RAD50 and MRE11. It helps to resect DNA near DSBs, providing single-stranded DNA for homologous recombination. NBS1 is recruited to HPV replication sites.
Polymerase η or POLη: error-prone translesion synthesis polymerase. POLη's flexible active site allows it to bypass replication fork impediments. HPV low mutation rate suggests that POLη is not used during viral replication.
RAD51: required for HPV replication. During homologous recombination, RAD51 facilitates the search for homology and strand invasion that helps to use sister

During amplification, there is extensive colocalization of homologous recombination factors with the HPV genome that can be detected by immunofluorescence microscopy [33]. HPV oncogenes are active participants in recruiting these repair factors. When expressed without other viral factors or DNA, HPV E6 and E7 cause FANCD2 to be moved away from sites of DNA damage limiting the ability of RAD51 to localize to DSBs [30,34]. When expressed as part of the whole viral genome, RAD51 and BRCA1 are preferentially recruited away from cellular damage to the viral genome [35]. Notably, RAD51 and BRCA1 are required for HPV replication [36].

HPV E6 and E7 also inhibit homologous recombination indirectly by deregulating cell cycle checkpoints. Because homologous recombination relies on a homologous template to complete repair, it typically cannot be finished without a sister chromatid. As a result, cells avoid beginning homologous recombination during G1. Instead they use an alternative repair pathway (nonhomologous end joining) to fix breaks with minimal loss of sequence [36]. HPV E6 and E7 make it significantly more likely that nuclear RPA foci (an indirect indicator of resected single-stranded DNA) appear during G1 [30]. DDR proteins form increasingly large complexes around this type of hard-to-resolve lesion [37]. This would provide a noteworthy opportunity for HPV to 'steal' homologous recombination proteins. The fact that most HPV replication occurs during G2 is contrary to this idea, though. Perhaps it is an unintended consequence resulting from widespread deregulation of cell signaling, or maybe it creates a 'G2-like' environment where HPV can replicate [38].

Stressing the Cell to Gain Access

HPV amplification requires replication of typically quiescent cells. To satisfy this need, HPV E7 degrades Rb and RB-family proteins leading to increased E2F transcription and effectively preventing G1/S checkpoints [39]. By removing this constraint on cell proliferation, HPV E7 allows dysregulated growth that depletes nucleoside pools causing **replication stress** [40]. In response, the host cell undergoes multiple efforts to mitigate the replication stress. It becomes addicted to two demethylases (KDM6A and KDM6B), resulting in widespread methylation and gene expression changes [41–44]. A ribonucleotide reductase, RRM2, is also overexpressed, providing an alternative source of nucleosides [45].

In this environment, replication forks are presumably stalling as they wait for necessary building blocks. This should decouple replication fork progression from the **MCM helicase** activity and result in long stretches of single-stranded DNA (ssDNA). ssDNA is rapidly bound by the RPA complex (RPA14, RPA32, and RPA70) to help prevent fork collapse and activate **ATR** signaling [46]. ATR activation stabilizes the error prone **polymerase η** or **POLη**, beginning a process known as **translesion synthesis** (**TLS**) [47]. The stalled fork also promotes PCNA ubiquitination, allowing POLη to displace the replicative polymerase, easing replication restraints and preventing fork collapse into DSBs. Since the pathway responds to other replication stressors, TLS is presumably activated by HPV E7-induced replication stress. However, TLS likely falters before completion as HPV E7 induces double-strand breaks consistent with fork collapse [48]. Further, HPV's constitutive activation of ATR occurs via a TOPBP1-dependent mechanism, which would be expected if TLS begins, but is not completed [24]. This is clearly important for HPV replication as ATR activation promotes HPV replication.

On the surface, this seems disadvantageous for the virus as failed TLS results in DSBs that promote viral episome integration, after which HPV can no longer produce infectious virions [30]. However, there would be advantages for HPV that could outweigh the detriments. First, failed TLS leads to the ATR activation that is at least partially required for recruitment of DSB repair factors to viral replication centers [49]. Further, the DSBs that result from replication fork collapse are overwhelmingly repaired by homologous recombination increasing the availability of these factors. Finally, because the need for TLS reaches its maxima during amplification as HPV E7 levels rise, if the pathway failed then homologous recombination proteins would also peak during amplification when HPV has the greatest need for them.

chromatin as template for error-free repair.
Replication stress: general term encompassing the strain resulting from any impediment to replication. Common source of genome instability in cancers. HPV E7 induces replication stress by depleting nucleoside pools.
RPA70: a member of the RPA trimer that protects single-stranded DNA from degradation. HPV oncogenes increase RPA70 abundance and phosphorylation of fellow RPA trimer partner, RPA32.
SIRT1: host NAD-dependent deacetylase that controls HPV replication through histone modifications and recruitment of RAD51 and NBS1 to replication centers.
STAT5: a member of the JAK/STAT signaling family. STAT5 is required for ATM activation during HPV amplification.
Synthetic lethality: occurs when the combination of two conditions is exponentially more deleterious together than separately. Often the result of blocking two interconnected signaling pathways.
Translesion synthesis (TLS): translesion synthesis mitigates replication stress via polymerase barrier bypass. It is a recently identified mediator of chemotherapy resistance. Inhibition of the pathway could explain some of the DNA repair activation seen in cells expressing HPV oncogenes.

(A)

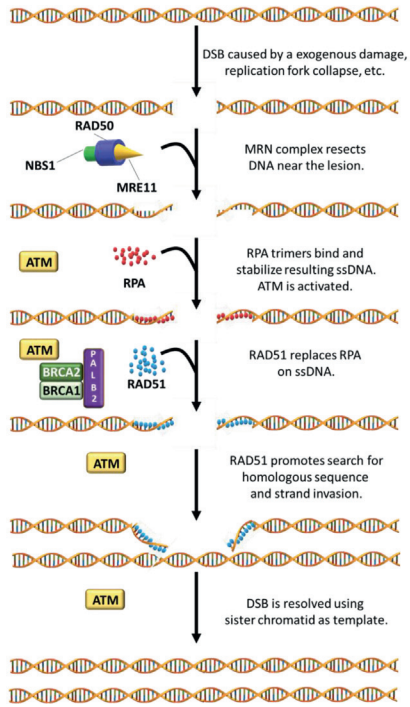

(B)

Protein(s)	Change in abundance	Localized to HPV replication foci
MRE11 [22]	UP	YES
RAD50 [22]	UP	YES
NBS1[22]	UP	YES
ATM [18]	UP	YES
RPA Complex [22, 34]	UP	YES
BRCA1 [23, 34]	UP	YES
BRCA2 [34]	UP	???
PALB2 [30]	DOWN	???
RAD51 [23, 34]	UP	YES
CHK2 [18]	UP	YES
SIRT1 [31, 32]	UP	YES

Trends in Microbiology

Figure 1. The Homologous Recombination Pathway Is Altered by Human Papillomavirus (HPV) Replication.
(A) Schematic of canonical homologous recombination pathway. (B) Table showing how HPV replication/gene expression alters the homologous recombination proteins. The column lists (left) genes involved in homologous recombination, (middle) changes in protein abundance during HPV replication or oncogene expression, and (right) whether the indicated protein localizes to HPV replication sites. CHK2 is phosphorylated by the DNA repair kinase ATM in response to a double-strand break (DSB) which induces a cell cycle checkpoint. SIRT1 promotes homologous recombination via deacetylation of target proteins. References [18,22,23,30,34] are provided in the first column.

Box 1. How Conserved Is the Abrogation of Homologous Recombination among Human Papillomaviruses?

This review focuses on cancer-associated HPVs from the alpha genus, but there is considerably more diversity in the genus. There are only 12 recognized 'high risk' αHPVs (HPV 16, HPV 18, HPV 31, HPV 33, HPV 35, HPV 45, HPV 51, HPV 52, HPV 56, HPV 58, HPV 59, and HPV 68). The other viruses in this genus are collectively referred to as 'low risk' HPVs and lack the ability to abolish p53- and RB-mediated cell signaling. Because they do not cause deadly cancers, these viruses are often neglected by researchers. When 'low risk' HPVs are studied, HPV 6 or HPV 11 are used as surrogates for the rest of the genus. These are chosen because they cause genital warts and reoccurring respiratory papillomas, more than for their ability to reflect the biology of the rest of the genus [83]. Even among the 'high risk' HPVs there is considerable bias towards studying the more clinically relevant viruses, with most studies investigating HPV 16, HPV18, and HPV31 biology. While there is good reason to believe that all 'high risk' HPVs share the ability to hinder homologous recombination, subtle differences in their manipulation of the pathway could explain why 70% of cervical cancers are caused by HPV 16 and HPV 18. There are more knowledge gaps with regard to the attenuation of repair by 'low risk' HPVs. The wart-causing 'low risk' HPVs (HPV 6 and HPV 11) have a significantly muted ability to alter DNA repair, compared to 'high risk' HPVs. However, less is known about how representative HPV 6 and HPV 11 are of less pathogenic 'low risk' HPVs. A more complete understanding of how other alpha genus HPVs thrive is an area ripe for investigation.

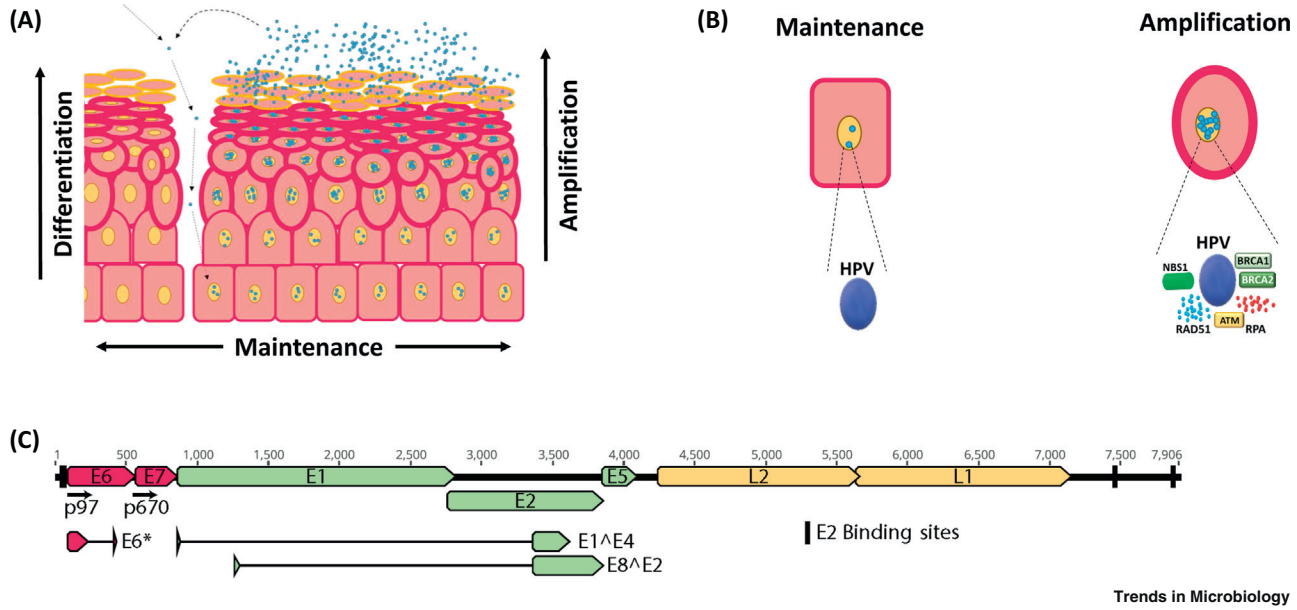

Figure 2. Homologous Recombination Proteins Localize to Viral Replication Sites during Amplification.

(A) Image depicts high-risk α-HPV life cycle in stratified epithelia. Differentiation in these cells is represented by changes in their shape. More differentiated cells are flatter ovals, while less differentiated cells are rectangular. Arrow and blue circle represent infectious viral particles infecting the basal layer and gaining access via microabrasions in the skin. Yellow circles depict nuclei. During horizontal replication of the host cells, high-risk α-HPV enters the maintenance phase of its life cycle where it maintains a relatively low genome copy number. As cells differentiate towards the surface, the number of viral genomes increase to remarkable levels, shown as a rising number of blue circles within cells. Human Papillomavirus (HPV) does not induce lysis; instead, it leaves as cells slough off naturally. Lighter pink cells with yellow borders represent this portion of the viral life cycle. (B) Enlarged image of cells [matching the morphology from (A)] highlighting the recruitment of homologous recombination proteins to sites of HPV replication, shown as blue spheres. (C) Linearized HPV genome with major transcripts. HPV genes are grouped by function and designated by color: HPV oncogenes (HPV E6, HPV E7, and splice variant HPV E6*) are pink, other early genes (HPV E1, HPV E2, HPV E5, HPV E1^E4, and HPV E8^E2) are green, and capsid genes (HPV L1 and L2) are yellow. The two primary promoters are noted with black arrows and numbers, indicating their location in the genome (p97 and p670). The HPV E2 bindings sites crucial for segregating HPV genomes during division are also noted.

Hurting without Killing: HPV's Repurposing of Homologous Recombination Factors Has Severe Consequences for Host Cells

Of course, HPV is not the only entity with an interest in how the cell responds to DSBs. Protecting genome fidelity is essential to the host cell's survival. HPV infections further complicate the host's mandate to protect its own DNA. The replication stress caused by the virus represents a notable challenge to cellular genome integrity [50]. As discussed in a preceding section, these responses are evidently unable to keep up as HPV oncogenes cause DSBs consistent with a failed or overwhelmed replication stress response. Unsurprisingly, HPV oncogenes make cells significantly more sensitive to replication stress from DNA crosslinking drugs, hydroxyurea, and UV [51,52].

HPV E6 and E7 also make DSBs more persistent, particularly in the host genome [30,35]. They lower homologous recombination efficiency by 50–60%, by causing a defect in the resolution of RAD51 foci [30]. The decreased homologous recombination efficiency suggests that the inhibitory effects of HPV oncogenes outpace any benefit to host that might come from the increased homologous recombination protein abundance. As expected from attenuated DSB repair, HPV oncogene-expressing cell lines are sensitive to endogenous and exogenous sources of DSBs [53–55].

It should be noted that the toxicity of replication stress and DSBs would likely be worse if HPV oncogenes were not simultaneously blocking repair and apoptosis. Apoptosis inhibition is often linked to HPV E6's promotion of p53 degradation, but the viral oncogenes have several other antiapoptotic activities [56]. This effectively amounts to a triple blockade of the cellular response to HPV E7-induced

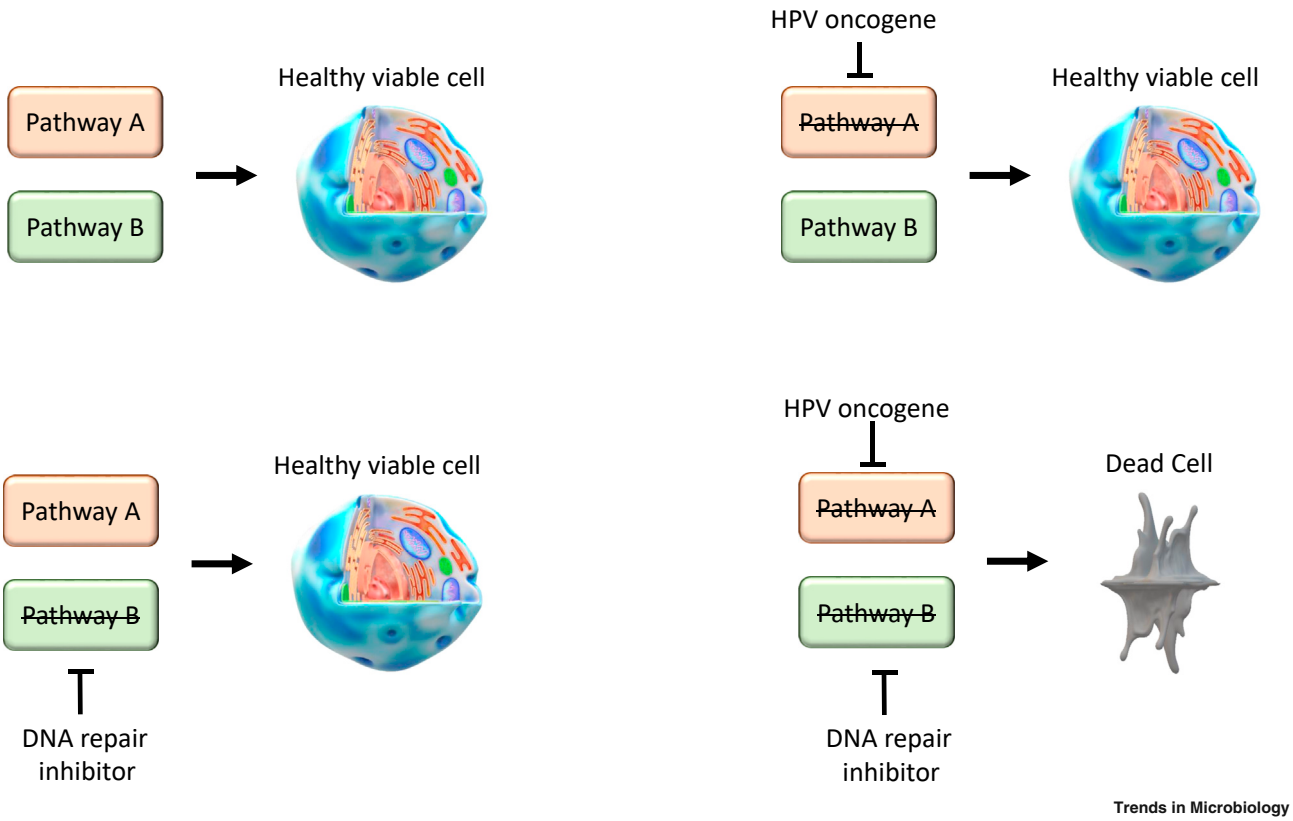

Figure 3. Potential Synthetic Lethal Relationship Where Human Papillomavirus (HPV) Oncogene Expression Is Combined with DNA Repair Inhibition.

On their own, the inhibition of Pathway A by HPV oncogene(s) or Pathway B by a DNA repair inhibitor are not deleterious to cells. However, when combined, they cause significant cytotoxicity. This would provide very targeted killing of HPV-associated cancer cells and requires continued characterization of DNA damage repair (DDR) pathways inhibited by HPV oncogenes. For example, HPV E6 and E7 inhibit the homologous recombination pathway (Pathway A), which is expected to create the potential for a synthetic lethal relationship with PARP1 inhibition (Pathway B).

replication stress. First, HPV oncogenes increase the likelihood of replication forks collapse. The repair of the resulting DSBs is attenuated and the last-ditch effort of programmed cell death is inhibited. Despite greater sensitivity, far more cells survive than would be prudent, and the host genome acquires tumorigenic mutations.

Targeting HPV Oncogene Biology for Direct Translational Implications

HPV-associated tumors are addicted to HPV oncogene expression. Even though HeLa cells have been grown in laboratories around the world for decades, they remain sensitive to reduction of HPV E6 or E7 [57]. This is notable given that HPV oncogenes promote acquisition of the additional mutations required for transformation. If cells with a notably impaired DDR do not acquire the necessary mutations to become independent of HPV oncogene expression after nearly 70 years in culture, it is unlikely that HPV-associated cancers would gain said mutations over the markedly shorter period that tumors exist *in vivo*. This results in a degree of tumor homogeneity that may be therapeutically targetable.

Synthetic lethality refers to gene mutations/chemical inhibitions that are very toxic together, but not particularly deleterious individually [58]. This concept has been the rationale for some chemotherapeutic regiments, where small-molecule inhibitors are more effective in certain genetic backgrounds. However, either extensive individual tumor profiling or biomarker development is required for this

approach. This may not be necessary in cervical cancers, where nearly all of the tumors are caused by constitutive HPV oncogene expression [59]. HPV-associated malignancies likely have an unusually high replication stress burden and a limited ability to complete homologous recombination. Figure 3 illustrates the concept of HPV oncogene-induced synthetic lethality. The efficacy of cisplatin and carboplatin at treating cervical cancers is consistent with this idea, as these drugs are more effective when replication stress is high or homologous recombination is impaired [60]. Using synthetic lethality approaches to target tumors with altered DNA repair is an area of considerable promise [61]. Breast cancers harboring BRCA1 or BRCA2 mutations can be effectively treated with PARP1 inhibitors [62]. PARP1 inhibition increases the number of DSBs during replication that would typically be repaired by homologous recombination, but BRCA1/BRCA2 mutations prevent the pathway from responding. HPV oncogenes also inhibit homologous recombination, and several ongoing clinical trials are using PARP1 inhibitors to treat cervical cancer [63–65].

The homogeneity resulting from HPV oncogene expression provides opportunities for improving biomarkers against HPV-associated tumors. DNA repair protein abundance increases in parallel with cervical premalignant lesion progression and was predicted based on HPV oncogene-driven changes first observed in tissue culture [66]. This approach is particularly helpful for tumors that may or may not be caused by HPV. Management of the ongoing HPV-positive head and neck squamous cell carcinoma (HPV^+ HNSCCs) epidemic would especially benefit, because response to therapy varies significantly between HPV-positive and -negative cancers [67]. In fact, individuals with HPV^+ HNSCCs are candidates for de-escalated therapies [68]. HPV status is currently determined using p16 status as a surrogate marker, but there are mutations that can change p16 abundance independently of HPV [69]. Since homologous recombination and other repair proteins are increased by HPV oncogenes, these proteins may be able to act as biomarkers, improving the specificity of p16 for predicting HPV status.

Cutaneous HPV Infections Repress Homologous Recombination

Although we have focused exclusively on high-risk members of the α-Papillomavirus genus to this point, other human papillomaviruses have clinically relevant interactions with the homologous recombination pathway. Members of the β-Papillomavirus genus (β-HPVs) have a tropism for cutaneous rather than anogenital and oropharyngeal keratinocytes. β-HPVs augment nonmelanoma skin cancer development, especially in people with immunosuppression [70]. The World Health Organization and the International Agency for Research on Cancer (IARC) recognize the oncogenic potential of two β-HPVs among the genus, designating β-HPV 5 and β-HPV 8 as possibly carcinogenic [71]. Although other members of the β-HPV genus may also be oncogenic [70,72,73], we follow the IARC's lead focusing only on β-HPV 5 and 8 and referring to them collectively as β-HPV (see Box 2

Box 2. Which β-HPVs Should We Worry about?

In this review, we focus on HPV 5 and HPV 8 as representative of β-HPVs, primarily because of their IARC designation. However, there is epidemiological evidence that more β-HPVs increase the risk of skin cancer. Along with HPV 5 and HPV 8, at least six other members of the genus (HPV 15, HPV 17, HPV 20, HPV 24, HPV 36, and HPV 38) are associated with a mild, yet significant, risk factor in cutaneous squamous-cell carcinoma [73]. There is also a variety of molecular evidence supporting broad, but mild, oncogenic potential within this genus. Many β-HPV E6s limit cells from undergoing UV-induced apoptosis [84]. Also, HPV 38 and HPV 49 oncogenes transform primary skin cells *in vitro* [85,86]. Among β-HPVs not designated 'possibly carcinogenic' by the IARC, HPV 38 is the best characterized. Transient expression of HPV 38 E6 and E7 promotes tumorigenesis in mice exposed to UV [72]. HPV 38E6 also reduces homologous recombination efficiency and activates telomerase [77,87]. Finally, HPV 38E6 binds p300, although more weakly than HPV 8E6 or 5E6, but does not cause its destabilization [88]. These data seem to justify reconsideration of IARC's characterization of β-HPVs. Further, given the diversity among β-HPVs, they may each have a specific genetic/immune environment where they are most transforming. Ultimately, continued interrogation of these viruses is necessary to understand the relative cancer risk associated with them and to identify appropriate antiviral treatments for any that are dangerous.

Key Figure

When a Double-Strand Break (DSB) Occurs in an S- or G2/M-Phase Cell's DNA, Homologous Recombination Proteins Assemble at the Lesion to Repair the Lesion (Repair Factor Color and Shape Match Those from Figures 1 and 2).

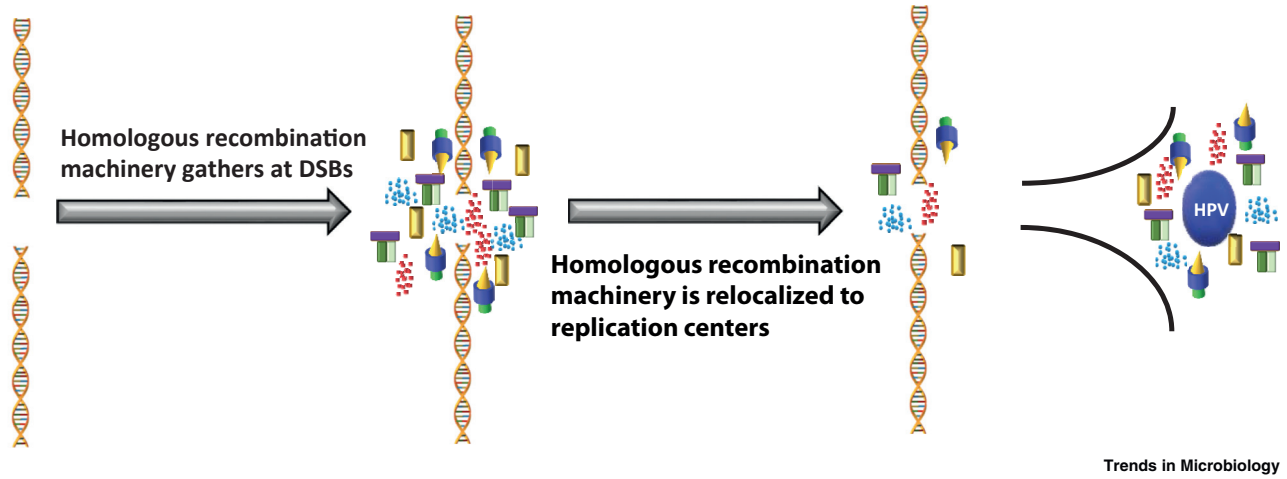

Figure 4. During an infection by human Papillomavirus (HPV), this repair machinery is leached away from cellular damage to viral replication centers (shown as a blue sphere).

for an expanded discussion of other β-HPVs). β-HPV infections appear to act by augmenting UV's mutagenic potential, making it more oncogenic. Unlike high-risk HPVs, β-HPV infections are transient. Indeed, their gene expression peaks in precancerous lesions and appears to be dispensable in tumors [74]. Similar to other HPVs, β-HPV have E6 and E7 genes (β-HPV E6 and β-HPV E7) that contain most of the virus's transforming potential. β-HPV E7 binds and destabilizes RB, but less completely than HPV E7 proteins from high-risk HPVs [71]. This likely removes cell cycle constraints, allowing cells to spend more time in parts of the cell cycle (S and G2/M phases), where DSBs are preferentially repaired via homologous recombination. β-HPV E6 attenuates multiple repair pathways, including homologous recombination, by binding and destabilizing the cellular histone acetyltransferase, p300 [75–77]. This makes UV more likely to result in a DSB and increases the risk that chromosome abnormalities (large deletions, fusions, etc.) result from crosslinked DNA [77]. Decreased p300 availability likely reaches further as p300 is a master transcription regulator [78]. We have already shown that, by destabilizing p300, β-HPV reduces the expression of four repair genes (ATM, ATR, BRCA1, BRCA2) that play critical roles in multiple repair pathways [75–77]. Presumably, by hindering repair, these viruses escape the cell cycle arrest associated with UV damage. Recently described infection models and established animal models are driving a renewed interest in this field [72,74,79,80]; however, some question the importance of p300 degradation in carcinogenesis. There are considerable basic and epidemiological gaps left to determine the extent that transient cutaneous HPV infections contribute to skin cancers, but they undoubtedly contribute to the tremendous tumor burden caused by HPV.

Concluding Remarks

Nearly all of the death and disease caused by HPV infections can be avoided through vaccinations. Unfortunately, the antivaccine movement is a persistent scourge. In the developing world, fiscal and logistic restrictions represent additional barriers. Together, this has undermined the full benefits of HPV vaccination in most countries other than Australia [81]. For unvaccinated individuals, and

people who are already infected with HPV, alternative therapies and improved biomarkers are still needed. HPV's utilization of homologous recombination provides an opportunity to meet both of these needs (Figure 4, Key Figure). We are already beginning to see this potential explored. Impaired homologous recombination synthesizes cells to PARP inhibitors and these drugs are being tested in cervical cancers [64]. Chemotherapeutic drugs that inhibit specific cell signaling pathways are becoming increasingly available in clinical settings. This is improving the opportunities to leverage an intimate understanding of HPV oncogene biology toward better patient outcomes [82]. HPV oncogene-induced changes in homologous recombination protein abundance also lead to targeted preclinical biomarker development. While there is undoubtedly a litany of remaining questions important to the field, we suggest five knowledge gaps that we find particularly compelling in the Outstanding Questions box. Using the knowledge of viral oncogene biology to improve treatment of the associated malignancies is not limited to homologous recombination and HPV-associated disease. Rather, these principles can be applied to the 15–20% of tumors with infectious origins. The lessons learned from HPV biology and therapeutic applications could thus have even larger public health consequences.

Outstanding Questions

What prevents translesion synthesis from mitigating HPV E7-induced replication stress?

Can changes in host DNA repair provide targets that improve care of HPV-associated cancers?

Why do cutaneous HPV infections take such a markedly different approach to homologous recombination?

To what extent is inhibition of homologous recombination shared among the Papillomavirus family?

Can HPV oncogenes serve as tools for dissecting homologous recombination and other DNA repair pathways?

Acknowledgments

I would like to thank Kansas State University's Johnson Cancer Research Center, and particularly the Les Clow family, for their support. Further, Dr Koenrad VanDoerslaer was instrumental in creating the stylized image of the HPV genome. Thanks Vanni.

References

1. Berman, T.A. and Schiller, J.T. (2017) Human papillomavirus in cervical cancer and oropharyngeal cancer: One cause, two diseases. *Cancer* 123, 2219–2229
2. Baldur-Felskov, B. *et al.* (2014) Early impact of human papillomavirus vaccination on cervical neoplasia – nationwide follow-up of young Danish women. *J. Natl. Cancer Inst.* 106, djt460
3. Kang, W.D. *et al.* (2013) Is vaccination with quadrivalent HPV vaccine after loop electrosurgical excision procedure effective in preventing recurrence in patients with high-grade cervical intraepithelial neoplasia (CIN2-3)? *Gynecol. Oncol.* 130, 264–268
4. Madeleine, M.M. *et al.* (2016) Natural antibodies to human papillomavirus 16 and recurrence of vulvar high-grade intraepithelial neoplasia (VIN3). *J. Low Genit. Tract. Dis.* 20, 257–260
5. Swedish, K.A. *et al.* (2012) Prevention of recurrent high-grade anal neoplasia with quadrivalent human papillomavirus vaccination of men who have sex with men: a nonconcurrent cohort study. *Clin. Infect. Dis.* 54, 891–898
6. de Martel, C. *et al.* (2017) Worldwide burden of cancer attributable to HPV by site, country and HPV type. *Int. J. Cancer* 141, 664–670
7. Sudenga, S.L. *et al.* (2016) Cervical HPV natural history among young Western Cape, South African women: the randomized control EVRI trial. *J. Infect.* 72, 60–69
8. Vink, M.A. *et al.* (2013) Clinical progression of high-grade cervical intraepithelial neoplasia: estimating the time to preclinical cervical cancer from doubly censored national registry data. *Am. J. Epidemiol.* 178, 1161–1169
9. Marur, S. *et al.* (2010) HPV-associated head and neck cancer: a virus-related cancer epidemic. *Lancet Oncol.* 11, 781–789
10. Jackson, S.P. and Bartek, J. (2009) The DNA-damage response in human biology and disease. *Nature* 461, 1071–1078
11. Bristol, M.L. *et al.* (2017) Why human papillomaviruses activate the DNA damage response (DDR) and how cellular and viral replication persists in the presence of DDR signaling. *Viruses* 9, E268
12. Hollingworth, R. and Grand, R.J. (2015) Modulation of DNA damage and repair pathways by human tumour viruses. *Viruses* 7, 2542–2591
13. Hustedt, N. and Durocher, D. (2016) The control of DNA repair by the cell cycle. *Nat. Cell Biol.* 19, 1–9
14. Nowsheen, S. and Yang, E.S. (2012) The intersection between DNA damage response and cell death pathways. *Exp. Oncol.* 34, 243–254
15. Jasin, M. and Rothstein, R. (2013) Repair of strand breaks by homologous recombination. *Cold Spring Harb. Perspect. Biol.* 5, a012740
16. Van Doorslaer, K. *et al.* (2017) The papillomavirus episteme: a major update to the papillomavirus sequence database. *Nucleic. Acids Res.* 45, D499–D506
17. Doorbar, J. *et al.* (2012) The biology and life-cycle of human papillomaviruses. *Vaccine* 30 (*Suppl.* 5), F55–F70
18. Moody, C.A. and Laimins, L.A. (2009) Human papillomaviruses activate the ATM DNA damage pathway for viral genome amplification upon differentiation. *PLoS Pathog.* 5, e1000605
19. Blackford, A.N. and Jackson, S.P. (2017) ATM, ATR, and DNA-PK: the trinity at the heart of the DNA damage response. *Mol. Cell* 66, 801–817
20. Mehta, K. *et al.* (2015) Human papillomaviruses activate and recruit SMC1 cohesin proteins for the differentiation-dependent life cycle through association with CTCF insulators. *PLoS Pathog.* 11, e1004763
21. Potts, P.R. *et al.* (2006) Human SMC5/6 complex promotes sister chromatid homologous recombination by recruiting the SMC1/3 cohesin complex to double-strand breaks. *EMBO J.* 25, 3377–3388
22. Anacker, D.C. *et al.* (2014) Productive replication of human papillomavirus 31 requires DNA repair factor Nbs1. *J. Virol.* 88, 8528–8544
23. Chappell, W.H. *et al.* (2015) Homologous recombination repair factors Rad51 and BRCA1 are

necessary for productive replication of human papillomavirus 31. *J. Virol.* 90, 2639–2652
24. Hong, S. *et al.* (2015) STAT-5 regulates transcription of the topoisomerase IIβ-binding protein 1 (TopBP1) gene to activate the ATR pathway and promote human papillomavirus replication. *mBio* 6, e02006–e02015
25. Hong, S. and Laimins, L.A. (2013) The JAK-STAT transcriptional regulator, STAT-5, activates the ATM DNA damage pathway to induce HPV 31 genome amplification upon epithelial differentiation. *PLoS Pathog.* 9, e1003295
26. Fradet-Turcotte, A. *et al.* (2011) Nuclear accumulation of the papillomavirus E1 helicase blocks S-phase progression and triggers an ATM-dependent DNA damage response. *J. Virol.* 85, 8996–9012
27. Sakakibara, N. *et al.* (2011) The papillomavirus E1 helicase activates a cellular DNA damage response in viral replication foci. *J. Virol.* 85, 8981–8995
28. Bristol, M.L. *et al.* (2016) DNA damage reduces the quality, but not the quantity of human papillomavirus 16 E1 and E2 DNA replication. *Viruses* 8, 175
29. Johnson, B.A. *et al.* (2017) The Rb binding domain of HPV31 E7 is required to maintain high levels of DNA repair factors in infected cells. *Virology* 500, 22–34
30. Wallace, N.A. *et al.* (2017) High risk alpha papillomavirus oncogenes impair the homologous recombination pathway. *J. Virol.* 91, e01084-17.
31. Langsfeld, E.S. *et al.* (2015) The deacetylase sirtuin 1 regulates human papillomavirus replication by modulating histone acetylation and recruitment of DNA damage factors NBS1 and Rad51 to viral genomes. *PLOS Pathog* 11, e1005181
32. Das, D. *et al.* (2017) The deacetylase SIRT1 regulates the replication properties of human papillomavirus 16 E1 and E2. *J. Virol.* 91, e00102–e00117
33. Gillespie, K.A. *et al.* (2012) Human papillomaviruses recruit cellular DNA repair and homologous recombination factors to viral replication centers. *J. Virol.* 86, 9520–9526
34. Khanal, S. and Galloway, D.A. (2019) High-risk human papillomavirus oncogenes disrupt the Fanconi anemia DNA repair pathway by impairing localization and de-ubiquitination of FancD2. *PLoS Pathog* 15, e1007442
35. Mehta, K. and Laimins, L. (2018) Human papillomaviruses preferentially recruit DNA repair factors to viral genomes for rapid repair and amplification. *mBio* 9, e00064–18.
36. Chang, H.H.Y. *et al.* (2017) Non-homologous DNA end joining and alternative pathways to double-strand break repair. *Nat. Rev. Mol. Cell Biol.* 18, 495–506
37. Lee, C.-S. *et al.* (2014) Dynamics of yeast histone H2A and H2B phosphorylation in response to a double-strand break. *Nat. Struct. Mol. Biol.* 21, 103–109
38. Reinson, T. *et al.* (2015) The cell cycle timing of human papillomavirus DNA replication. *PLoS One* 10, e0131675
39. McLaughlin-Drubin, M.E. and Münger, K. (2009) The human papillomavirus E7 oncoprotein. *Virology* 384, 335–344
40. Moody, C.A. (2019) The impact of replication stress in human papillomavirus pathogenesis. *J. Virol.* 93, e01003–e01018
41. Gameiro, S.F. *et al.* (2017) Human papillomavirus dysregulates the cellular apparatus controlling the methylation status of H3K27 in different human cancers to consistently alter gene expression regardless of tissue of origin. *Oncotarget* 8, 72564–72576
42. McLaughlin-Drubin, M.E. *et al.* (2011) Human papillomavirus E7 oncoprotein induces KDM6A and KDM6B histone demethylase expression and causes epigenetic reprogramming. *Proc. Natl. Acad. Sci. U. S. A.* 108, 2130–2135
43. McLaughlin-Drubin, M.E. *et al.* (2013) Tumor suppressor p16INK4A is necessary for survival of cervical carcinoma cell lines. *Proc. Natl. Acad. Sci. U. S. A.* 110, 16175–16180
44. Soto, D.R. *et al.* (2017) KDM6A addiction of cervical carcinoma cell lines is triggered by E7 and mediated by p21CIP1 suppression of replication stress. *PLOS Pathog.* 13, e1006661
45. Anacker, D.C. *et al.* (2016) HPV31 utilizes the ATR-Chk1 pathway to maintain elevated RRM2 levels and a replication-competent environment in differentiating keratinocytes. *Virology* 499, 383–396
46. Zou, L. (2007) Single- and double-stranded DNA: building a trigger of ATR-mediated DNA damage response. *Genes Dev.* 21, 879–885
47. Göhler, T. *et al.* (2011) ATR-mediated phosphorylation of DNA polymerase η is needed for efficient recovery from UV damage. *J. Cell Biol.* 192, 219–227
48. Leung, W. *et al.* (2019) Mechanisms of DNA damage tolerance: post-translational regulation of PCNA. *Genes (Basel)* 10, 10
49. Reinson, T. *et al.* (2013) Engagement of the ATR-dependent DNA damage response at the human papillomavirus 18 replication centers during the initial amplification. *J. Virol.* 87, 951–964
50. Singh, B. and Wu, P.-Y.J. (2019) Linking the organization of DNA replication with genome maintenance. *Curr. Genet.* 65, 677–683
51. Chen, B. *et al.* (2009) Human papilloma virus type16 E6 deregulates CHK1 and sensitizes human fibroblasts to environmental carcinogens independently of its effect on p53. *Cell Cycle* 8, 1775–1787
52. Gu, W. *et al.* (2019) Cervical cancer cell lines are sensitive to sub-erythemal UV exposure. *Gene* 688, 44–53
53. Mirghani, H. *et al.* (2015) Increased radiosensitivity of HPV-positive head and neck cancers: molecular basis and therapeutic perspectives. *Cancer Treat. Rev.* 41, 844–852
54. Nickson, C.M. *et al.* (2017) Misregulation of DNA damage repair pathways in HPV-positive head and neck squamous cell carcinoma contributes to cellular radiosensitivity. *Oncotarget* 8, 29963–29975
55. Park, J.W. *et al.* (2014) Human papillomavirus type 16 E7 oncoprotein causes a delay in repair of DNA damage. *Radiother. Oncol.* 113, 337–344
56. Yuan, C.-H. *et al.* (2012) Modulation of apoptotic pathways by human papillomaviruses (HPV): mechanisms and implications for therapy. *Viruses* 4, 3831–3850
57. Hall, A.H.S. and Alexander, K.A. (2003) RNA interference of human papillomavirus type 18 E6 and E7 induces senescence in HeLa cells. *J. Virol.* 77, 6066–6069
58. O'Neil, N.J. *et al.* (2017) Synthetic lethality and cancer. *Nat. Rev. Genet.* 18, 613–623
59. Cohen, P.A. *et al.* (2019) Cervical cancer. *Lancet* 393, 169–182
60. Puigvert, J.C. *et al.* (2016) Targeting DNA repair, DNA metabolism and replication stress as anti-cancer strategies. *FEBS J.* 283, 232–245
61. Shaheen, M. *et al.* (2011) Synthetic lethality: exploiting the addiction of cancer to DNA repair. *Blood* 117, 6074–6082
62. Zimmer, A.S. *et al.* (2018) Update on PARP inhibitors in breast cancer. *Curr. Treat. Options Oncol.* 19, 21
63. Kunos, C. *et al.* (2015) A phase I–II evaluation of veliparib (NSC#737664), topotecan, and filgrastim or pegfilgrastim in the treatment of persistent or recurrent carcinoma of the uterine cervix: an NRG

Oncology/Gynecologic Oncology Group study. *Int. J. Gynecol. Cancer* 25, 484–492
64. Matulonis, U.A. and Monk, B.J. (2017) PARP inhibitor and chemotherapy combination trials for the treatment of advanced malignancies: does a development pathway forward exist? *Ann. Oncol.* 28, 443–447
65. Thaker, P.H. *et al.* (2017) A phase I trial of paclitaxel, cisplatin, and veliparib in the treatment of persistent or recurrent carcinoma of the cervix: an NRG Oncology Study (NCT#01281852). *Ann. Oncol.* 28, 505–511
66. Spriggs, C.C. *et al.* (2019) Expression of HPV-induced DNA damage repair factors correlates with CIN progression. *Int. J. Gynecol. Pathol.* 38, 1–10
67. Dok, R. and Nuyts, S. (2016) HPV positive head and neck cancers: molecular pathogenesis and evolving treatment strategies. *Cancers (Basel)* 8, 41
68. Mirghani, H. and Blanchard, P. (2018) Treatment de-escalation for HPV-driven oropharyngeal cancer: where do we stand? *Clin. Transl. Radiat. Oncol.* 8, 4–11
69. Vokes, E.E. *et al.* (2015) HPV-associated head and neck cancer. *J. Natl. Cancer Inst.* 107, djv344
70. Tommasino, M. (2017) The biology of beta human papillomaviruses. *Virus Res.* 231, 128–138
71. Wendel, S.O. and Wallace, N.A. (2017) Loss of genome fidelity: beta HPVs and the DNA damage response. *Front. Microbiol.* 8
72. Viarisio, D. *et al.* (2018) Beta HPV38 oncoproteins act with a hit-and-run mechanism in ultraviolet radiation-induced skin carcinogenesis in mice. *PLoS Pathog.* 14, e1006783
73. Rollison, D.E. *et al.* (2019) An emerging issue in oncogenic virology: the role of beta human papillomavirus types in the development of cutaneous squamous cell carcinoma. *J. Virol.* 93, e01003–e01018
74. Hufbauer, M. and Akgül, B. (2017) Molecular mechanisms of human papillomavirus induced skin carcinogenesis. *Viruses* 9, 187
75. Wallace, N.A. *et al.* (2012) HPV 5 and 8 E6 abrogate ATR activity resulting in increased persistence of UVB induced DNA damage. *PLoS Pathog.* 8, e1002807
76. Wallace, N.A. *et al.* (2013) HPV 5 and 8 E6 expression reduces ATM protein levels and attenuates LINE-1 retrotransposition. *Virology* 443, 69–79
77. Wallace, N.A. *et al.* (2015) β-HPV 5 and 8 E6 disrupt homology dependent double strand break repair by attenuating BRCA1 and BRCA2 expression and foci formation. *PLoS Pathog.* 11, e1004687
78. Bedford, D.C. and Brindle, P.K. (2012) Is histone acetylation the most important physiological function for CBP and p300? *Aging (Albany NY)* 4, 247–255
79. Meyers, J.M. *et al.* (2017) Cutaneous HPV8 and MmuPV1 E6 proteins target the NOTCH and TGF-β tumor suppressors to inhibit differentiation and sustain keratinocyte proliferation. *PLOS Pathog.* 13, e1006171
80. Xue, X.-Y. *et al.* (2017) The full transcription map of mouse papillomavirus type 1 (MmuPV1) in mouse wart tissues. *PLoS Pathog.* 13, e1006715
81. Lee, L. and Garland, S.M. (2017) Human papillomavirus vaccination: the population impact. *F1000Res* 6, 866
82. Kelley, M.R. *et al.* (2014) Targeting DNA repair pathways for cancer treatment: what's new? *Future Oncol.* 10, 1215–1237
83. Egawa, N. and Doorbar, J. (2017) The low-risk papillomaviruses. *Virus Res.* 231, 119–127
84. Underbrink, M.P. *et al.* (2008) E6 proteins from multiple human betapapillomavirus types degrade Bak and protect keratinocytes from apoptosis after UVB irradiation. *J. Virol.* 82, 10408–10417
85. Cornet, I. *et al.* (2012) Comparative analysis of transforming properties of E6 and E7 from different beta human papillomavirus types. *J. Virol.* 86, 2366–2370
86. Muench, P. *et al.* (2010) Cutaneous Papillomavirus E6 proteins must interact with p300 and block p53-mediated apoptosis for cellular immortalization and tumorigenesis. *Cancer Res.* 70, 6913–6924
87. Bedard, K.M. *et al.* (2008) The E6 oncoproteins from human betapapillomaviruses differentially activate telomerase through an E6AP-dependent mechanism and prolong the lifespan of primary keratinocytes. *J. Virol.* 82, 3894–3902
88. Howie, H.L. *et al.* (2011) Beta-HPV 5 and 8 E6 promote p300 degradation by blocking AKT/p300 association. *PLoS Pathog.* 7, e1002211

pathogens

MDPI

Article

β-HPV 8E6 Attenuates ATM and ATR Signaling in Response to UV Damage

Jazmine A. Snow, Vaibhav Murthy, Dalton Dacus, Changkun Hu and Nicholas A. Wallace *

Division of Biology, Kansas State University, Manhattan, KS 66502, USA; jazasnow@ksu.edu (J.A.S.); murthy.39@buckeyemail.osu.edu (V.M.); dacus@ksu.edu (D.D.); Chu1@ksu.edu (C.H.)
* Correspondence: nwallac@ksu.edu

Received: 27 September 2019; Accepted: 22 November 2019; Published: 26 November 2019

Abstract: Given the high prevalence of cutaneous genus beta human papillomavirus (β-HPV) infections, it is important to understand how they manipulate their host cells. This is particularly true for cellular responses to UV damage, since our skin is continually exposed to UV. The E6 protein from β-genus HPV (β-HPV E6) decreases the abundance of two essential UV-repair kinases (ATM and ATR). Although β-HPV E6 reduces their availability, the impact on downstream signaling events is unclear. We demonstrate that β-HPV E6 decreases ATM and ATR activation. This inhibition extended to XPA, an ATR target necessary for UV repair, lowering both its phosphorylation and accumulation. β-HPV E6 also hindered POLη accumulation and foci formation, critical steps in translesion synthesis. ATM's phosphorylation of BRCA1 is also attenuated by β-HPV E6. While there was a striking decrease in phosphorylation of direct ATM/ATR targets, events further down the cascade were not reduced. In summary, despite being incomplete, β-HPV 8E6's hindrance of ATM/ATR has functional consequences.

Keywords: genus beta human papillomavirus; ATM; ATR; nucleotide excision repair; translesion synthesis; cell cycle; UV

1. Introduction

The human papillomavirus (HPV) family is made up of five genera (alpha, beta, gamma, mu and nu papillomaviruses), each containing a large number of individual HPV types [1,2]. The division into these groups is based on differences in the major capsid gene's sequence [3,4]. Although all these genera contain members capable of causing disease, the alpha (α-HPV) and beta (β-HPV) genera have received the most research attention because of their connection and potential connection to cancer, respectively [5–8]. Certain members of the alpha papillomavirus genus are known to cause tumors in the anogenital tract and in the oropharynx [9]. These so-called high risk, or HR α-HPVs, cause tumors that are dependent on continued viral oncogene (HR α-HPV E6 and E7) expression, making it somewhat straightforward to connect their infections with tumorigenesis [10,11].

β-HPVs are far more difficult to definitively tie to malignancies but may contribute to non-melanoma skin cancer (NMSC) development in certain populations and potentially more broadly [12]. The difficulty in linking β-HPVs to NMSCs is that, unlike HR-α HPVs, they do not cause an infection that lingers in the tumor [13,14]. Their infections are more transient, lasting for months rather than decades like HR-α HPVs [15]. As a result, β-HPV infections are thought to act through a "hit and run" mechanism of oncogenesis [16,17]. This hypothesis holds that β-HPV infections act synergistically along with UV radiation to promote tumorigenic mutations that cause lasting changes to the cellular environment without being dependent on continued expression of β-HPV's putative oncogenes (β-HPV E6 and E7) [18].

The "hit and run" hypothesis presents a challenge for epidemiologists that is further compounded by the fact that neither β-HPV infections nor NMSCs are rare. In fact, most people are sero-positive for at least one β-HPV and there are millions of NMSCs diagnosed each year [19–21]. The purposed link between β-HPV and NMSCs is best characterized in individuals with *Epidermodysplasia verruciformis* (EV), a genetic disease that is associated with an increased susceptibility to HPV infections, and in solid organ transplant recipients [22–24]. While a potential role in cancer warrants further investigation, the ubiquitous presence of β-HPV in our skin alone makes it important to further understand β-HPV biology.

Of β-HPV's genes, β-HPV E6 is the most well characterized [25]. It alters multiple cell signaling pathways including MAML1, TGFβ, NOTCH and EGFR signaling [26–28]. It also binds and destabilizes the cellular histone acetyltransferase, p300 [29]. We have previously shown p300's role as a transcription factor is required for robust expression of at least four essential DNA repair genes, including two essential repair kinases (ATM and ATR) [30–32]. Because of their position atop multiple repair pathways, we hypothesize that diminished ATM and ATR availability has a far-reaching impact on the ability of cells to protect themselves from UV radiation [33–36]. We test this hypothesis with a combination of in silico and in vitro analyses, specifically focusing on phosphorylation events that facilitate cell cycle regulation, nucleotide excision repair (NER), and translesion synthesis (TLS). NER is responsible for physically removing UV-induced DNA lesions and it has been shown that an essential protein, XPA, is stabilized by ATR phosphorylation [37,38]. The TLS pathway helps bypass UV lesions primarily through the TLS polymerase, POLη, which is regulated by ATR and p53 [39,40]. Finally, ATM and ATR control cell cycle progression via phosphorylation of CHK1 and CHK2 [41–43].

2. Results

2.1. ATR, ATM and p53 Have Distinct Transcription Effector Profiles

We have previously reported that β-HPV 8E6 decreases ATM and ATR abundance [30,31]. However, the extent that β-HPV 8E6 disrupts ATM and ATR signaling remains poorly defined. This motivated us to characterize the extent that β-HPV 8E6 alters ATM and ATR signaling pathways. As a first step, we performed an in silico screen of previously collected transcriptomic data featuring 877 different cell lines [44–46]. Cell lines with ATM/ATR expression with z-scores below −2 were considered to have low expression (28 and 22 cell lines respectively) and compared to the remaining cell lines. We focused our analysis on genes that belonged to two pathways involved in UV repair responses, namely nucleotide excision repair (NER) and translesion synthesis (TLS) as well as a few canonical ATR/ATM targets (BRCA1, CHEK1, CDC25A, and TP53) [47–51]. We were unable to perform this analysis for CHEK2, one of the most characterized ATM targets, as there was no data available in the transcriptomic data. Gene expression was plotted against statistical significance in volcano plots to highlight significant robust correlations (Figure 1).

As expected, ATM and ATR expression positively correlated with UV responsive and canonical target gene expressions. We complimented this approach by performing the reciprocal analysis of cells that had high expression of these kinases. Despite comparing different subsets of cell lines, we found similar correlations among ATM/ATR and UV-responsive gene expression (28 and 45 cell lines were observed to have excess ATM/ATR, respectively) (Supplemental Figure S1). As a final computational effort, we compared expression profiles in cell lines segregated by the presence or absence of ATM/ATR truncating mutations (Supplemental Figure S2). However, there was only a small number of cell lines with ATM/ATR truncating mutations available for analysis, therefore the significant gene expression changes are not as robust. This also supported the role of these kinases as broad regulators of UV responsive gene expression. For both low and high expression of ATM/ATR, the changes in all three gene expression groups were more strongly correlated with ATM expression than ATR expression (Figure 1, Supplemental Figure S1).

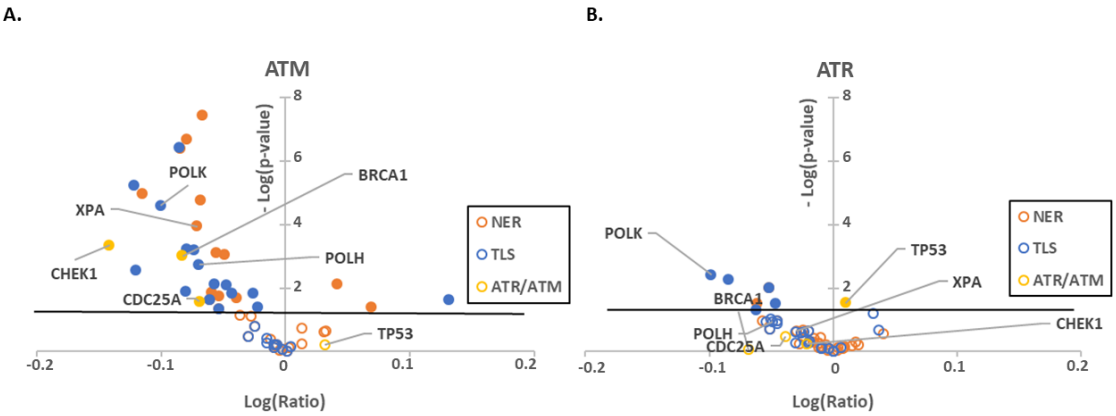

Figure 1. Low expression of ATR/ATM mRNA correlates with a decrease in UV damage repair pathways gene expression. Volcano plots comparing RNAseq data of NER (orange), TLS (blue) and ATR/ATM target (yellow) genes between cell lines (**A**) with low ATM expression (z-score > 2) and without decreased ATM expression (z-score < 2) or (**B**) between cells with (z-score > 2) and without (z-score < 2) low ATR expression. Outlined circles represent non-significant expression changes. Filled in circles represent significant expression changes. The black line represents significance cutoff ($p < 0.05$). The x-axis depicts the log of the ratio of each gene's expression levels in cell lines with high expression of ATM/ATR versus all other cell lines in the cancer cell line encyclopedia. The y-axis shows the negative log of the *p*-value. Genes with reduced expression appear to the left of the y-axis, while genes with increased expression are on the right.

Both capstone DNA repair kinases have multiple targets that they regulate primarily via phosphorylation [34]. p53 is preeminent among those targets for both ATM and ATR [52]. We have also previously shown that β-HPV 8E6 delays p53 stabilization in response to UV damage [53]. p53 is also a well-recognized transcription factor [54]. To gain some insight into how much of the expression profiles was the result of ATM/ATR signaling through p53, we characterized expression of ATM/ATR responsive genes in transcriptomic data from cell lines segregated by p53 expression (Table 1). This was distinct from both ATM and ATR expression profiles but shared some notable overlap. POLK had a positive correlation in all three settings suggesting that POLK may be regulated by ATM, ATR and p53. This includes the possibility that each regulates POLK expression independently as well as the possibility that ATM and ATR regulate POLK by stabilizing p53. We interpret these data as consistent with other reports describing distinct but overlapping roles for ATM, ATR and p53 in response to UV. However, not all of these changes remained significant when accounting for the false discovery rate associated with multiple comparisons (Supplemental Table S1). This prompted us to test our hypothesis using in vitro approaches.

Table 1. Different expression profiles in cells with lower ATM, ATR and p53 expression. n.s. denotes a non-significant relationship. −/+ denote significant relationships $p < 0.05$ with low magnitude. −−/++ denote relationships with $0.05 < p > 0.001$ and $0.02 >$ log ration > 0.01. −−−/+++ denote relationships with $p < 0.001$ and log ratio > 0.02. (sign denotes negative and positive regulation).

	p53	ATR	ATM
BRCA1	n.s.	++	+++
CDC25A	n.s.	n.s.	++
CHEK1	−	n.s.	+++
POLH	+++	n.s.	++
POLK	+	++	+++
XPA	−	n.s.	+++

2.2. β-HPV E6 Decreases ATM and ATR Activation

The correlations demonstrated by these data motivated us to interrogate β-HPV E6's ability to decrease ATR/ATM signaling with in vitro systems, beginning with the ATM activation that occurs via autophosphorylation at Ser1981 (pATM). β-HPV infection occurs in keratinocytes, making them the preferred cell culture model. We used p300 abundance as a surrogate marker for β-HPV E6 expression to confirm expression of β-HPV E6 in primary keratinocytes (LXSN and β-HPV 8E6 HFKs). Since these cells are derived from patients, it was important to control for donor variability using lines derived from separate sources. To this end, we also tested our hypothesis in keratinocytes derived from a different donor and immortalized by exogenous hTERT expression (hTERT HFKs). Probing for the HA-tag on the β-HPV 8E6 expressed in hTERT HFKs provided proof of expression (Supplemental Figure S3). Finally, hTERT HFKs mimic the telomerase activation that is a common in NMSCs providing insight into β-HPV E6 phenotypes in a relevant cellular environment [55].

β-HPV 8E6 decreased total and activated ATM in each of these cell lines (Figure 2A). This loss is seen more clearly in primary HFKs. The difference in activated ATM remained over 8 h after UV-induced ATM activation (Figure 2B,C, Supplemental Figure S4A–D). To determine if β-HPV 8E6 prevents ATM from phosphorylating its downstream targets, we probed for two canonical ATM targets associated with the DNA damage response, Ser1423 of BRCA1 (pBRCA1) and Thr68 of CHK2 (pCHK2) [43,56]. β-HPV 8E6 caused aberrations in both proteins' reaction to UV (Figure 2B,C). pCHK2 accumulation and total CHK2 abundance were both decreased by β-HPV 8E6. pBRCA1 levels peaked higher, but this buildup was delayed, occurring several hours after they reach their maxima in vector control hTERT HFKs, demonstrating a delayed response similar to what we have reported for p53 for hTERT HFKs [30] (Figure 2B, Supplemental Figure S4E–H). We did not see this delayed peak in pBRCA1 occur in the primary HFKs (Figure 2C). β-HPV 8E6 also decreased p53 stabilization, but we cannot distinguish whether this is an ATM or ATR effect as both kinases stabilize p53 (Supplemental Figure S5). To determine if β-HPV 8E6 changed ATM's cellular position, we performed subcellular fractionation on cells before and after UV treatment. There were no robust differences in nuclear localization, suggesting that β-HPV 8E6 primarily impairs ATM activation via decreased expression and autophosphorylation. Interestingly, we did observe some changes in cytoplasmic localization between LXSN, vector control, and β-HPV 8E6 in untreated cells (Figure 2D). We then moved to ATR's activation by autophosphorylation at Thr1989 (pATR). This typically occurs in response to single stranded DNA associated with replication stress [57]. β-HPV E6 decreased pATR in hTERT HFKs (Figure 3A). pATR levels increased in vector control HFKs and in β-HPV E6 over 6/8-h post UV. However, β-HPV E6 diminished pATR induction. This resulted in notably less pATR in cells with β-HPV 8E6 after UV (Figure 3B,C, Supplemental Figure S4I,J). Subcellular fractionation did not provide evidence that β-HPV E6 attenuated localization of pATR to the nucleus (Figure 3D).

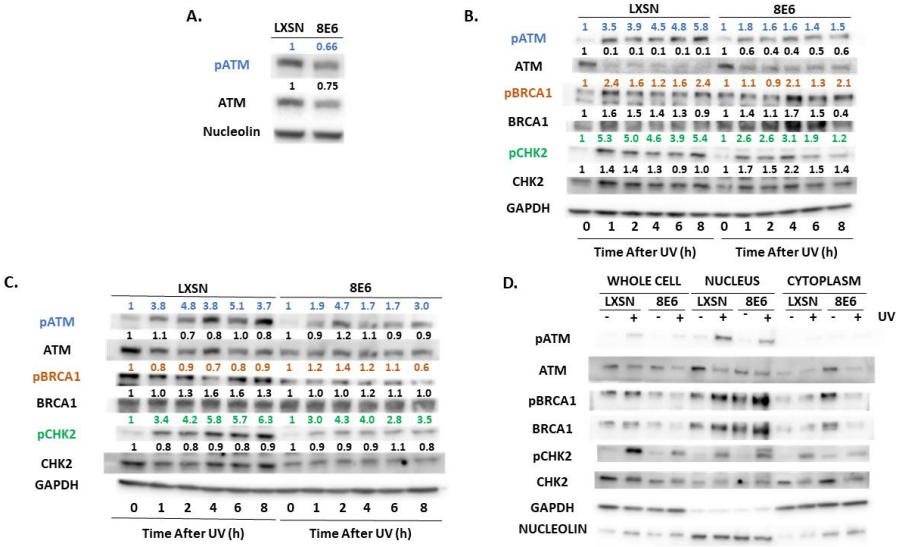

Figure 2. β-HPV 8E6 attenuates ATM activation. (**A**) Representative immunoblots of untreated hTERT HFKs with vector control (LXSN) and β-HPV 8E6 cell lines. Nucleolin was used as a loading control. (**B**) Representative immunoblots of hTERT HFKs with vector control (LXSN) and β-HPV 8E6 harvested 0–8 h post 5 mJ/cm^2 UVR. GAPDH was used as a loading control. (**C**) Representative immunoblots of primary HFKs with vector control (LXSN) and β-HPV 8E6 harvested 0–8 h post 5 mJ/cm^2 UVR. GAPDH was used as a loading control. (**A**–**C**) The numbers above bands represent quantification by densitometry. This is shown relative to untreated cells within the same cell line and normalized to the loading control. (**D**) Subcellular fractionation of hTERT HFKs with vector control (LXSN) and β-HPV 8E6 cell line lysates harvested 6 h post exposure to 5 mJ/cm^2 UVR were observed via immunoblot. GAPDH was used as a cytoplasmic loading control and Nucleolin was used as a nuclear loading control.

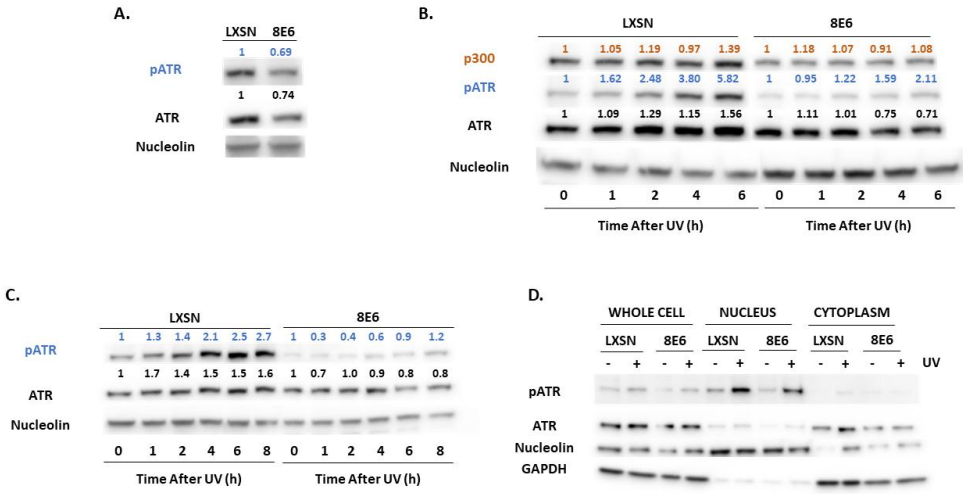

Figure 3. β-HPV 8E6 attenuates ATR activation. (**A**) Representative immunoblots of untreated hTERT HFKs with vector control (LXSN) and β-HPV 8E6 cell lines. Nucleolin was used as a loading control. (**B**) Representative immunoblots of hTERT HFKs with vector control (LXSN) and β-HPV 8E6 harvested 0–6 h post 5 mJ/cm^2 UVR. Nucleolin was used as a loading control. (**C**) Representative immunoblots of primary HFKs with vector control (LXSN) and β-HPV 8E6 harvested 0–8 h post 5 mJ/cm^2 UVR. Nucleolin was used as a loading control. (**A**–**C**) The numbers above bands represent quantification by densitometry. This is shown relative to untreated cells within the same cell line and normalized to the loading control. (**D**) Subcellular fractionation of hTERT HFKs with vector control (LXSN) and β-HPV 8E6 cell line lysates harvested 6 h post exposure to 5 mJ/cm^2 UVR were observed via immunoblot. GAPDH was used as a cytoplasmic loading control and Nucleolin was used as a nuclear loading control.

2.3. β-HPV 8E6 Decreases Phosphorylation of ATR Target Proteins

We continued our characterization of β-HPV 8E6's impact on UV signaling by examining ATR's most established target, CHK1 [57–59]. ATR phosphorylates CHK1 at Ser345 (pCHK1) in response to replication stress and UV [59]. We saw a mild increase in a replication stress marker (RPA32 at Ser8 (pRPA32)) accompanying β-HPV 8E6 expression (Supplemental Figure S6). In contrast, pCHK1 was decreased by β-HPV 8E6 (Figure 4A). To determine if CHEK1 transcription changed, RT-PCR was performed. β-HPV 8E6 caused a modest but non-significant decrease in CHEK1 mRNA consistent with our in silico data (Figures 1 and 4B). Next, we probed pCHK1 and total CHK1 by immunoblot over a 6/8-h time course after UV. While UV elicited a sizable increase in pCHK1 within an hour of exposure in vector control cells, β-HPV 8E6 prevent all but a mild induction of pCHK1 (Figure 4C,D, Supplemental Figure S4K,L). These changes were independent of foreskin donor or hTERT activation.

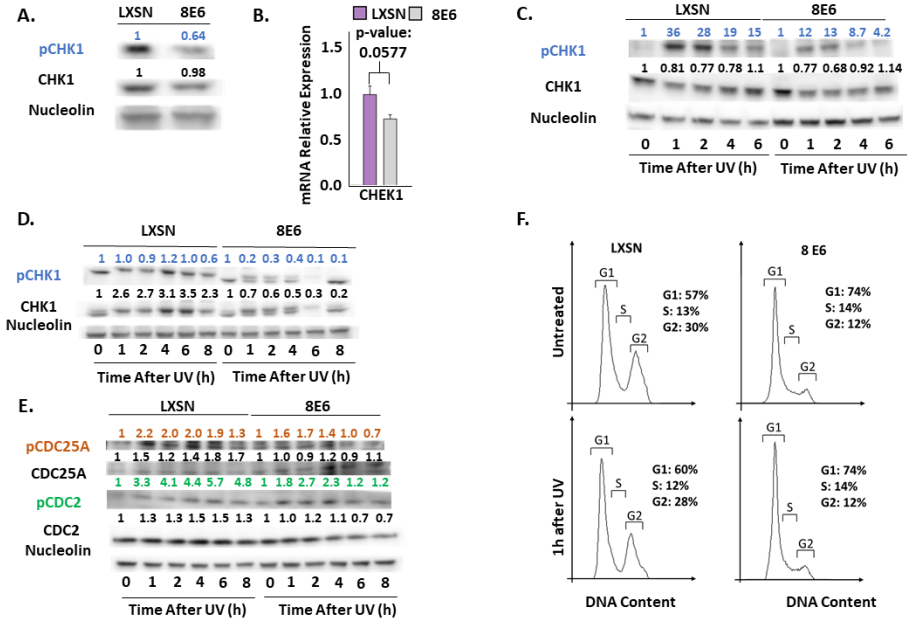

Figure 4. β-HPV 8E6 attenuates CHK1 phosphorylation. (**A**) Representative immunoblots of untreated hTERT HFKs with vector control (LXSN) and β-HPV 8E6 cell lines. Nucleolin was used as a loading control. (**B**) mRNA expression level of CHEK1 in vector control (LXSN) and β-HPV 8E6 expressing primary HFKs as measured by RT-qPCR and normalized towards the expression level of β-actin. Data shown in figures are the means of ±SE of three independent experiments. (**C**) Representative immunoblots of hTERT HFKs with vector control (LXSN) and β-HPV 8E6 harvested 0–6 h post 5mJ/cm^2 UVR. Nucleolin was used as a loading control. (**D**) Representative immunoblots of primary HFKs with vector control (LXSN) and β-HPV 8E6 harvested 0–8 h post 5 mJ/cm^2 UVR. Nucleolin was used as a loading control. (**E**) Representative immunoblots of hTERT HFKs with vector control (LXSN) and β-HPV 8E6 harvested 0–8 h post 5 mJ/cm^2 UVR. Nucleolin was used as a loading control. (**A, C**–**E**) The numbers above bands represent quantification by densitometry. This is shown relative to untreated cells within the same cell line and normalized to the loading control. (**F**) Cell cycle analysis of hTERT HFKs with LXSN vector control and β-HPV 8E6 1 h post 5 mJ/cm^2 UVR.

CHK1 coordinates cell cycle progression at the G1-S boundary [60]. To determine if β-HPV 8E6 diminished phosphorylation downstream of CHK1 activation, we defined the phosphorylation status of CHK1 targets, beginning with CDC25A [42]. This dual–specificity protein phosphatase removes inhibitory phosphorylates from cyclin-dependent kinases, like CDK2, and other regulatory factors, like CDC2, allowing them to promote cell cycle progression. Highlighting the key role of CDC25A in tumorigenesis, it is frequently overexpressed in cancer cells and associated with poor cancer patient outcomes [61]. In response to UV, pCHK1 phosphorylates CDC25A increasing its

proteasome-mediated turnover [42]. To our surprise, β-HPV 8E6 did not reliably change total CDC25A abundance or the protein's phosphorylation at Thr507 (pCDC25A) (Figure 4E and Supplemental Figure S7). β-HPV 8E6 caused inconsistent changes to pCDC2 (at Thr14) (Figure 4E and Supplemental Figure S7). This could be explained either by β-HPV 8E6 not completely inhibiting ATR signaling or by redundant kinase activity. Despite not completely blocking ATR signaling, β-HPV 8E6 subtly changed cell cycle distribution, mildly increasing the proportion of cells in G1 (Figure 4F).

ATR promotes NER by phosphorylating and stabilizing XPA in response to UV [62,63]. We measured total XPA and XPA phosphorylation at Ser196 (pXPA) by immunoblot (Figure 5A). A small but insignificant decrease in XPA mRNA accompanied β-HPV 8E6 expression indicating that this decrease in abundance is not likely due to reduced transcription (Figure 5B). Next, we looked at pXPA and XPA by immunoblot over a 6/8-h time course after UV. We observed that pXPA was increased in LXSN, vector control, after cells were exposed to UV. However, in the presence of β-HPV 8E6, pXPA protein abundance was decreased even after exposure to UV (Figure 5C,D, Supplemental Figure S4M,N). While there was only a subtle decrease in pXPA in hTERT HFKs following UV, this decline is more visible in primary HFKs. For further validation, we observed XPA phosphorylation in a previously described osteosarcoma cell line expressing β-HPV 8E6. β-HPV 8E6 attenuated XPA phosphorylation in these cells (Supplemental Figure S8). Consistent with our previous experiments, we found that β-HPV 8E6 did not affect XPA's distribution in subcellular fraction experiments. (Figure 5E). However, immunofluorescence microscopy showed mild differences in XPA localization associated with β-HPV 8E6. Specifically, XPA remained dispersed throughout the cell. This contrasts with XPA's localization in control cells where it is nearly exclusively nuclear. This data suggests that β-HPV 8E6 may have some ability to decrease nuclear localization of XPA after UV exposure. (Supplemental Figure S9).

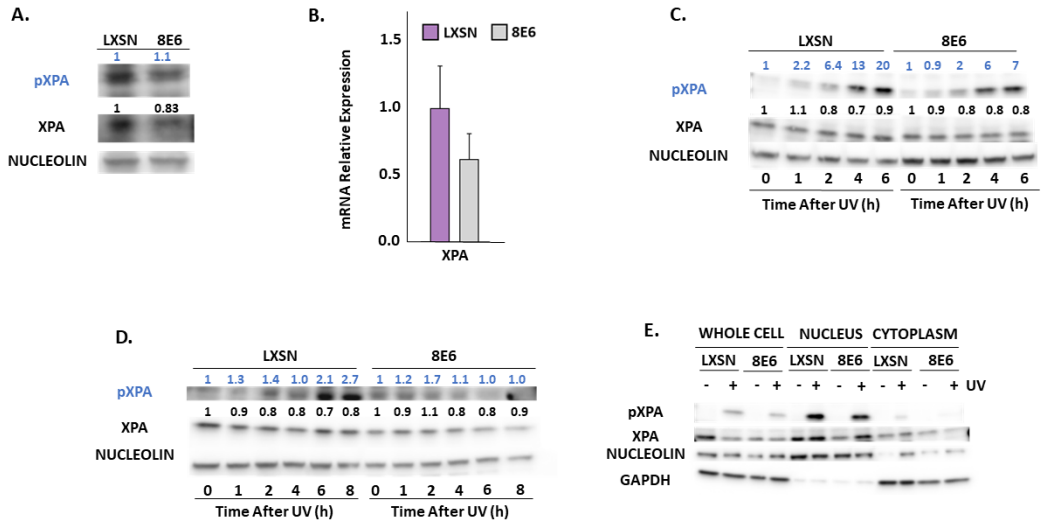

Figure 5. β-HPV 8E6 attenuates XPA phosphorylation. (**A**) Representative immunoblots of untreated hTERT HFKs with vector control (LXSN) and β-HPV 8E6 cell lines. Nucleolin was used as a loading control. (**B**) mRNA expression level of XPA in vector control (LXSN) and β-HPV 8E6 expressing primary HFKs as measured by RT-qPCR and normalized towards the expression level of β-actin. Data shown in figures are the means of ±SE of three independent experiments. (**C**) Representative immunoblots of hTERT HFKs with vector control (LXSN) and β-HPV 8E6 harvested 0–6 h post 5 mJ/cm^2 UVR. Nucleolin was used as a loading control. (**D**) Representative immunoblots of primary HFKs with vector control (LXSN) and β-HPV 8E6 harvested 0–8 h post 5 mJ/cm^2 UVR. Nucleolin was used as a loading control. (**A**,**C**,**D**) The numbers above bands represent quantification by densitometry. This is shown relative to untreated cells within the same cell line and normalized to the loading control. (**E**) Subcellular fractionation of hTERT HFKs with vector control (LXSN) and β-HPV 8E6 cell line lysates harvested 6 h post exposure to 5 mJ/cm^2 UVR were observed via immunoblot. GAPDH was used as a cytoplasmic loading control and Nucleolin was used as a nuclear loading control.

Immunoblot analysis also shows β-HPV 8E6 causes a decrease in POLη (Figure 6A). This reduction of POLη is more consistent in primary HFKs throughout the figure. In contrast, we did not find significant differences in the abundance of another TLS polymerase, POLκ (Figure 6A) [64]. β-HPV 8E6 marginally decreased POLH (gene for POLη) expression consistent with our in silico data, but this modest difference failed to reach statistical significance (Figures 1 and 6B). Previous reports have shown that POLη stability is dependent on ATR phosphorylation during UV damage [39], leading us to speculate that β-HPV 8E6 altered POLη stability. β-HPV 8E6 does not change the abundance of other TLS proteins, such as RAD18 and ubiquitinated PCNA (Supplemental Figure S10). Exposure to UV increased the abundance of POLη and POLκ in control cells (Figure 6C,D, Supplemental Figure S4O–R). While β-HPV 8E6 prevented POLη induction, POLκ rose more sharply after UV (Figure 6C,D, Supplemental Figure S4O–R). This may represent a compensatory response. Neither of these phenotypes were altered by hTERT activation and both were consistent among cells derived from different donors (Figure 6C,D, Supplemental Figure S4O–R). There are likely functional ramifications of the reduced POLη abundance as immunofluorescence microscopy demonstrated that β-HPV 8E6 reduced UV-induced POLη nuclear foci (Figure 6E, Supplemental Figure S11).

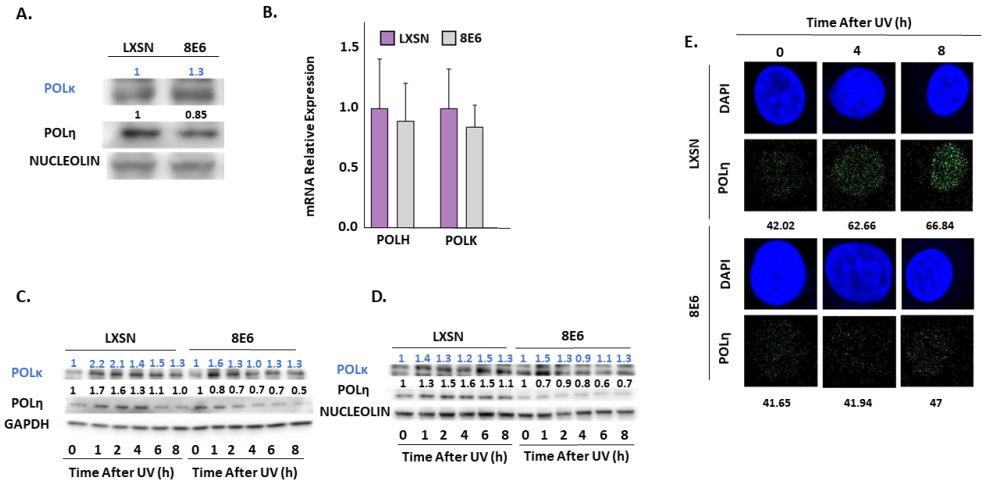

Figure 6. β-HPV 8E6 attenuates POLη abundance. (**A**) Representative immunoblots of untreated hTERT HFKs vector control (LXSN) and β-HPV 8E6 cell lines. Nucleolin was used as a loading control. (**B**) mRNA expression level of POLH and POLK in vector control (LXSN) and β-HPV 8E6 expressing primary HFKs as measured by RT-qPCR and normalized towards the expression level of β-actin. Data shown in figures are the means of ±SE of three independent experiments. (**C**) Representative immunoblots of hTERT HFKs with vector control (LXSN) and β-HPV 8E6 harvested 0–8 h post 5 mJ/cm^2 UVR. GAPDH was used as a loading control. (**D**) Representative immunoblots of primary HFKs with vector control (LXSN) and β-HPV 8E6 harvested 0–8 h post 5 mJ/cm^2 UVR. Nucleolin was used as a loading control. (**A**,**C**,**D**) The numbers above bands represent quantification by densitometry. This is shown relative to untreated cells within the same cell line and normalized to the loading control. (**E**) Representative immunofluorescence microscopy images of hTERT HFKs. POLη (green) and nuclei stained (blue) with DAPI.

3. Discussion

Pre-clinical studies and observations in immunocompromised people with NMSC support the role of β-HPV in NMSC development [65,66]. Yet, gaps in the molecular details of how β-HPV E6 changes the cellular environment remain. To address this challenge, we defined how β-HPV 8E6's reduction of ATR and ATM impacted cell signaling in response to UV. This work expands the breadth of known UV-responsive pathways impaired by β-HPV E6 to include nucleotide excision repair and translesion synthesis (Figures 5 and 6, respectively). Figure 7 details the β-HPV E6 induced changes to DNA repair and cell cycle regulation described throughout this paper.

First, we performed an in silico screen to find candidate genes likely to be regulated by ATM/ATR. We saw a positive correlation between ATM/ATR expression and the expression of UV responsive and canonical target gene expression (Figure 1). Moving from in silico analysis to in vitro, we show that β-HPV E6 decreases the autophosphorylation of ATM and ATR in primary and hTERT HFKs (Figures 2 and 3, respectively). This led us to study proteins that are dependent on ATM- and/or ATR- phosphorylation. We saw that phosphorylation of two key ATM targets, BRCA1 and CHK2, was lessened by β-HPV E6 with and without UV exposure (Figure 2). Further studies will need to be done to determine the extent of which decreased phosphorylation of BRCA1 and CHK2 impacts their downstream signaling pathways.

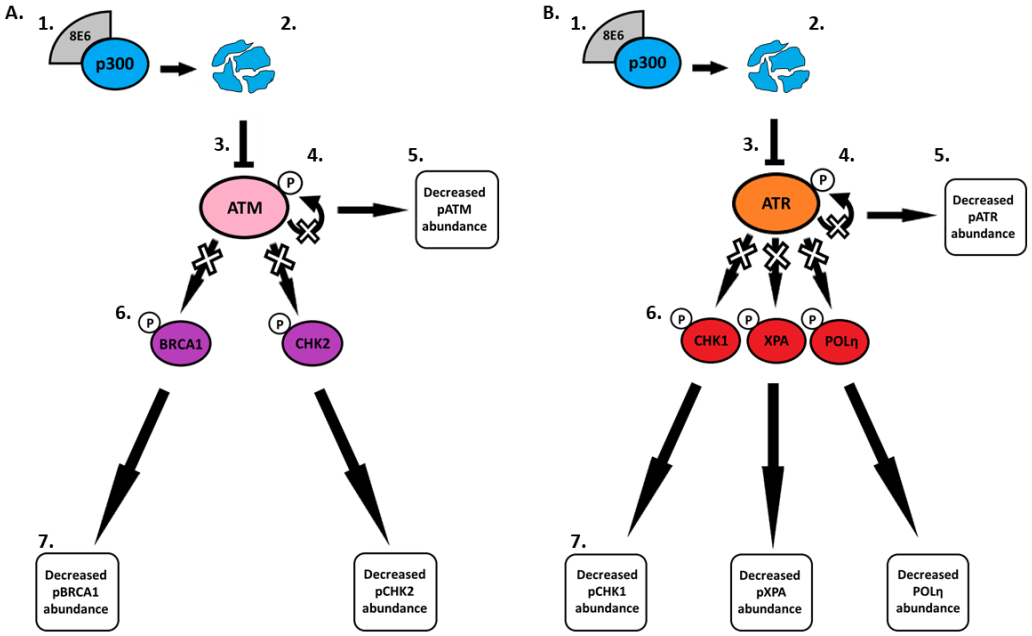

Figure 7. Schematic diagram of the effects of β-HPV 8E6 on downstream ATM and ATR targets. (**A**) β-HPV 8E6 binds to p300 (1) causing p300 to become destabilized and subsequentially degraded (2). The decrease in p300 levels leads to less ATM transcription (3). This leads to a decrease in ATM autophosphorylation (4) resulting in less activated ATM available (5). Limited availability of activated ATM leads to a decrease in ATM-dependent phosphorylation of downstream proteins (6) causing changes in β-HPV 8E6 infected cells (7). (**B**) β-HPV 8E6 binds to p300 (1) causing p300 to become destabilized and subsequentially degraded (2). The decrease in p300 levels leads to less ATR transcription (3). This leads to a decrease in ATR autophosphorylation (4) resulting in less activated ATR available (5). Limited availability of activated ATR leads to a decrease in ATR-dependent phosphorylation of downstream proteins (6) causing changes in β-HPV 8E6 infected cells (7).

Since ATM is mainly involved in double strand break repair rather than UV repair, we moved on to ATR and its downstream targets. Beginning with phosphorylation of one of the most characterized ATR targets, CHK1. We found that pCHK1 was diminished by β-HPV E6. Since CHK1 phosphorylation halts the cell cycle, we hypothesized that β-HPV 8E6 reduced cell cycle arrest after UV. To test this, we examined the phosphorylation of CHK1 targets. Surprisingly, there were no appreciable changes to the downstream proteins, CDC25A and CDC2, and only modest changes in the cell cycle profile in cells with β-HPV E6 (Figure 4). This partial inhibition may be attributed to β-HPV 8E6's inability to completely eliminate p300, ATM or ATR. Alternatively, the phenotypes could be explained by the presence of secondary kinases capable of filling in for ATR. In either case, we suspect that there will be other examples where β-HPV 8E6's inhibition of signaling pathways is significant but limited. As a result, the continued interrogation of abrogated signaling is both warranted and necessary.

β-HPV E6 was able to attenuate phosphorylation of XPA, a rate-limiting protein for NER. This may also result in altered subcellular localization of XPA, but our data do not support a strong conclusion in this regard (Figure 5 and Supplemental Figure S8). With less pXPA protein present, we hypothesize that NER function will be attenuated in cells expressing β-HPV E6. This could lead to genomic instability due to the persistence of UV lesions that would typically be resolved by the NER pathway. It would also be advantageous for β-HPV. The virus is dependent on cellular replication but infects an anatomical site that is frequently exposed to UV. Failure to initiate NER could increase the likelihood that β-HPV infected cells continue to proliferate after UV damage, offering a more conducive environment for β-HPV replication. Clearly, future studies on β-HPV E6's impact on NER are needed to better clarify the functional consequences of reduced XPA phosphorylation.

Lastly, we looked at POLη, the TLS polymerase most relevant for bypassing UV lesions. β-HPV E6 decreased POLη abundance with and without UV. POLη foci formation and localization were reduced with β-HPV E6 (Figure 6). The levels of another TLS polymerase, POLκ, were not by β-HPV E6. Thus, β-HPV E6 is not universally reducing the availability of TLS polymerases. Decreased POLη is expected to promote genomic instability by forcing TLS to rely on TLS polymerases less suited to bypass UV lesions. The experiments described here have a limited ability to test these ideas, but they justify further investigation.

Together these data better elucidate β-HPV E6's manipulation of UV damage repair. While there were inconsistencies between primary HFKs and hTERT HFKs in our immunoblots, we put more emphasis on the phenotypes seen in the primary HFKs. Primary HFKs only grow for a limited time in culture and thus more closely mirror the typically transient β-HPV infection. Further, it would not be surprising if the differences were attributable to the known interactions between telomerase and DNA repair machinery [67]. However, lack of functional analysis limits the breadth of our conclusions. This will require a more detailed interrogation of cell cycle, NER, and TLS in the presence of β-HPV E6. Organotypic raft cultures and animal models could also provide biologically relevant insight in the monoculture experiments described here. Further, it would be beneficial to repeat these experiments in the presence of other β-HPV proteins (particularly β-HPV 8E7) and genes from other disease associated β-HPVs (e.g., HPV 38 and HPV 49).

4. Materials and Methods

4.1. Cell Culture

Primary human foreskin keratinocytes (HFKs) were isolated from neonatal human foreskins. HFKs were grown in EpiLife medium (Gibco, Billings, MT, USA) supplemented with calcium chloride (Gibco), human keratinocyte growth supplement (Gibco), and penicillin-streptomycin (Caisson, North Logan, UT, USA) or Keratinocyte Growth Medium 2 (Promocell, Heidelberg, Germany), Supplement Mix (Promocell), and penicillin-streptomycin (Caisson). hTERT human foreskin keratinocytes (hTERT HFKs), provided by Michael Underbrink (University of Texas Medical Branch, Galveston, TX, USA), are immortalized keratinocytes that constituently express telomerase (hTERT). hTERT HFKs were grown in EpiLife medium (Gibco) supplemented with calcium chloride (Gibco), human keratinocyte growth supplement (Gibco), and penicillin-streptomycin (Caisson). Multiple passages were used throughout these experiments for both cell lines with hTERT HFK passaging ranging from 15–80 and primary HFKs passaging ranging from 9–11. hTERT HFKs and primary HFKs both expressed the control vector (LXSN) and β-HPV 8E6; hTERT HFKs expressed HA-tagged β-HPV 8E6. In total, one primary HFK and one hTERT HFK cell line (each from separate donors) was used in these experiments.

4.2. Cell Cycle Analysis

Cells were harvested by trypsinization from 10-cm dishes, with cells being 70–90% confluent. After washing with cold 1× phosphate-buffered saline (PBS), cells were fixed with 4% paraformaldehyde (PFA) in 1×PBS for 15 min, and permeabilized in PBS containing 0.2% Triton X-100 for 30 min at room

temperature. After washing with PBS, cells were resuspended in 0.2 mL of PBS and 3 µM of DAPI was added, then incubated at room temperature for 30 min in the dark [68].

Samples were analyzed by using an LSRFortessa X20 Flow Cytometer (BD, Franklin Lakes, NJ). Cells were gated on the Forward versus Side Scatter plot to eliminate debris, and then single cells were gated by using a dot-plot showing the pulse width versus pulse area of the DAPI channel. Post-acquisition analysis was performed with Flowing software 2.5.1. [68].

4.3. Comparative Transcriptomic Analysis

Web-based software on cBioPortal for Cancer Genomics (ww.cbioportal.org) was used to analyze RNAseq data from the *Cancer Cell Line Encyclopedia* [44–46]. List of genes for each category in Figure 1 and Supplemental Figure S1 is provided here: NER genes: UBE2B, FAAP20, POLK, PRIMPOL, RFC1, POLE3, RPA1, POLD1, RPA3, PCLAF, POLE2, RFC5, DTL, PCNA, RFC4, POLD3, RFC2, RPA2, ZBTB1, POLI, REV3L, REV1, POLH, VCP, RAD18, ISG15, SPRTN. TLS genes: CDK7, POLE, POLE2, POLE3, POLD1, POLD2, GTF2H1, GTF2H4, POLD3, POLD4, POLE4, RBX1, PCNA, CCNH, DDB2, ERCC8, DDB1, RPA3, LIG1, RFC1, RFC2, RFC3, RFC4, RFC5, XPC, ERCC6, MNAT1, ERCC3, ERCC2, GTF2H5, XPA, ERCC4, ERCC1. ATR/ATM genes: CHEK1, CDC25A, BRCA1, TP53. List of genes in Supplementary Figure S2 is provided here: BRCA1, MRE11, RAD9A, RAD9B, RAD50, TP53, NBN, PRKDC, RBBP8, ATMIN, HIF1A, TOPBP1, TP53BP1, MDC1, H2AFX, STRAP, SMC1B, E2F1, AATF, DCLRE1C, MDC1, EXO1, DNA2

4.4. Immunoblot

Once cell lines were 85% confluent after being seeded onto 6-well plates, they were exposed to 5 mJ/cm^2 UV radiation for the appropriate time. Then, whole cell lysates were prepared by washing cells in cold 1×PBS before incubating on ice in complete RIPA lysis buffer (RIPA lysis buffer, protease inhibitor, phosphatase inhibitor) and mechanically harvested. Lysates were then centrifuged for higher purification and protein concentration was determined via BCA assay. 20 µg protein lysates were electrophoresed on SDS-PAGE and transferred to Immobilon-P membranes (Millipore, Burlington, MA, USA). The membranes were then probed with primary and secondary antibodies. All key immunoblot results were repeated at least five times (three times in hTERT HFKs and twice in HFKs to confirm the phenotype). Negative results (e.g., sub-cellular fractionation experiments) were done in duplicate. Quantification was performed using ImageJ (NIH, Rockville, MD, USA).

4.5. Antibodies

The following primary antibodies were used: pATM (Ser1981) (D25E5) (13050S, Cell Signaling, Danvers, MA), ATM (11G12) (92356S, Cell Signaling), pATR (Thr1989) (58014S, Cell Signaling), ATR (2790S, Cell Signaling), pBRCA1 (Ser1423) (ab90528, Abcam, Cambridge, United Kingdom), BRCA1 (9010S, Cell Signaling), pCHK2 (Thr68) (C13C1)(2197S, Cell Signaling), CHK2 (2662S, Cell Signaling), pCHK1 (Ser345) (133D3) (2348S, Cell Signaling), CHK1 (2G1D5) (2360S, Cell Signaling), pCDC25A (Thr507) (PA512564, Thermo Fisher, Waltham, MA), CDC25A (DCS121) (MA112293, Thermo Fisher), pCDC2 (Thr14) (2543S, Cell Signaling), CDC2 (77055S, Cell Signaling), pCDK2 (Tyr15) (PA5-77907, Fisher Scientific, Hampton, NH), CDK2 (78B2) (2546S, Cell Signaling), pXPA (Ser196) (PA5-64730, Thermo Fisher), XPA (5F12) (ab65963, Abcam), RAD18 (ab57447, Abcam), UB. PCNA (Lys164) (D5C7P) (13439S, Cell Signaling), PCNA (PC10) (2586S, Cell Signaling), POLκ (ab57070, Abcam), POLη (B-7) (sc-17770, Santa Cruz, Dallas, TX), pRPA32/RPA2 (Ser8) (83745S, Cell Signaling), RPA32/RPA2 (52448S, Cell Signaling), RPA70/RPA1 (2267S, Cell Signaling), TOPBP1 (B-7) (sc-271043, Santa Cruz), GAPDH (0411) (sc-47724, Santa Cruz), Nucleolin (C23) (MS-3) (sc-803, Santa Cruz).

The following secondary antibodies were used: Peroxidase AffiniPure Goat Anti Mouse IgG (H + L) (115-035-003, Jackson ImmunoResearch, West Grove, PA), Anti Rabbit IgG, HRP-linked (7074S, Cell Signaling), Goat anti-Rabbit IgG (H + L) Cross-Adsorbed Secondary Antibody, Goat anti-Mouse

IgG (H + L) Cross-Adsorbed Secondary Antibody, Alexa Fluor 488 (A-11001, Thermo Fisher, Waltham, MA), Alexa Fluor 594 (A-11012, Thermo Fisher).

4.6. Immunofluorescent Microscopy

Cells were seeded onto glass bottom plates (Cellvis, Mountain View, CA, USA), grown for 24 h and exposed to 5 mJ/cm^2 UV radiation. Then once it was the appropriate time after 5 mJ/cm2 UV exposure, the cells were incubated in 4% formaldehyde for 15 min. Then the cells were permeabilized with 0.1% Triton X for 10 min. Next, the cells were blocked with 3% BSA and incubated with primary antibody overnight at 4 °C. The next day, the cells were incubated with fluorescent secondary antibodies (1:500) for 1 h and stained with 300 nM DAPI (D1306, Thermo Fisher) for 9 min. Cells were imaged using the Carl Zeiss 700 confocal microscope (Oberkochen, Germany) using the 40× (1.4 NA Oil) objective. Foci and intensity analyses were completed using ImageJ.

4.7. Subcellular Fractionation

Cells were seeded and grown for 24 h before being exposed to 5 mJ/cm^2 UV and incubated for the appropriate time after radiation. Whole cell lysates were prepared by washing cells in cold 1×PBS before mechanically harvesting the cells in Subcellular Fractionation Buffer (HEPES, KCl, MgCl2, EDTA, EGA, pH 7.4, 1mM DTT, protease inhibitor, and phosphatase inhibitor). Nuclear and cytoplasmic lysates were separated through centrifugation. 20 µg protein lysates were electrophoresed on SDS-PAGE and transferred to Immobilon-P membranes (Millipore, Burlington, MA, USA). The membranes were then probed with primary and secondary antibodies.

4.8. mRNA Quantification

Cell were lysed using Trizol (Invitrogen, Carlsbad, CA, USA) and RNA isolated with the RNeasy kit (Qiagen, Hilden, Germany). Two µg of RNA were reverse transcribed using the iScript™ cDNA Synthesis Kit (Bio-Rad, Hercules, CA). Quantitative reverse transcription-PCR was performed in triplicate with the TaqMan™ FAM-MGB Gene Expression Assay (Applied Biosystems, Foster City, CA) and C1000 Touch Thermal Cycler (Bio-Rad). The following probes (Thermo Scientific) were used: ACTB (Hs01060665_g1), POLH (Hs00197814_m1), POLK (Hs00211965_m1), CHEK1 (Hs00967506_m1), XPA (Hs00166045_m1)

4.9. UV Radiation

Cells were washed with 1×PBS and then irradiated at 5 mJ/cm^2 using the UV Stratalinker 2400 (Stratagene, San Diego, CA, USA). Then media was added back to the cells and they were allowed to incubate for the appropriate time after UV exposure.

4.10. Statistical Analysis

Statistical significance was determined using student's *t*-test. p values less than or equal to 0.05 were reported as significant.

Supplementary Materials: The following are available online at http://www.mdpi.com/2076-0817/8/4/267/s1, Figure S1: High expression of ATR/ATM mRNA correlates with an increase in UV damage repair pathways gene expression. Figure S2: Truncation of ATR/ATM weakly correlates with UV damage repair pathways gene expression., Figure S3: Confirmation of β-HPV 8E6 expression. Figure S4: Quantification of hTERT HFK and primary HFK UV time course immunoblots. Figure S5: β-HPV 8E6 reduces p53 accumulation after UV exposure. Figure S6: β-HPV 8E6 increases phosphorylation of RPA32. Figure S7: Quantification of hTERT HFK UV time course immunoblots for CHK1 downstream targets. Figure S8: β-HPV 8E6 attenuates XPA phosphorylation in U2OS cells. Figure S9: β-HPV 8E6 attenuates XPA localization in U2OS cells. Figure S10: β-HPV 8E6 does not attenuate other TLS proteins. Figure S11: β-HPV 8E6 diminished POLη foci formation and intensity. Table S1: Multiple comparison (False discovery rate).

Author Contributions: Conceptualization, N.A.W.; Resources, N.A.W.; Supervision, N.A.W.; Funding acquisition, N.A.W.; Investigation, J.A.S., V.M., D.D., C.H.; Validation, J.A.S., V.M., D.D., C.H.; Writing—original draft preparation, J.A.S., N.A.W.; Writing—review and editing, J.A.S., N.A.W., C.H., D.D., V.M.; Visualization, J.A.S.

Funding: We would like to thank the Terry Johnson Basic Cancer Research Center and the Les Clow family for their support of this project. We also received support from a career development award provided by the United States' Department of Defense's Congressionally Directed Medical Research Program's Peer Reviewed Cancer Research Program (CMDRP PRCRP CA160224 (NW)).

Acknowledgments: Special thanks to Michael Underbrink for providing hTERT HFKs.

Conflicts of Interest: The authors declare no conflict of interest.

References

1. de Villiers, E.-M. Cross-roads in the classification of papillomaviruses. *Virology* **2013**, *445*, 2–10. [CrossRef] [PubMed]
2. Bernard, H.-U.; Burk, R.D.; Chen, Z.; van Doorslaer, K.; zur Hausen, H.; de Villiers, E.-M. Classification of papillomaviruses (PVs) based on 189 PV types and proposal of taxonomic amendments. *Virology* **2010**, *401*, 70–79. [CrossRef] [PubMed]
3. de Villiers, E.-M.; Fauquet, C.; Broker, T.R.; Bernard, H.-U.; zur Hausen, H. Classification of papillomaviruses. *Virology* **2004**, *324*, 17–27. [CrossRef] [PubMed]
4. Bzhalava, D.; Eklund, C.; Dillner, J. International standardization and classification of human papillomavirus types. *Virology* **2015**, *476*, 341–344. [CrossRef] [PubMed]
5. Munger, K.; Baldwin, A.; Edwards, K.M.; Hayakawa, H.; Nguyen, C.L.; Owens, M.; Grace, M.; Huh, K. Mechanisms of human papillomavirus-induced oncogenesis. *J. Virol.* **2004**, *78*, 11451–11460. [CrossRef] [PubMed]
6. Gheit, T. Mucosal and cutaneous human papillomavirus infections and cancer biology. *Front. Oncol.* **2019**, *9*, 355. [CrossRef]
7. Brianti, P.; Flammineis, E.D.; Mercuri, S.R. Review of HPV-related diseases and cancers. *New Microbiol.* **2007**, *40*, 80–85.
8. Egawa, N.; Doorbar, J. The low-risk papillomaviruses. *Virus Res.* **2017**, *231*, 119–127. [CrossRef]
9. Longworth, M.S.; Laimins, L.A. Pathogenesis of human papillomaviruses in differentiating epithelia. *Microbiol. Mol. Biol. Rev.* **2004**, *68*, 362–372. [CrossRef]
10. Muñoz, N.; Castellsagué, X.; de González, A.B.; Gissmann, L. Chapter 1: HPV in the etiology of human cancer. *Vaccine* **2006**, *24*, S1–S10. [CrossRef]
11. Duensing, S.; Münger, K. Mechanisms of genomic instability in human cancer: Insights from studies with human papillomavirus oncoproteins: Genomic Instability and Cervical Cancer. *Int. J. Cancer* **2004**, *109*, 157–162. [CrossRef] [PubMed]
12. Wendel, S.O.; Wallace, N.A. Loss of genome fidelity: Beta HPVs and the DNA damage response. *Front. Microbiol.* **2017**, *8*, 2250. [CrossRef] [PubMed]
13. Pfister, H. Chapter 8: Human papillomavirus and skin cancer. *JNCI Monogr.* **2003**, *2003*, 52–56. [CrossRef] [PubMed]
14. Hufbauer, M.; Akgül, B. Molecular mechanisms of human papillomavirus induced skin carcinogenesis. *Viruses* **2017**, *9*, 187. [CrossRef] [PubMed]
15. Shanmugasundaram, S.; You, J.X. Targeting persistent human papillomavirus infection. *Viruses* **2017**, *9*, 229. [CrossRef] [PubMed]
16. Howley, P.M.; Pfister, H.J. Beta genus papillomaviruses and skin cancer. *Virology* **2015**, *479–480*, 290–296. [CrossRef]
17. Weissenborn, S.J.; Nindl, I.; Purdie, K.; Harwood, C.; Proby, C.; Breuer, J.; Majewski, S.; Pfister, H.; Wieland, U. Human papillomavirus-DNA loads in actinic keratoses exceed those in non-melanoma skin cancers. *J. Investig. Dermatol.* **2005**, *125*, 93–97. [CrossRef]
18. Ramasamy, K.; Shanmugam, M.; Balupillai, A.; Govindhasamy, K.; Gunaseelan, S.; Muthusamy, G.; Robert, B.; Nagarajan, R. Ultraviolet radiation-induced carcinogenesis: Mechanisms and experimental models. *J. Radiat. Cancer Res.* **2017**, *8*, 4–19.

19. Rollison, D.E.; Viarisio, D.; Amorrortu, R.P.; Gheit, T.; Tommasino, M. An emerging issue in oncogenic virology: The role of beta human papillomavirus types in the development of cutaneous squamous cell carcinoma. *J. Virol.* **2019**, *93*, e01003-18. [CrossRef]
20. Lomas, A.; Leonardi-Bee, J.; Bath-Hextall, F. A systematic review of worldwide incidence of nonmelanoma skin cancer: Worldwide incidence of nonmelanoma skin cancer. *Br. J. Dermatol.* **2012**, *166*, 1069–1080. [CrossRef]
21. Apalla, Z.; Lallas, A.; Sotiriou, E.; Lazaridou, E.; Ioannides, D. Epidemiological trends in skin cancer. *Dermatol. Pract. Concept.* **2017**, *7*, 1–6. [CrossRef] [PubMed]
22. Patel, T.; Morrison, L.K.; Rady, P.; Tyring, S. Epidermodysplasia verruciformis and susceptibility to HPV. *Dis. Markers* **2010**, *29*, 199–206. [CrossRef] [PubMed]
23. Nindl, I.; Rösl, F. Molecular concepts of virus infections causing skin cancer in organ transplant recipients. *Am. J. Transplant.* **2008**, *8*, 2199–2204. [CrossRef] [PubMed]
24. Bavinck, J.N.B.; Feltkamp, M.; Struijk, L.; ter Schegget, J. Human papillomavirus infection and skin cancer risk in organ transplant recipients. *J. Investig. Dermatol. Symp. Proc.* **2001**, *6*, 207–211. [CrossRef] [PubMed]
25. Tomaić, V. Functional roles of E6 and E7 oncoproteins in HPV-induced malignancies at diverse anatomical sites. *Cancers* **2016**, *8*, 95. [CrossRef]
26. Meyers, J.M.; Spangle, J.M.; Munger, K. The human papillomavirus type 8 E6 protein interferes with NOTCH activation during keratinocyte differentiation. *J. Virol.* **2013**, *87*, 4762–4767. [CrossRef]
27. Meyers, J.M.; Uberoi, A.; Grace, M.; Lambert, P.F.; Munger, K. Cutaneous HPV8 and MmuPV1 E6 proteins target the NOTCH and TGF-β tumor suppressors to inhibit differentiation and sustain keratinocyte proliferation. *PLoS Pathog.* **2017**, *13*, e1006171. [CrossRef]
28. Taute, S.; Pfister, H.J.; Steger, G. Induction of tyrosine phosphorylation of UV-activated EGFR by the beta-human papillomavirus type 8 E6 leads to papillomatosis. *Front. Microbiol.* **2017**, *8*, 2197. [CrossRef]
29. Howie, H.L.; Koop, J.I.; Weese, J.; Robinson, K.; Wipf, G.; Kim, L.; Galloway, D.A. Beta-HPV 5 and 8 E6 promote p300 degradation by blocking AKT/p300 association. *PLoS Pathog.* **2011**, *7*, e1002211. [CrossRef]
30. Wallace, N.A.; Robinson, K.; Howie, H.L.; Galloway, D.A. HPV 5 and 8 E6 abrogate ATR activity resulting in increased persistence of UVB induced DNA damage. *PLoS Pathog.* **2012**, *8*, e1002807. [CrossRef]
31. Wallace, N.A.; Gasior, S.L.; Faber, Z.J.; Howie, H.L.; Deininger, P.L.; Galloway, D.A. HPV 5 and 8 E6 expression reduces ATM protein levels and attenuates LINE-1 retrotransposition. *Virology* **2013**, *443*, 69–79. [CrossRef] [PubMed]
32. Stauffer, D.; Chang, B.; Huang, J.; Dunn, A.; Thayer, M. p300/CREB-binding protein interacts with ATR and is required for the DNA replication checkpoint. *J. Biol. Chem.* **2007**, *282*, 9678–9687. [CrossRef] [PubMed]
33. Marechal, A.; Zou, L. DNA damage sensing by the ATM and ATR kinases. *Cold Spring Harb. Perspect. Biol.* **2013**, *5*, a012716. [CrossRef] [PubMed]
34. Blackford, A.N.; Jackson, S.P. ATM, ATR, and DNA-PK: The trinity at the heart of the DNA damage response. *Mol. Cell* **2017**, *66*, 801–817. [CrossRef] [PubMed]
35. O'Connor, M.J. Targeting the DNA damage response in cancer. *Mol. Cell* **2015**, *60*, 547–560. [CrossRef] [PubMed]
36. Hufbauer, M.; Cooke, J.; van der Horst, G.T.J.; Pfister, H.; Storey, A.; Akgül, B. Human papillomavirus mediated inhibition of DNA damage sensing and repair drives skin carcinogenesis. *Mol. Cancer* **2015**, *14*, 183. [CrossRef]
37. Sugitani, N.; Sivley, R.M.; Perry, K.E.; Capra, J.A.; Chazin, W.J. XPA: A key scaffold for human nucleotide excision repair. *DNA Repair* **2016**, *44*, 123–135. [CrossRef]
38. Park, J.-M.; Kang, T.-H. Transcriptional and posttranslational regulation of nucleotide excision repair: The guardian of the genome against ultraviolet radiation. *Int. J. Mol. Sci.* **2016**, *17*, 1840. [CrossRef]
39. Göhler, T.; Sabbioneda, S.; Green, C.M.; Lehmann, A.R. ATR-mediated phosphorylation of DNA polymerase η is needed for efficient recovery from UV damage. *J. Cell Biol.* **2011**, *192*, 219–227. [CrossRef]
40. Tonzi, P.; Huang, T.T. Role of Y-family translesion DNA polymerases in replication stress: Implications for new cancer therapeutic targets. *DNA Repair* **2019**, *78*, 20–26. [CrossRef]
41. Zhang, Y.; Hunter, T. Roles of Chk1 in cell biology and cancer therapy: Chk1 review. *Int. J. Cancer* **2014**, *134*, 1013–1023. [CrossRef] [PubMed]

42. Xiao, Z.; Chen, Z.; Gunasekera, A.H.; Sowin, T.J.; Rosenberg, S.H.; Fesik, S.; Zhang, H. Chk1 mediates S and G_2 arrests through Cdc25A degradation in response to DNA-damaging agents. *J. Biol. Chem.* **2003**, *278*, 21767–21773. [CrossRef] [PubMed]
43. Matsuoka, S.; Rotman, G.; Ogawa, A.; Shiloh, Y.; Tamai, K.; Elledge, S.J. Ataxia telangiectasia-mutated phosphorylates Chk2 in vivo and in vitro. *Proc. Natl. Acad. Sci. USA* **2000**, *97*, 10389–10394. [CrossRef] [PubMed]
44. Barretina, J.; Caponigro, G.; Stransky, N.; Venkatesan, K.; Margolin, A.A.; Kim, S.; Wilson, C.J.; Lehár, J.; Kryukov, G.V.; Sonkin, D.; et al. The Cancer Cell Line Encyclopedia enables predictive modelling of anticancer drug sensitivity. *Nature* **2012**, *483*, 603–607. [CrossRef]
45. Cerami, E.; Gao, J.; Dogrusoz, U.; Gross, B.E.; Sumer, S.O.; Aksoy, B.A.; Jacobsen, A.; Byrne, C.J.; Heuer, M.L.; Larsson, E.; et al. The cBio cancer genomics portal: An open platform for exploring multidimensional cancer genomics data: Figure 1. *Cancer Discov.* **2012**, *2*, 401–404. [CrossRef]
46. Gao, J.; Aksoy, B.A.; Dogrusoz, U.; Dresdner, G.; Gross, B.; Sumer, S.O.; Sun, Y.; Jacobsen, A.; Sinha, R.; Larsson, E.; et al. Integrative analysis of complex cancer genomics and clinical profiles using the cBioPortal. *Sci. Signal.* **2013**, *6*, pl1. [CrossRef]
47. Abraham, R.T. Cell cycle checkpoint signaling through the ATM and ATR kinases. *Genes Dev.* **2001**, *15*, 2177–2196. [CrossRef]
48. Cortez, D. Requirement of ATM-dependent phosphorylation of brca1 in the DNA damage response to double-strand breaks. *Science* **1999**, *286*, 1162–1166. [CrossRef]
49. Canman, C.E. Activation of the ATM kinase by ionizing radiation and phosphorylation of p53. *Science* **1998**, *281*, 1677–1679. [CrossRef]
50. Tibbetts, R.S.; Brumbaugh, K.M.; Williams, J.M.; Sarkaria, J.N.; Cliby, W.A.; Shieh, S.-Y.; Taya, Y.; Prives, C.; Abraham, R.T. A role for ATR in the DNA damage-induced phosphorylation of p53. *Genes Dev.* **1999**, *13*, 152–157. [CrossRef]
51. Lavin, M.F.; Gueven, N. The complexity of p53 stabilization and activation. *Cell Death Differ.* **2006**, *13*, 941–950. [CrossRef] [PubMed]
52. Awasthi, P.; Foiani, M.; Kumar, A. ATM and ATR signaling at a glance. *J. Cell Sci.* **2015**, *128*, 4255–4262. [CrossRef] [PubMed]
53. Wallace, N.A.; Robinson, K.; Galloway, D.A. Beta human papillomavirus E6 expression inhibits stabilization of p53 and increases tolerance of genomic instability. *J. Virol.* **2014**, *88*, 6112–6127. [CrossRef] [PubMed]
54. Sullivan, K.D.; Galbraith, M.D.; Andrysik, Z.; Espinosa, J.M. Mechanisms of transcriptional regulation by p53. *Cell Death Differ.* **2018**, *25*, 133–143. [CrossRef] [PubMed]
55. Griewank, K.G.; Murali, R.; Schilling, B.; Schimming, T.; Möller, I.; Moll, I.; Schwamborn, M.; Sucker, A.; Zimmer, L.; Schadendorf, D.; et al. TERT promoter mutations are frequent in cutaneous basal cell carcinoma and squamous cell carcinoma. *PLoS ONE* **2013**, *8*, e80354. [CrossRef]
56. Gatei, M.; Scott, S.P.; Filippovitch, I.; Soronika, N.; Lavin, M.F.; Weber, B.; Khanna, K.K. Role for ATM in DNA damage-induced phosphorylation of BRCA1. *Cancer Res.* **2000**, *60*, 3299–3304.
57. Liu, S.; Shiotani, B.; Lahiri, M.; Maréchal, A.; Tse, A.; Leung, C.C.Y.; Glover, J.N.M.; Yang, X.H.; Zou, L. ATR autophosphorylation as a molecular switch for checkpoint activation. *Mol. Cell* **2011**, *43*, 192–202. [CrossRef]
58. Stokes, M.P.; Rush, J.; MacNeill, J.; Ren, J.M.; Sprott, K.; Nardone, J.; Yang, V.; Beausoleil, S.A.; Gygi, S.P.; Livingstone, M.; et al. Profiling of UV-induced ATM/ATR signaling pathways. *Proc. Natl. Acad. Sci. USA* **2007**, *104*, 19855–19860. [CrossRef]
59. Zhao, H.; Piwnica-Worms, H. ATR-mediated checkpoint pathways regulate phosphorylation and activation of human Chk1. *Mol. Cell. Biol.* **2001**, *21*, 4129–4139. [CrossRef]
60. Iyer, D.; Rhind, N. The intra-S checkpoint responses to DNA damage. *Genes* **2017**, *8*, 74. [CrossRef]
61. Shen, T.; Huang, S. The role of Cdc25A in the regulation of cell proliferation and apoptosis. *Anticancer Agents Med. Chem.* **2012**, *12*, 631–639. [CrossRef] [PubMed]
62. Lee, T.-H.; Park, J.-M.; Leem, S.-H.; Kang, T.-H. Coordinated regulation of XPA stability by ATR and HERC2 during nucleotide excision repair. *Oncogene* **2014**, *33*, 19–25. [CrossRef] [PubMed]
63. Shell, S.M.; Li, Z.; Shkriabai, N.; Kvaratskhelia, M.; Brosey, C.; Serrano, M.A.; Chazin, W.J.; Musich, P.R.; Zou, Y. Checkpoint kinase ATR promotes nucleotide excision repair of UV-induced DNA damage via physical interaction with xeroderma pigmentosum group A. *J. Biol. Chem.* **2009**, *284*, 24213–24222. [CrossRef] [PubMed]

64. Tonzi, P.; Yin, Y.; Lee, C.W.T.; Rothenberg, E.; Huang, T.T. Translesion polymerase kappa-dependent DNA synthesis underlies replication fork recovery. *ELife* **2018**, *7*, e41426. [CrossRef] [PubMed]
65. Hasche, D.; Vinzón, S.E.; Rösl, F. Cutaneous papillomaviruses and non-melanoma skin cancer: Causal agents or innocent bystanders? *Front. Microbiol.* **2018**, *9*, 874. [CrossRef] [PubMed]
66. Nindl, I.; Gottschling, M.; Stockfleth, E. Human papillomaviruses and non-melanoma skin cancer: Basic virology and clinical manifestations. *Dis. Markers* **2007**, *23*, 247–259. [CrossRef]
67. Webb, C.J.; Wu, Y.; Zakian, V.A. DNA repair at telomeres: Keeping the ends intact. *Cold Spring Harb. Perspect. Biol.* **2013**, *5*, a012666. [CrossRef]
68. Forment, J.V.; Walker, R.V.; Jackson, S.P. A high-throughput, flow cytometry-based method to quantify DNA-end resection in mammalian cells. *Cytom. Part A* **2012**, *81*, 922–928. [CrossRef]